SYSTEMS TECHNOLOGY, INC.

13766 SO. HAWTHORNE BOULEVARD • HAWTHORNE, CALIFORNIA 90250

Technical Report No. 1015-1

ANALYTICAL DESIGN AND SIMULATION EVALUATION OF AN APPROACH FLIGHT DIRECTOR SYSTEM FOR A JET STOL AIRCRAFT

May 1974

ANALYTICAL DESIGN AND SIMULATION EVALUATION

OF AN APPROACH FLIGHT DIRECTOR SYSTEM

FOR A JET STOL AIRCRAFT

Richard H. Klein
Lee Gregor Hofmann
Duane T. McRuer

May 1974

STI TR 1015-1

Distribution of this report is provided
in the interest of information exchange.
Responsibility for the contents resides in
the author or organization that prepared it.

I

SYSTEMS TECHNOLOGY, INC.

Technical Report No. 1015-1

ANALYTICAL DESIGN AND SIMULATION EVALUATION
OF AN APPROACH FLIGHT DIRECTOR SYSTEM
FOR A JET STOL AIRCRAFT

Richard H. Klein
Lee Gregor Hofmann
Duane T. McRuer

May 1974

i

ABSTRACT

The National Aeronautics and Space Administration has undertaken a program to develop design criteria and operational procedures for STOL transport aircraft. As part of that program, a series of flight tests shall be performed in an Augmentor Wing Jet STOL Aircraft. The objective of this set of flight tests is to evaluate the flying qualities of that aircraft, manual control techniques for powered-lift vehicles, and improvements possible in approach and landing performance through flight director displays and stability augmentation of the basic vehicle's dynamics.

In preparation for the flight test programs, an analytical study was conducted to gain an understanding of the characteristics of the vehicle for manual control, to assess the relative merits of the variety of manual control techniques available with attitude and thrust vector controllers, and to determine what improvements can be made over manual control of the bare airframe by providing the pilot with suitable command guidance information and by augmentation of the bare airframe dynamics. The objective of the study described in this report is to apply closed-loop pilot/vehicle analysis techniques to the analysis of manual flight control of powered-lift STOL aircraft in the landing approach and to the design and experimental verification of an advanced flight director display.

TABLE OF CONTENTS

LIST OF FIGURES

LIST OF TABLES

SECTION I

INTRODUCTION

Closed-loop pilot/vehicle analysis represents an effective way of reaching a near optimum system design prior to final simulation and flight test. The theory of closed-loop manual control rests on validated mathematical pilot models (Ref. 1), established control systems techniques (Ref. 2), and empirical data (Ref. 3) that have been derived from applied research.

A pertinent application of manual control theory is the design of a flight director. A flight director system consists of both a computer and a display as shown in Fig. 1. The computer combines various vehicle attitude and position errors from the guidance system to provide one signal in each axis of control. If the pilot nulls this signal the vehicle will follow the commanded guidance path.
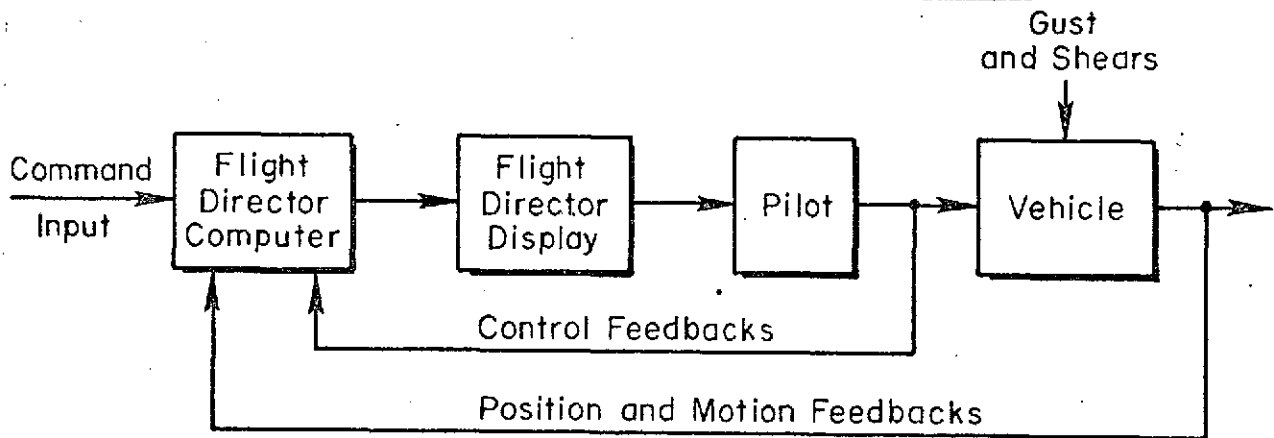
Figure 1. Flight Director System Elements

The display portion of Fig. 1 may be represented by the typical 3 cue (or element) STOL flight director indicator shown in Fig. 2. It has horizontal and vertical command bars as well as a lift command indication on the left side. The command elements form the basis for the pilot's control actions. In conventional aircraft there are only the two central command bars, one for column and one for wheel. For a STOL, however, the additional command bar is necessary since a major portion of the path control may be coming from thrust, thrust vectoring or direct lift control (DLC)

Vertical
Force
Command
Cue

Lateral
Command
Bar

Longitudinal
Command
Bar
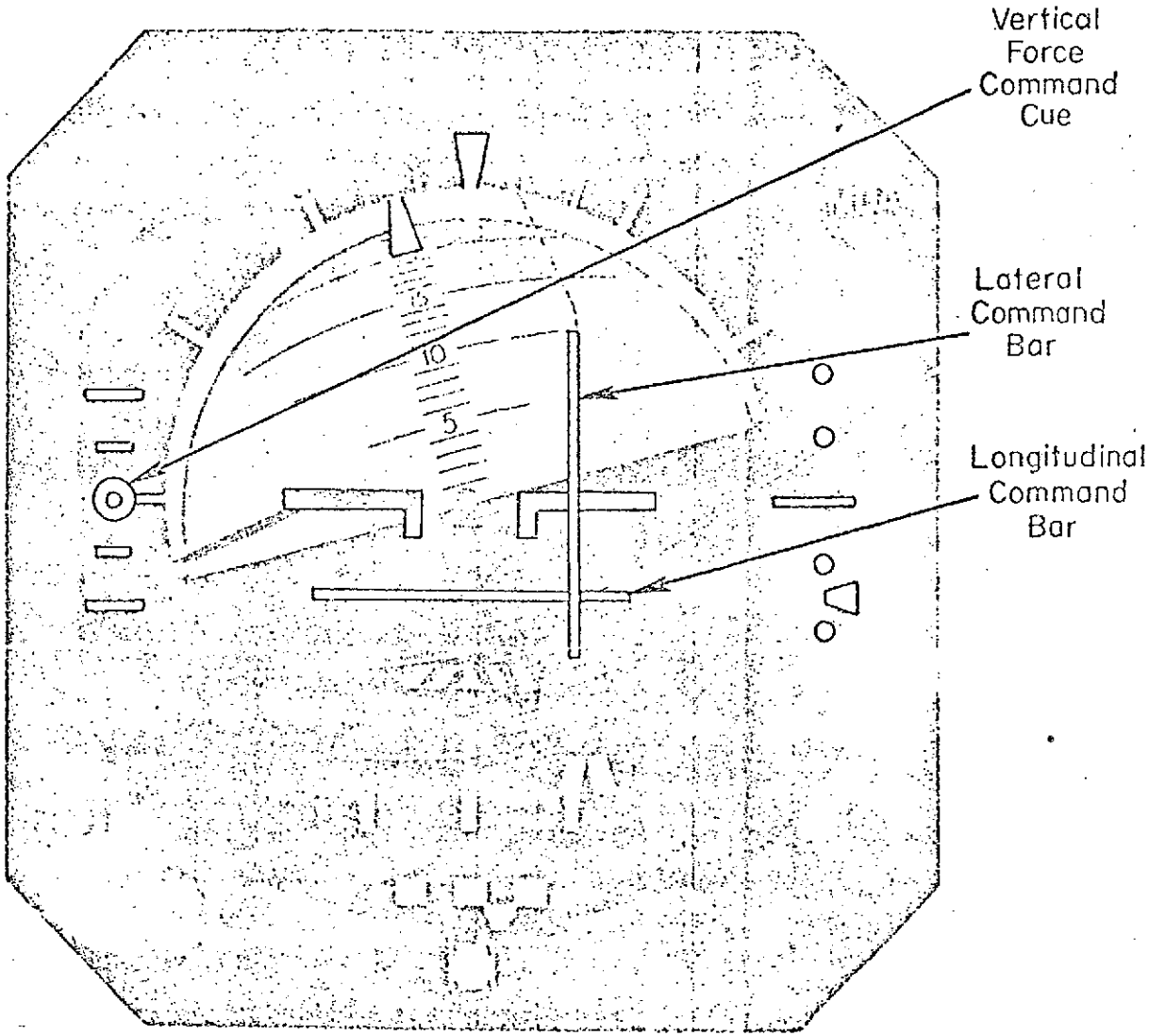
Figure 2. Typical Flight Director Display
Applicable for STOL Aircraft

The control laws for the command displays are derived so that when the pilot nulls the command bars the vehicle will be directed onto the approach path in accord with well-defined guidance and control requirements. In addition to the guidance requirements, the feedback quantities making up the "effective controlled element," i.e., the vehicle-plus-flight-director dynamics, must be weighted, filtered, and equalized in accord with a set of pilot-centered requirements so that the pilot can null the command bar with ease and efficiency.

The remaining elements of the integrated display indicate the aircraft's situation relative to the external world. This "status" information includes an artificial horizon, glide slope and localizer deviation, radar altitude, and turn and slip indication.

A. SCOPE OF THE REPORT

This report presents the development and simulation evaluation of the longitudinal and lateral flight director control laws for a jet STOL aircraft. Although this is a specific application, the requirements and design process developed are applicable to other STOL vehicles. The system developed is applicable to constant speed straight-in approaches on a glide path. Localizer capture is included but glide slope capture and transition from level flight to the − 7-1/2 deg glide path is not included. Particular emphasis is placed on windproofing the lateral director system.

B. OUTLINE OF THE REPORT

The requirements for the flight director systems are presented at the outset. This is primarily concerned with the various manual control aspects that need to be considered. A brief summary of the guidance and control requirements is also given. Sections III and IV present the longitudinal and lateral system development. This includes derivation of the feedbacks, weighting of the feedbacks to meet the requirements, and complementary filtering of the feedbacks to reflect practical implementation. Sections V and VI present the longitudinal and lateral simulation evaluation, respectively. Two pilots participated in the program and provided pilot ratings and comments of the proposed systems as well as various candidate

systems that were derived to research some of the pilot-centered principles that had never been verified. Changes in tracking performance with and without the directors is also discussed.

SECTION II

SYSTEM REQUIREMENTS

Manual or automatic approach control systems are designed to acquire
and track a landing guidance beam. The fundamental requirements are that
this be done in a stable and rapidly responding manner, independent of
both wind and noise disturbances. However, the manual approach situation
has the added requirement that the approach control system be compatible
with the human pilot. These requirements can thus be grouped into those
which are:

- Fundamental to guidance and control

- Pilot centered

These requirements have been elaborated in Ref. 4 for the longitudinal
control of a conventional aircraft and in Ref. 12 for both longitudinal
and lateral control of STOL aircraft. In this section the requirements
of Refs. 4 and 12 have been summarized.

A. GUIDANCE AND CONTROL REQUIREMENTS

In general, guidance and control requirements are independent of the
type of vehicle. For an approach control system, the fundamental require-
ment is path control. Thus, the guidance law must provide for a stable,
well-damped beam acquisition and subsequent beam following in the presence
of wind disturbances and unusual initial conditions. More advanced systems,
especially applicable to STOL aircraft, might also be required to follow
higher order approach paths (e.g., dual angle or curved path). Additional
requirements related to control include attitude regulation and damping,
as well as the more fundamental vehicle requirements (i.e., control power,
authority, etc.).

Meeting the guidance and control requirements in the lateral axis is
most difficult because ailerons alone control the path via roll attitude.
Longitudinally, there are at least two active controls, so lift control can
be independent of attitude control. This allows higher bandwidth beam
following than in CTOL aircraft without compromising attitude regulation.

B. PILOT-CENTERED REQUIREMENTS

The general pilot-centered requirements for STOL aircraft with more than two command bars are presented in the following paragraphs.

1. Minimum Pilot Workload

As a result of human pilot properties, a design requirement is that the effective control element, consisting of the vehicle plus flight director computer, be constructed to:

- Require no low-frequency pilot lead equalization.

- Permit pilot loop closure over a wide range of gains.

- Allow long dwell times on each instrument.

A flight director system meets this requirement when the weightings of the various motion feedbacks in the flight director computer produce an effective controlled element that approximates a pure integration, K/s, over the frequency range that the pilot closes the flight director loop. For this set of controlled element dynamics, the pilot response is approximately a gain plus time delay in the frequency region of control (near crossover).

2. Response Compatibility (Motion Harmony)

Response compatibility relates to the ways in which the various motions of the aircraft interrelate and how they affect the pilot. An example best illustrates this requirement. Assume the pilot controls flight path with a vertical force controller. If the vertical accelerations he generates in his attempts to center the command bar are greater than he would use on a VFR approach, the feedbacks and/or equalization should be changed.

3. Unattended Operation

Accounting for other pilot workload and for periods of unattended operation is accomplished with effective controlled element amplitude ratio and phase characteristics that permit wide variations in pilot gain

while retaining adequate gain and phase margins throughout the mid-frequency region. This implies that conditionally stable systems and feedback of beam integral are undesirable.

4. Command Bar Consistency

In a flight director the cue is different from status information since the command signal is a _mixture_ of control and vehicle motions rather than one real-world cue. However, some correspondence does exist between the command signal and the vehicle or control motions in each of several frequency bands. In each band, the flight director command should be dominated by a particular airplane motion or control quantity. So, even though there is no direct VFR cue which corresponds directly to the flight director command, nonetheless the command signal must have some degree of consistency with the status elements on the display. Typically, this means the high-frequency command bar motions relate to the vehicle attitude information and the low-frequency motions relate to the inertial path deviations.

5. Minimum Scanning Workload

Scanning is reduced by minimizing the number of director commands presented on the display. It is also reduced by integrating the status elements, thus increasing effectiveness of parafoveal viewing; both reduce the scanning remnant. Reducing the high frequency motion components present in the display also will reduce the required scan rate.

6. Non-Interacting Controls

For the case of more than one manipulator for each axis, the directors should be uniquely associated with their respective controllers. Primarily, this means that the feedbacks for each director are selected and weighted so that when the pilot uses a given manipulator he only generates a response on that respective director.

7. Minimum SAS Failure Transients

Due to the heavy stability augmentation necessary on many STOL vehicles, the flight director must provide a graceful degradation of system performance in the event of a SAS failure. This means that the pilot can sufficiently cope with the failure with minimum re-adaptation.

8. Wing Low Crosswind Approach

The forward slip technique is particularly appropriate for STOL approaches because crab angles are relatively larger for a given crosswind component than for a CTOL approach and the bank angle necessary for a STOL in a wing-low approach is less than that for a CTOL. Consequently the director system should be capable of allowing a forward slip or crab type approach without producing path standoff errors.

A summary of the above pilot-centered requirements and corresponding flight director implications is presented in Table 1.

TABLE 1

PILOT-CENTERED REQUIREMENTS

REQUIREMENT	FLIGHT DIRECTOR IMPLICATIONS
Reduced time delay Minimum remnant Best rating	K/s controlled element Proper display gain
Unattended operation	No integral feedbacks, or conditionally stable systems
Motion harmony	Closed-loop control does not induce attitudes and/or accelerations that are incompatible with other flight modes
Minimum scanning workload	Minimize number of director required; maximize effectiveness of parafoveal viewing; lag feedbacks in frequency region beyond crossover to avoid "busy" display.
Wing-low crosswind approach technique	Wash out inner-loop feedbacks
Noninteracting controls	Decouple axes so control of one director does not excite others
Minimum SAS failure transients	Maintain proper SAS-flight director feedback mix
Avoid busy display	Small display lag

SECTION III

LONGITUDINAL FLIGHT DIRECTOR SYSTEM DEVELOPMENT

For STOL vehicles utilizing some form of powered lift the pilot can effectively use an additional longitudinal control for modulating flight path without changing speed or attitude. With two active controllers, i.e., one for attitude and one for some form of powered lift, the longitudinal flight director should provide separate and unique command cues. Also since altitude (or flight path) can be changed with either attitude or direct lift, the design of the directors is not evolved through a clearcut tradeoff in pilot-centered versus guidance and control requirements as it is for the lateral system in Section IV (where only one control is used for three degrees of freedom). From the guidance and control standpoint the longitudinal system has an advantage, since it allows independent control of two of the three degrees of freedome (i.e., attitude, speed, and flight path). However, from the standpoint of determining the weightings of the various motion and position feedbacks best for manual control, it is a disadvantage, since the two director command signals are interactive. In other words, how and what the pilot does in closing one director loop influences the apparent dynamics of the other director command. This places a great deal of emphasis on the pilot's operating instructions — his technique must be such as to "make good" the assumptions on which the director was based.

We will set down the steps of the design process that consider these requirements in the derivation of the longitudinal director guidance laws for a powered lift STOL vehicle. We will also discuss the practical aspects of feedback signal derivation and range compensation which are then included in an overall block diagram defining the system.

A. DESIGN PROCESS

The first step in the design process is to determine the control structure. This is accomplished by pilot/vehicle analyses and by recommendations of test pilots participating in the simulation studies. For example, the control technique evolved for the C-8A jet STOL aircraft (with no longitudinal

SAS) was to control airspeed with attitude, and flight path with hot thrust vectoring. Throttle is assumed held constant once established on the 7.5 deg glide path. This structure dictates the fundamental feedbacks to each director. All other feedbacks with non-zero steady-state values should be washed out to avoid a glide slope standoff. The selection of washout time constants will be dealt with as part of the guidance law derivation.

The next step is to examine manual loop closure estimates used to determine approximate feedback gain ratios and lead requirements. Predicted pilot lead time constants greater than 1 sec should be included in the director guidance law since this would constitute a major source of pilot opinion degradation. However, in order to preserve high-frequency command bar consistency and to avoid a "busy" display, a 1/2 to 3/4 sec lag may also be required in conjunction with the lead equalization. The need for and degree of lag necessary for good pilot opinion is an important issue that is best determined by simulation.

The selection of gain ratios is based on the form of the effective controlled element, command bar consistency, (both pilot-centered requirements) and closed-loop responses (guidance and control requirements). Starting with estimated gains and lead equalization requirements from the manual control analysis, the effective controlled element frequency response for both director is examined. Gain ratios are varied to obtain K/s-like response characteristic over a broad range of frequencies. The "lift" director response is also checke with the column director loop closed. Additional feedbacks may be added to this director signal to increase the high-frequency response.

The final step is to close the director loops and compare closed-loop responses and rms beam errors to various inputs for variations in feedback quantities and/or equalization.

B. GUIDANCE LAWS

In the stick (or column) director, airspeed is controlled via attitude. To avoid standoff errors between attitude and airspeed, the pitch attitude feedback is washed out. This washout should be as rapid as possible in

order to minimize airspeed standoff errors. The use of beam rate, $\dot{d}$, feedback
provides the basis for achieving the faster washout as well as improving the
glide slope tracking performance. The kinematic relationship between pitch
attitude, θ, and beam rate, $\dot{d}$, is useful in defining the minimum attitude
washout time constant. For example, as described in Ref. 4, a good approxi-
mation relating $\dot{d}$ and θ in the low- to mid-frequency region is given by:

$$\frac{\dot{d}}{\theta} = \frac{U_o}{T_{\theta_2}s + 1} \tag{1}$$

Thus, for frequencies below $1/T_{\theta_2}$, beam rate can replace pitch attitude
because $\dot{d}$ and θ are equivalent (in the absence of winds). Consequently, we
can wash out θ with a time constant of at least T_{θ_2}. Note further that the
high-frequency gain ratio $K_{\dot{d}}/K_{\theta}$ desired between $\dot{d}$ and θ is likewise evident
from Eq. 1. That is:

$$K_{\dot{d}}/K_{\theta} = 1/U_o \tag{2}$$

The resulting system has essentially the same dynamic response as attitude
alone but improved glide slope tracking performance.

We must now look at the airspeed to attitude feedback weighting for the
flight director/pilot/vehicle system shown in Fig. 3. The effects of various
airspeed/attitude gain ratios can be seen by examination of the effective
controlled element responses, FD_s/δ_s, shown in Fig. 4. Notice that the
smallest gain ratio, −0.005 rad/ft/sec (as used in the manual closures)
produces a very low dc gain, which means the director bar will always be
wandering. The highest gain ratio, −0.02, has the least K/s-like response
and largest phase dip near 0.4 rad/sec. A reasonable compromise is the
−0.01 value. In all cases pilot lead would be anticipated near $1/T_{sp_2}$ to
extend the region of K/s-like response. This should not produce any degra-
dation in pilot rating for the flight director task. However, since the lead
is in the region of 1 to 1-1/2 rad/sec, it may or may not be included in the
guidance law. This can best be determined by simulation. Had the required
lead been less than 1 rad/sec, it definitely would have been incorporated in
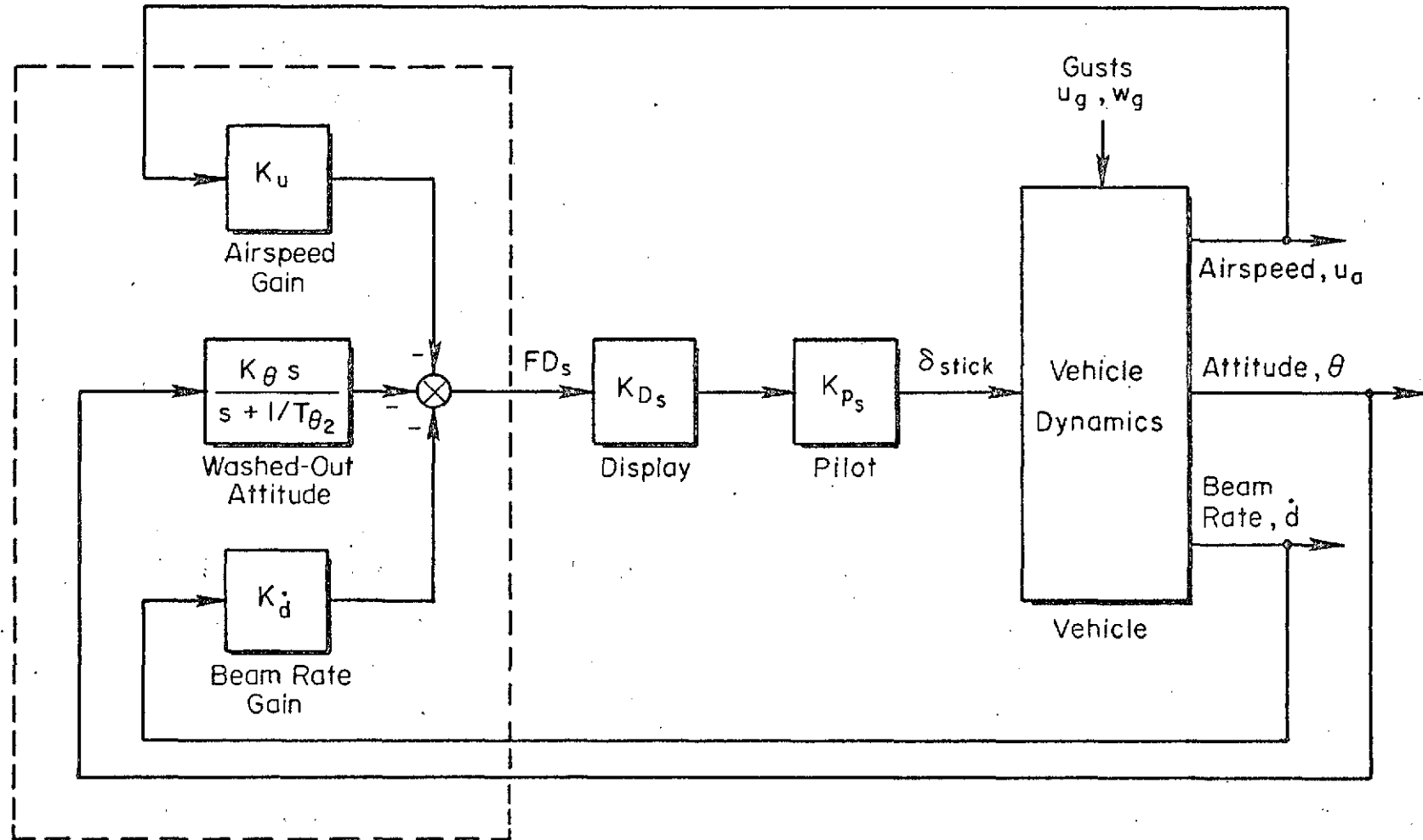
Figure 3. Simplified Pilot/Vehicle/Flight Director System for Stick Loop

$\left|\dfrac{FD_s}{\delta_s}\right|$

40

20

(dB)

0

-20

ω_p

$K_u/K_\theta = -.02$

$= -.01$

$= -.005$

$\dfrac{1}{T_{wo}}$

$\dfrac{1}{T_{sp_1}}$

$\dfrac{1}{T_{sp_2}}$

$\dfrac{K_{\dot{d}}}{K_\theta} = .01$

$\dfrac{1}{T_{wo}} = .35$

$$\frac{FD}{\delta_s} = \frac{K_\theta\left[\dfrac{s}{s+1/T_{wo}}N_{\delta_s}^\theta + \dfrac{K_{\dot{d}}}{K_\theta}N_{\delta_s}^{\dot{d}} + \dfrac{K_u}{K_\theta}N_{\delta_s}^u\right]}{(s+1/T_{sp_1})(s+1/T_{sp_2})\left[\zeta_p\,;\,\omega_p\right]}$$

$\measuredangle\dfrac{FD}{\delta_s}$

0

-100

(deg)

-180°

-200

$-.005$

$-.01$

$-.02$

0.01

0.1

1.0

10.0
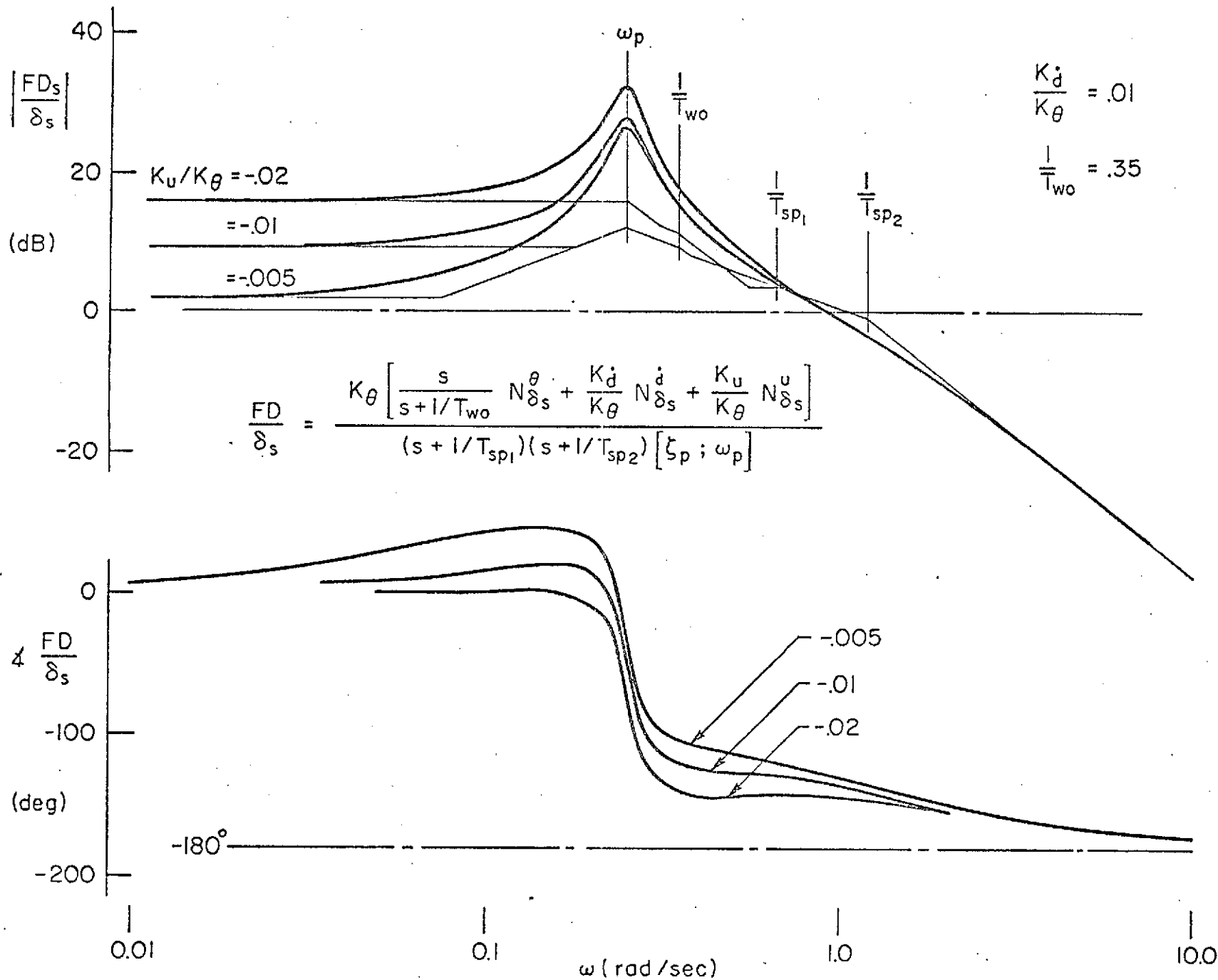
$\omega\,(\text{rad/sec})$

Figure 4. Effective Controlled Element for Stick as Function of Airspeed/Attitude Ratio

the director along with an associated lag at 1-1/2 to 2 rad/sec to maintain high-frequency command bar consistency.

A system survey for the FD_S/δ_S closure is shown in Fig. 5 for the following gain and washout values:

$$K_{\dot{d}}/K_\theta = 0.01 \ \text{rad/ft/sec} \quad (\doteq \ 1/2 \ \text{deg/ft/sec})$$

$$K_u/K_\theta = -0.01 \ \text{rad/ft/sec} \quad (\doteq \ 1 \ \text{deg/kt})$$

$$T_{wo} = 3.0 \ \text{sec}$$

An example pure gain loop closure has been made at 1 rad/sec, since this is the region of anticipated crossover. The resulting closed-loop roots for a pilot/attitude/display gain $(K_{p_S}K_\theta)$ of 1.17 rad-stick/rad-attitude error are indicated by the dark blocks on the root locus and Bode root locus sketches. The closed-loop characteristic equation is:

$$\Delta' = \frac{(0.243)[0.99; \ 0.503][0.45: \ 1.16]}{(0.35)}$$

Normally, lead equalization and pilot time delay effects would be included in this survey, but for purposes of deriving feedback weightings this added complexity will not alter the subsequent conclusions. The lead would increase the phase margin and extend the K/s-like region. The time delay reduces the phase margin and restricts the crossover to less than 2-1/2 to 3 rad/sec. The net effect at 1 rad/sec is negligible.

We can now turn attention to the vectored "thrust" or "nozzle" director and derive the effective controlled element with and without the stick director loop closed. From previous analysis it was apparent that flight path control with nozzle required low-frequency lead equalization $(1/T_L = 0.5)$ in the beam deviation to nozzle loop. Since this is not desirable from a pilot rating standpoint, the director signal should contain beam rate feedback in a ratio given by:

$$K_d/K_{\dot{d}} = 1/T_{LEAD} = 0.5 \ \text{rad/sec}$$

$$\frac{K_{\dot{d}}}{K_\theta} = .01$$

$$\frac{K_u}{K_\theta} = -.01$$

$$\frac{1}{T_{wo}} = .35$$
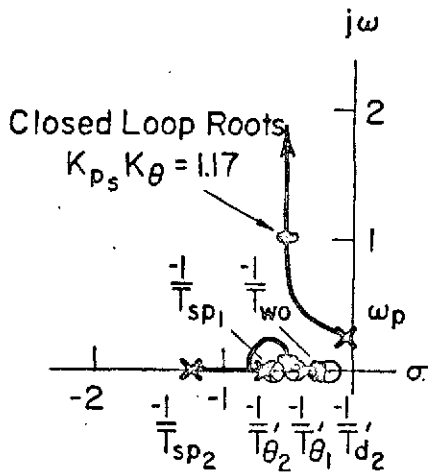
$$\frac{FD_s}{\delta_s} = \frac{1.28\,K_\theta(.163)(.380)(.592)}{(.35)(.66)(1.23)[.095;.25]}$$
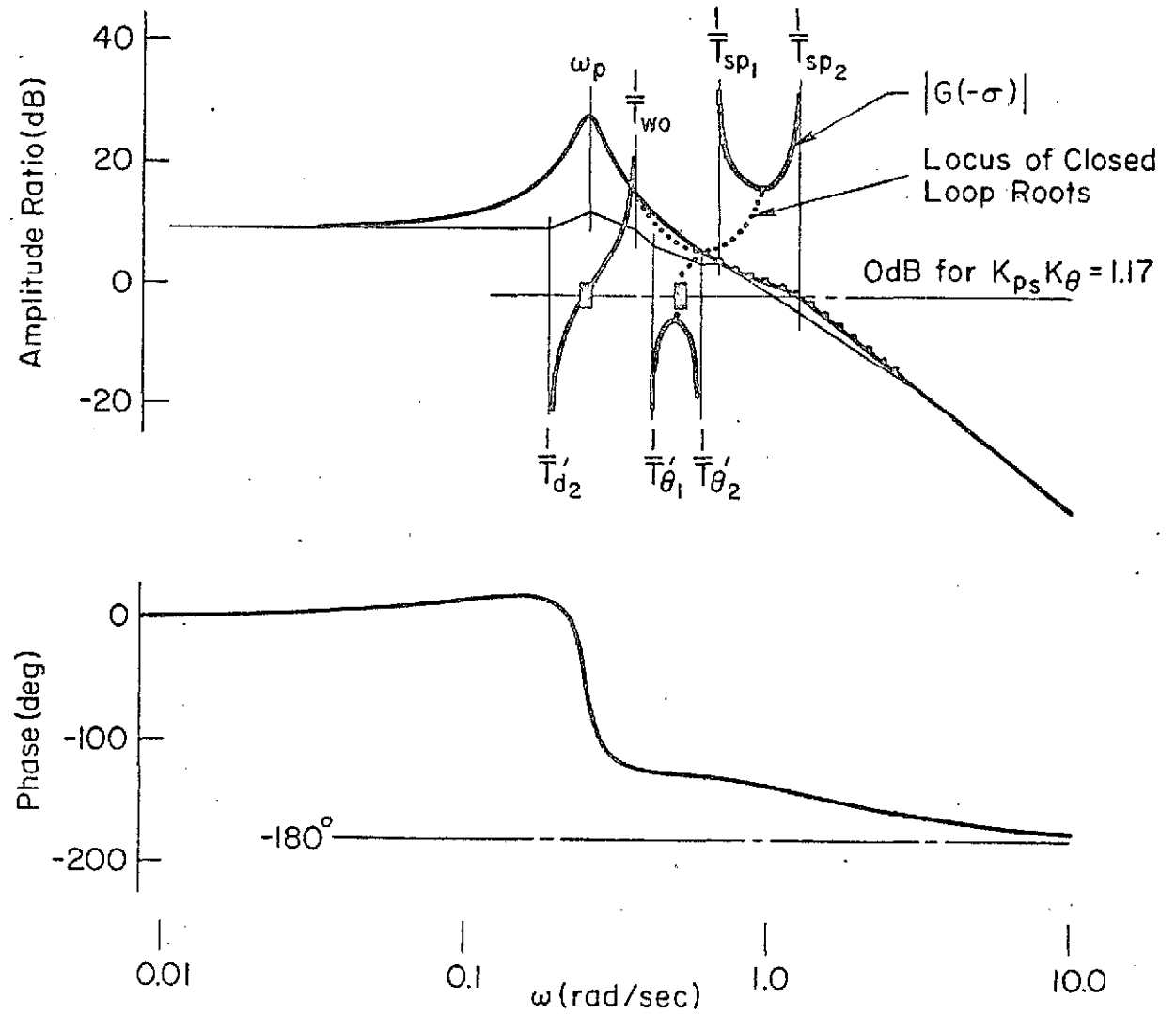
Figure 5. System Survey of Stick Effective Controlled Element for Chosen Gains

One set of Bode-root locus plots in Fig. 6 shows this effective controlled element as a single loop, i.e., without the stick loop closure. The transfer function is:

$$\frac{FD_N}{\delta_N} = \frac{K_{\dot{d}}(s + K_d/K_{\dot{d}})N_{\delta_N}^{\dot{d}}}{\underbrace{s(s + 1/T_{sp_1})(s + 1/T_{sp_2})[\zeta_p;\ \omega_p]}_{\Delta}}$$

The other set of Bode root loci show the nozzle director effective controlled element as seen by the pilot when the stick director loop is closed as an inner loop, i.e.,

$$\frac{FD_N}{\delta_N}\bigg]_{FD_s \to \delta_s} = \frac{K_{\dot{d}}(s + K_d/K_{\dot{d}})\left\{N_{\delta_N}^{\dot{d}} + Y_{p_s}K_\theta\left[\dfrac{sN_{\delta_s\delta_N}^{\theta\ \dot{d}}}{s + 1/T_{wo}} + \dfrac{K_u}{K_\theta}N_{\delta_s\delta_N}^{u\ \dot{d}}\right]\right\}}{s\ (s + 1/T'_{wo})[\zeta'_p;\ \omega'_p][\zeta'_{sp};\ \omega'_{sp}]} \qquad (4)$$

where the prime indicates the inner flight director loop has been closed. Note the long region of K/s-like amplitude response for the closed-loop case. For the single-loop case, the attenuation at high frequency will make the director bug appear quite sluggish, and it will not reflect any mid- or high-frequency motions.

The apparent lack of director response to rapid control inputs violates the requirement for command bar consistency. Although it is not apparent what the director should be consistent with, the director should give a positive indication when the pilot moves the nozzle lever. For most aircraft this can be accomplished with a vertical acceleration or control position feedback. One problem with acceleration feedback is that it will reflect gust inputs and can be changed by other control inputs. Control position feedback is much more direct and less contaminated. However, this too has several drawbacks that must be accounted for. These include:

- High gains will make the display too sensitive to control movements, thus causing other essential feedbacks to be obscured.

$$\frac{FD_N}{\delta_N}\bigg]_{SL} = \frac{6.5K_d'(.5)(.081)}{(0)(.66)(1.23)[.095;.25]}$$

$$\frac{FD_N}{\delta_N}\bigg]_{ML} = \frac{6.5K_d'(.5)(.192)(1.20)}{(0)(.243)[.99;.503][.45;1.16]}$$
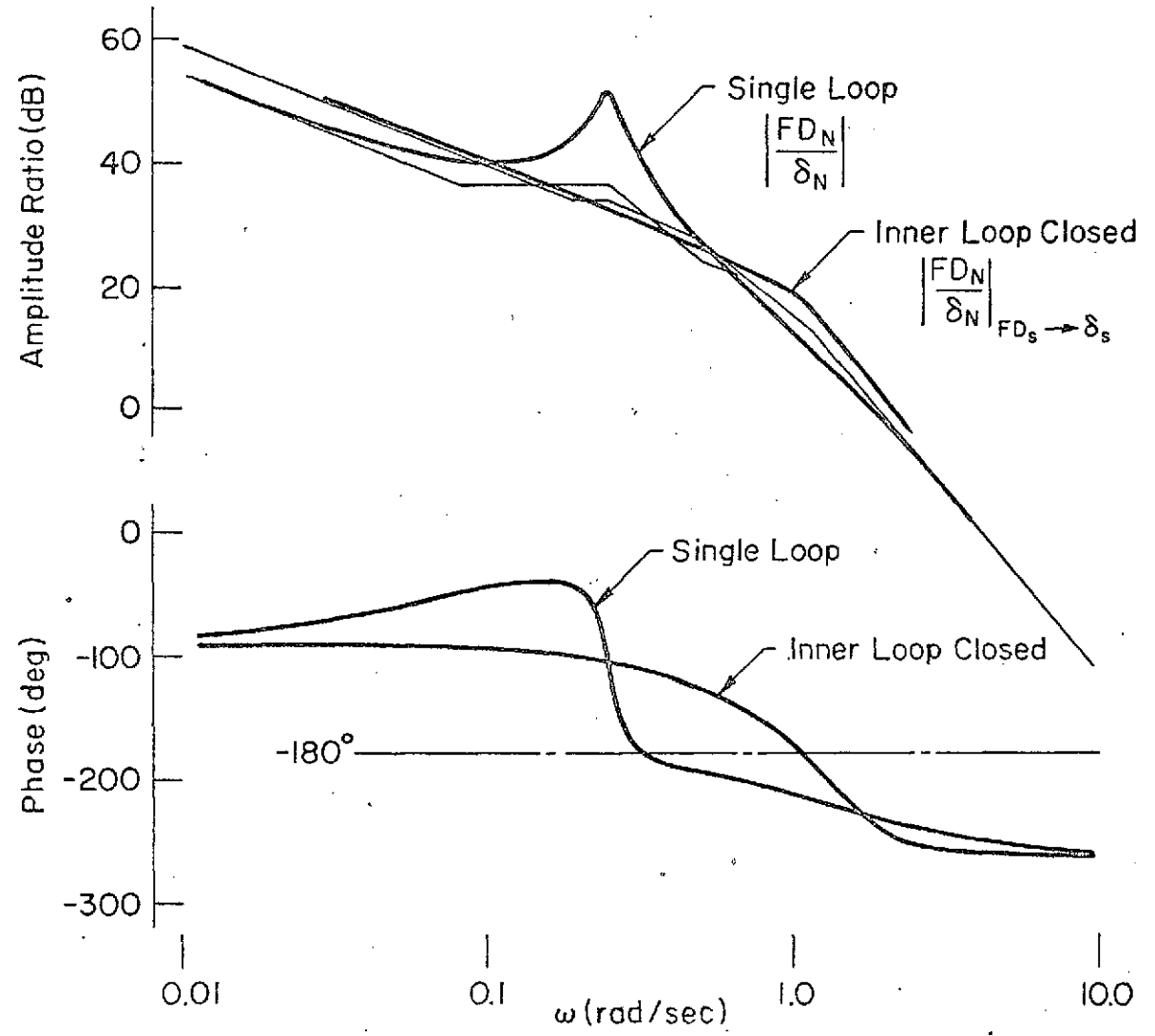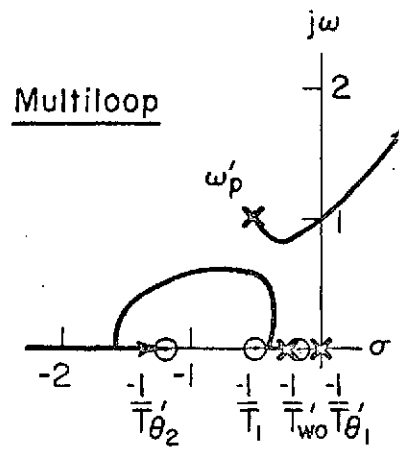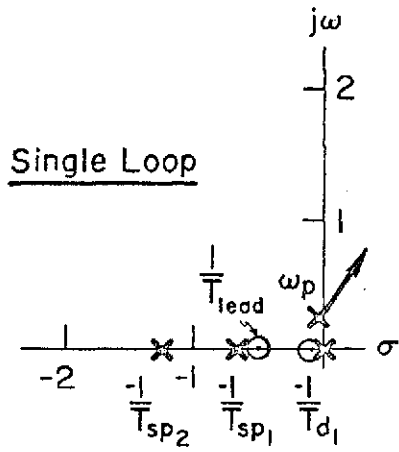
Figure 6. Nozzle Effective Controlled Element with and without Stick Director Loop Closed

- Undesirable feedback of pilot remnant may result. This problem is eliminated with lag filtering of the control position signal.

- Aircraft trim changes will result in director standoff errors. This is avoided by washing out the feedback signal at low frequencies.

The effective controlled element transfer function for the single-loop nozzle director shown in Fig. 7 is given by:

$$\frac{FD_N}{\delta_N} = \overbrace{\frac{K_{\dot{d}}(s + K_d/K_{\dot{d}})N_{\delta_N}^{\dot{d}}}{s\Delta}}^{G_{d_N}} + \overbrace{\frac{(K_{\delta_N}/T_L)s}{(s + 1/T_{WO})(s + 1/T_L)}}^{G_{\delta_N}} \qquad (5)$$

Control position feedback is equalized with a washout, $1/T_{WO}$, and lag, $1/T_L$. Notice that at high frequency $FD_N/\delta_N = K_{\delta_N}/(T_L s + 1)$. For the multiloop situation the control position feedback times the washout and lag equalization is just added to the closed-loop FD/δ_N transfer function of Eq. 4. This can be written as:

$$\frac{FD_N}{\delta_N} = \left. \frac{FD_N}{\delta_N} \right]_{FD_S \rightarrow \delta_S} + \frac{K_{\delta_N}s}{(s + 1/T_{WO})(T_L s + 1)} \qquad (6)$$
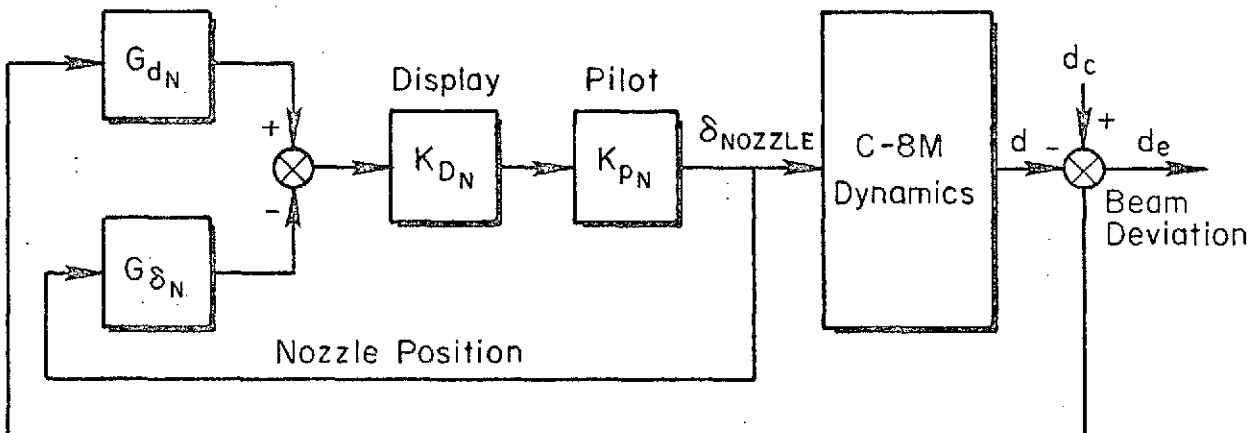
Figure 7. Pilot/Vehicle/Flight Director System
for Nozzle Loop

Since the control position washout is only required for low frequency ($1/T_{WO} < 0.1$ rad/sec) compatibility, it can be neglected in the subsequent analysis of the effective controlled element.

An appropriate gain ratio, $K_{\delta_N}/K_{\dot{d}}$, can be found by computing the FD_N/δ_N transfer function for various values of $K_{\delta_N}/K_{\dot{d}}$. The numerical equation, assuming a control position lag of 1 sec is given below:

$$\frac{FD_N}{\delta_N} = \frac{K_{\dot{d}}\left\{\dfrac{6.5(0.5)(0.192)(1.2)}{(0)(0.35)} + \dfrac{K_{\delta_N}}{K_{\dot{d}}}\dfrac{(0.243)[0.99;\ 0.503][0.45;\ 1.16]}{(1)(0.35)}\right\}}{\dfrac{(0.243)[0.99;\ 0.503][0.45;\ 1.16]}{(0.35)}} \tag{7}$$

Figure 8 shows the change in the high-frequency portions of the nozzle director effective controlled element as the gain ratio $K_{\delta_N}/K_{\dot{d}}$ is increased from zero to 0.5 ft/sec/deg. This latter gain was selected to give a K/s-like response at low as well as high frequencies.

The last step in the analysis was to check the d/d_C responses and rms values of d/w_g for representative input spectrums. Figures 9a-9c show representative d/d_C responses throughout the stages of director development. For purposes of comparison, both cases without nozzle position feedback have the stick director loop closed at 1 rad/sec and the nozzle director loop closed at 0.4 rad/sec, both assuming a pure gain pilot. In the last case, the nozzle loop was closed at 1 rad/sec due to the high-frequency K/s-like response. The first response in Fig. 9 represents u + θ feedbacks to the stick director and d + $\dot{d}$ to the nozzle director. The attitude washout was 10 sec in order to provide path damping. The bandwidth (3 dB down point) is about 0.7 rad/sec. When beam rate is utilized in the column director and the attitude washout reduced to 3 sec, the bandwidth of the response (Fig. 9b) is increased to 1.1 rad/sec. In the last figure, it can be seen that the lagged nozzle position feedback does not alter the high-frequency break, although it does produce a mid-frequency droop in the response.

A comparison of rms beam error to vertical gust inputs is given in Table 2 for these three systems. The u + θ system with an attitude washout of 10 sec has 30% more error than the u + θ + $\dot{d}$ system when the attitude

Without Nozzle Feedback

$$\frac{FD}{\delta_N} = \frac{6.5K_{\dot{d}}(.5)(.192)(1.20)}{(0)(.243)[.99;.503][45;1.16]}$$

With Nozzle Feedback $K_{\delta_N}/K_{\dot{d}} = 28.7\frac{ft/sec}{rad} = 0.5\frac{ft/sec}{deg}$

$$\frac{FD}{\delta_N} = \frac{28.7K_{\dot{d}}(.165)(.473)[.87;.51][.33;1.14]}{(0)(1.0)(.243)[.99;.503][45;1.16]}$$

$\frac{1}{T_{LAG}}$

$\frac{K_{\delta_N}}{K_{\dot{d}}} = 28.7$

$\frac{K_{\delta_N}}{K_{\dot{d}}} = 0$

$\frac{K_{\delta_N}}{K_{\dot{d}}} = 28.7$

-180°

$\frac{K_{\delta_N}}{K_{\dot{d}}} = 0$

ω(rad/sec)
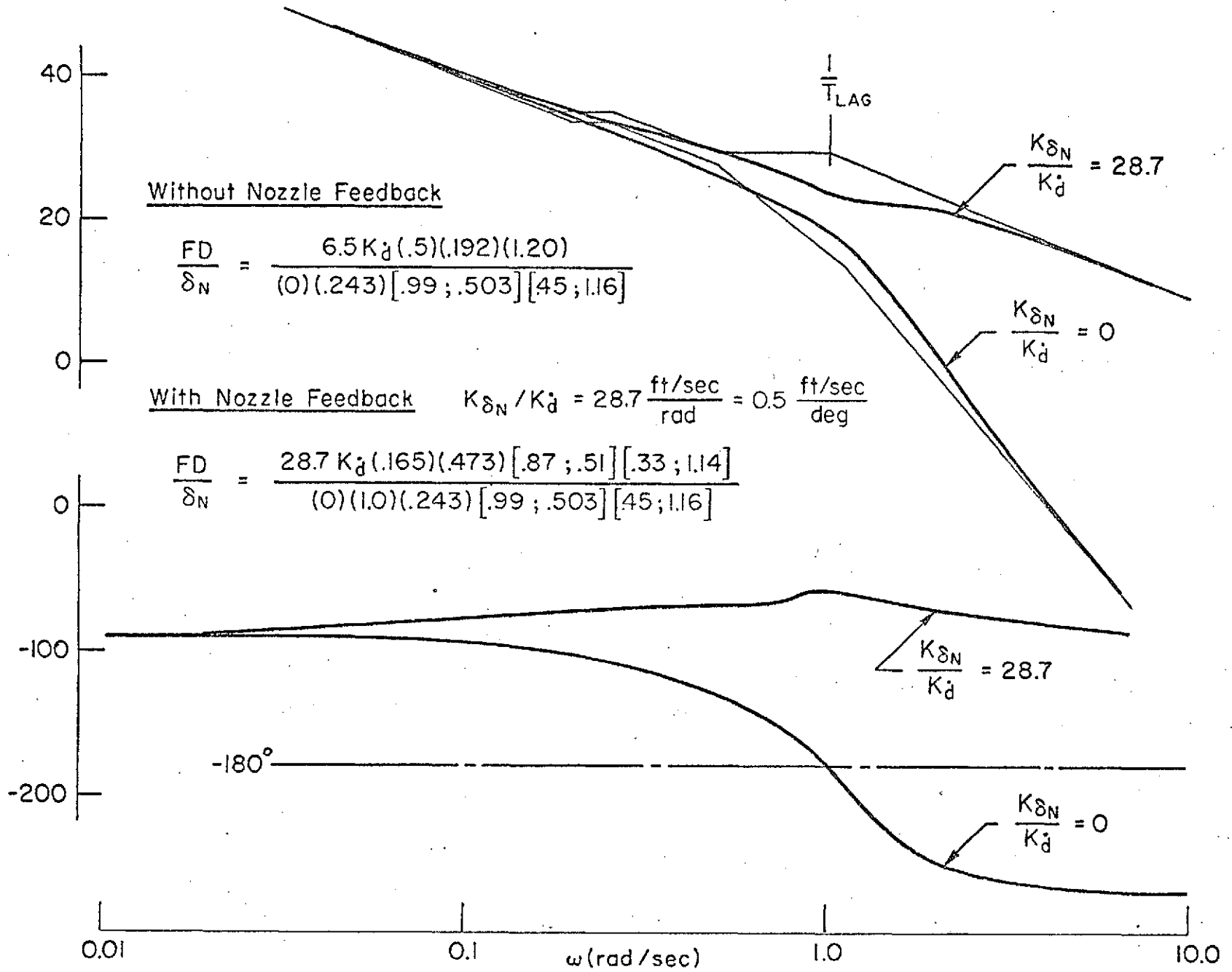
Figure 8. Effect of Nozzle Position Feedback on Nozzle Effective Controlled Element

$$\frac{d}{d_c} = \frac{.189(.5)(.059)(1.23)}{(.052)(.277)[.29;.55][.56;1.26]}$$

(a)

$$\frac{d}{d_c} = \frac{.93(.275)[.67;.36]}{(.181)(.51)[.59;.58][.46;.99]}$$

(b)

$$\frac{d}{d_c} = \frac{1.08(.322)(2.48)[.52;.336]}{(.158)(.503)(2.92)[.87;40][.40;1.11]}$$

(c)

Figure 9. Comparison of d/d_c Responses
at Various Design Stages

TABLE 2

RMS BEAM DEVIATIONS TO VERTICAL GUSTS
FOR THREE LONGITUDINAL DIRECTOR DESIGNS

System Gust Input	$u + \theta \rightarrow \delta_S$ $d + \dot{d} \rightarrow \delta_N$ $1/T_{wo_\theta} = 0.1$	$u + \theta + \dot{d} \rightarrow \delta_S$ $d + \dot{d} \rightarrow \delta_N$ $1/T_{wo_\theta} = 0.35$	$u + \theta + \dot{d} \rightarrow \delta_S$ $d + \dot{d} + \delta_N \rightarrow \delta_N$ $1/T_{wo_\theta} = 0.35$
$w_g/(s + 1)$	2.3 ft/(ft/sec)	1.7	2.8
$w_g/(s + 0.5)$	3.0	2.3	3.9

washout is 3 sec. However, the use of nozzle position feedback more than negates this improvement. Whether this drawback outweighs the improvement gained by producing a more desirable controlled element response is another tradeoff best determined by simulation.

C. PRACTICAL ASPECTS

The derivation of the director guidance laws have, up to this point, not been concerned with signal sensing or operational effects such as varying range and signal limiting. The most pressing problem is the derivation of beam rate, $\dot{d}$, which has been difficult to obtain in the past without incurring excessive noise penalties. Range compensation and command limiting are simpler problems.

We will first deal with the generation of beam rate using the technique of complementary filtering. In brief, complementary filtering mixes similar information from several sources in such a way as to derive the pure signal plus heavily filtered noise. We will assume the radio guidance signal as given at the receiver output, wherein smoothing, damping and extrapolation of the received data has been carried out. The important fact to note here is that the equivalent continuous transfer function for this processing has a bandwidth which greatly exceeds the bandwidth required for the complementary filtering scheme described below. Therefore, its effect can be neglected.

A mechanization for deriving beam rate which uses barometric measurements to wash out the steady-state rate of descent and accelerometer bias is given in Fig. 10. The lower washout compensation block could also be mechanized in the alternate form given below:

$$\frac{s(s + \omega_1 + \omega_2)}{(s + \omega_1)(s + \omega_2)} = 1 - \frac{(\omega_1\omega_2)/(\omega_2 - \omega_1)}{s + \omega_1} \quad \frac{(\omega_1\omega_2)/(\omega_2 - \omega_1)}{s + \omega_2}$$

The choice of the filter break frequencies, ω_1, ω_2, and ω_3, are based on the following:

- ⊛ ω_1 cuts off the pseudo-differentiation of beam error; therefore, it may not be overly large. A range 0.3 to 1.0 is a likely possibility. The actual value is determined on two bases: 1) "best" total signal reconstruction in, say, rms sense; and 2) effective bandwidth of noise, as opposed to signal, from standpoint of regression phenomenon.
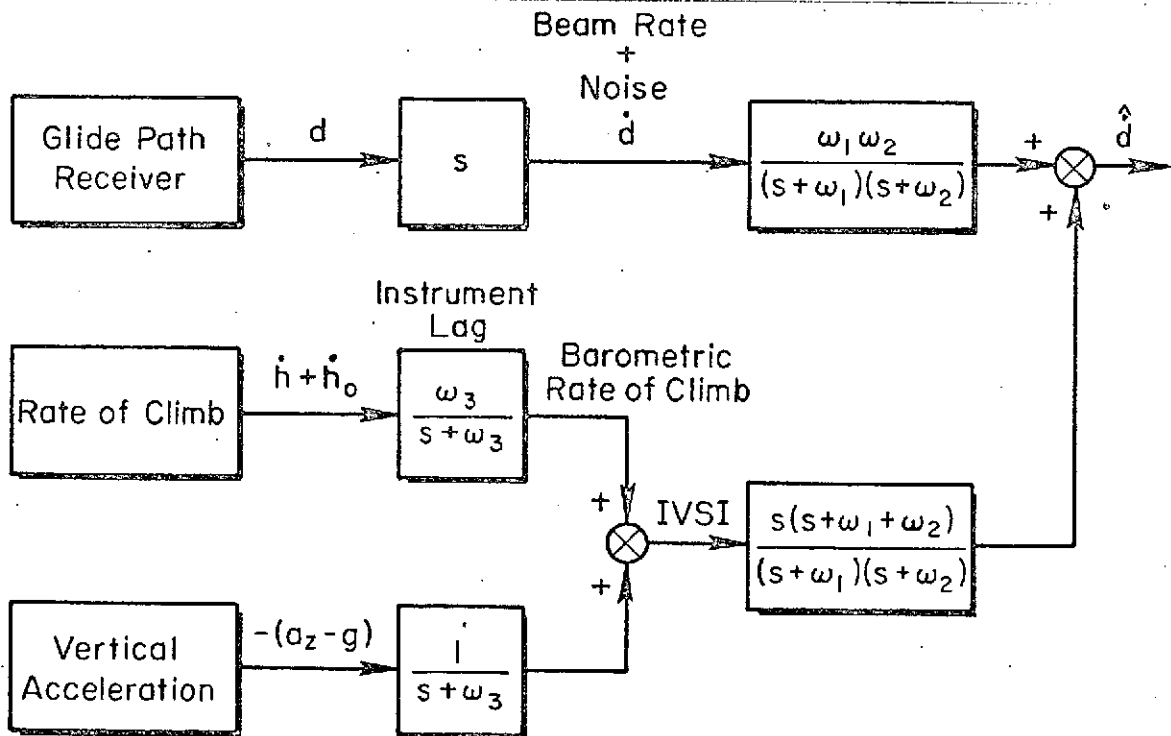
Figure 10. Mechanization of Beam Rate Signal

- ω_2 cuts off the noise on the pseudo-differentiated beam error. A good range of values is between 1.0 ω_1 and 3.0 ω_1.

- ω_3 must be chosen to approximate the barometric vertical speed lag as closely as possible. If instantaneous vertical speed (IVSI) is used, ω_3 should be zero.

Due to the use of beam rate feedback in the stick director command, it will be necessary to range compensate the received output. This can be appreciated by inspecting the Bode and root locus plots in Fig. 11. In this figure we have assumed a nominal range of 10,000 ft (approximately where beam capture would occur when flying at 1500 ft altitude). As the range decreases, the beam deviation gain effectively increases, which moves the low-frequency zero, $1/T_{d_1}'$, into the right half plane. In essence, the effective controlled element appears more and more like the beam rate feedback only. This will result in a maximum pilot gain restriction, since a closure drives $1/T_{sp_1}$ toward this zero.

More important are the display gain effects. Since the beam rate feedback was scaled to match the attitude feedback gain, the decreasing range will effectively increase the display gain and make it inconsistent with the attitude status information. This, when coupled with a display limiter will surely result in an unstable Pilot Induced Oscillation (PIO).

The nozzle director would also have an increasing display gain. However, if beam deviation and beam rate are the only feedbacks the dynamic response of the effective controlled element would be unchanged by range variations. From the standpoint of keeping the pilot/display gain constant throughout the approach, it would be desirable to provide range compensation. This can be done directly using DME range or can utilize a more conventional mechanization using a timer or radar altimeter.

The last point bearing mention regards signal limiting. Again, the two axis director system has no requirement, since beam deviation does not generate an attitude command as in CTOL systems. Limiters would only be required on the displayed signal to keep the bars within reasonable bounds. A limiter on the airspeed feedback may, however, be desirable in case the system were to be engaged at a speed much different from the reference.

An overall block diagram of the preliminary system including all gains, time constants, complementary filters, and limiters is presented in Fig. 12.

Range
10,000 ft

$$\frac{FD}{\delta_s} = \frac{1.28 K_\theta (.163)(.38)(.60)}{(.35)(.66)(1.23)[.095;.25]}$$

Range
1000 ft

$$\frac{FD_s}{\delta_s} = \frac{1.28 K_\theta (-.055)(.351)(4.72)}{(.35)(.66)(1.23)[.005;.25]}$$
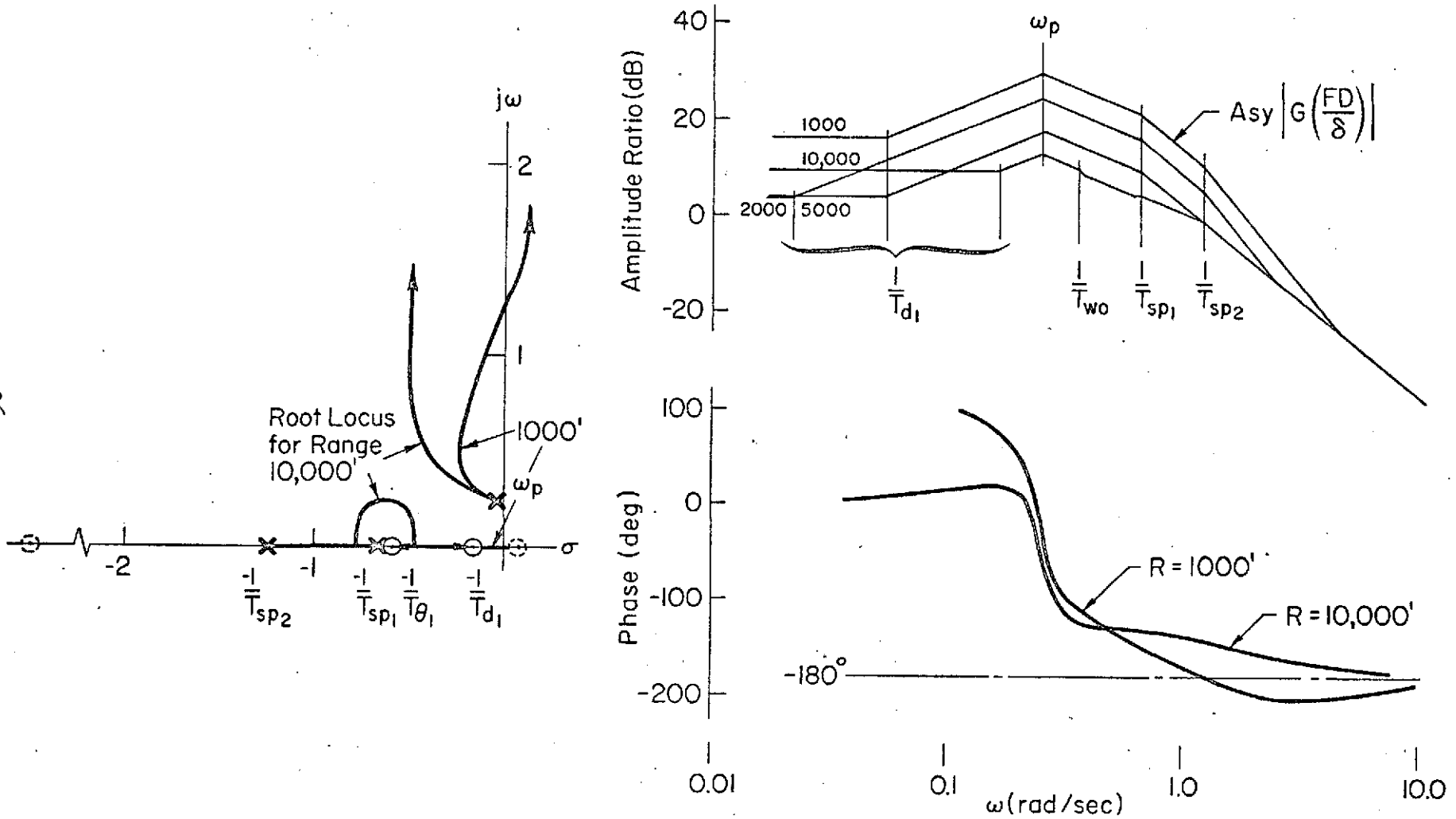
Figure 11. Effect of Decreasing Range on Stick Director Effective Controlled Element
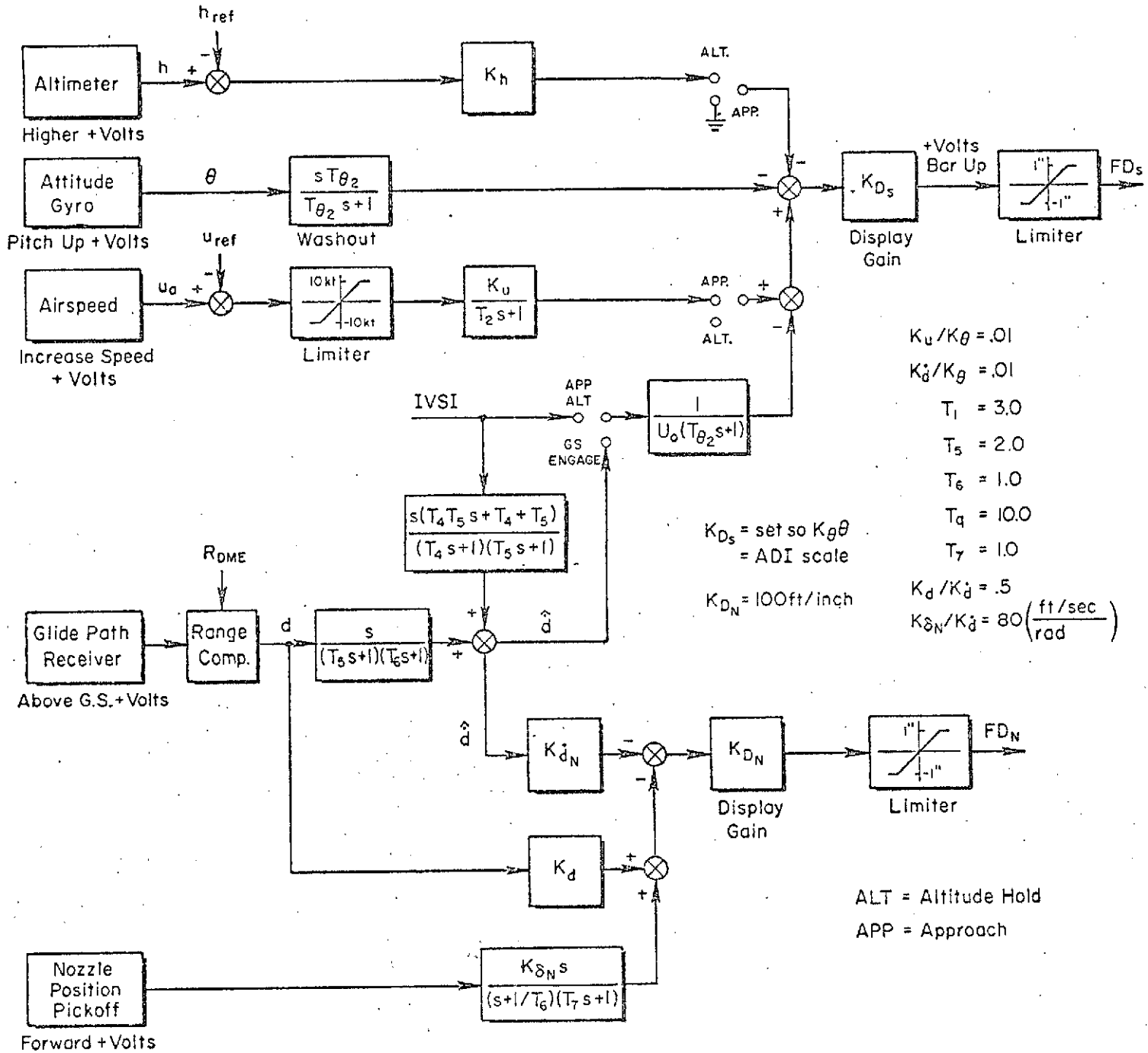
Figure 12.   Preliminary Longitudinal Flight Director Block Diagram

SECTION IV

LATERAL FLIGHT DIRECTOR SYSTEM DEVELOPMENT

The lateral flight director system provides the pilot with a single cue upon which to base his control actions. By following this command signal, the vehicle will be directed onto the approach path in accord with the guidance and control requirements. In addition to the guidance requirements the "effective controlled element," i.e., the vehicle plus flight director dynamics defined by the transfer function FD/δ, must also reflect the pilot-centered requirements discussed in Section II.

An analysis and design of a lateral director system that meets the above requirements is given in this section. This includes the practical mechanization details of feedback signal derivation, command limiting, and range compensation.

A. SIMPLIFIED SYSTEM ANALYSIS

The steady-state path errors to wind and beam command inputs were derived using a low-frequency (i.e., path mode) analysis of the lateral system. This was done as a function of the various conventional feedback quantities and equalization shown in Fig. 13, i.e., φ, ψ, λ, y, to derive the most effective system. More complex forms of equalization, such as rapid reset integrators, and feedforwards of direct wind inputs or beam commands, were beyond the scope of this part of this phase of the program. Hence, the results and conclusions drawn from the analysis may not be optimum, although they will be better than for conventional systems.

The simplified analysis assumes the flight director signal represents an attitude command which the pilot closes tightly (i.e., $\varphi/FD \doteq 1/G_\varphi$). The resulting block diagram of the pilot/vehicle/flight-director system is shown in Fig. 14.
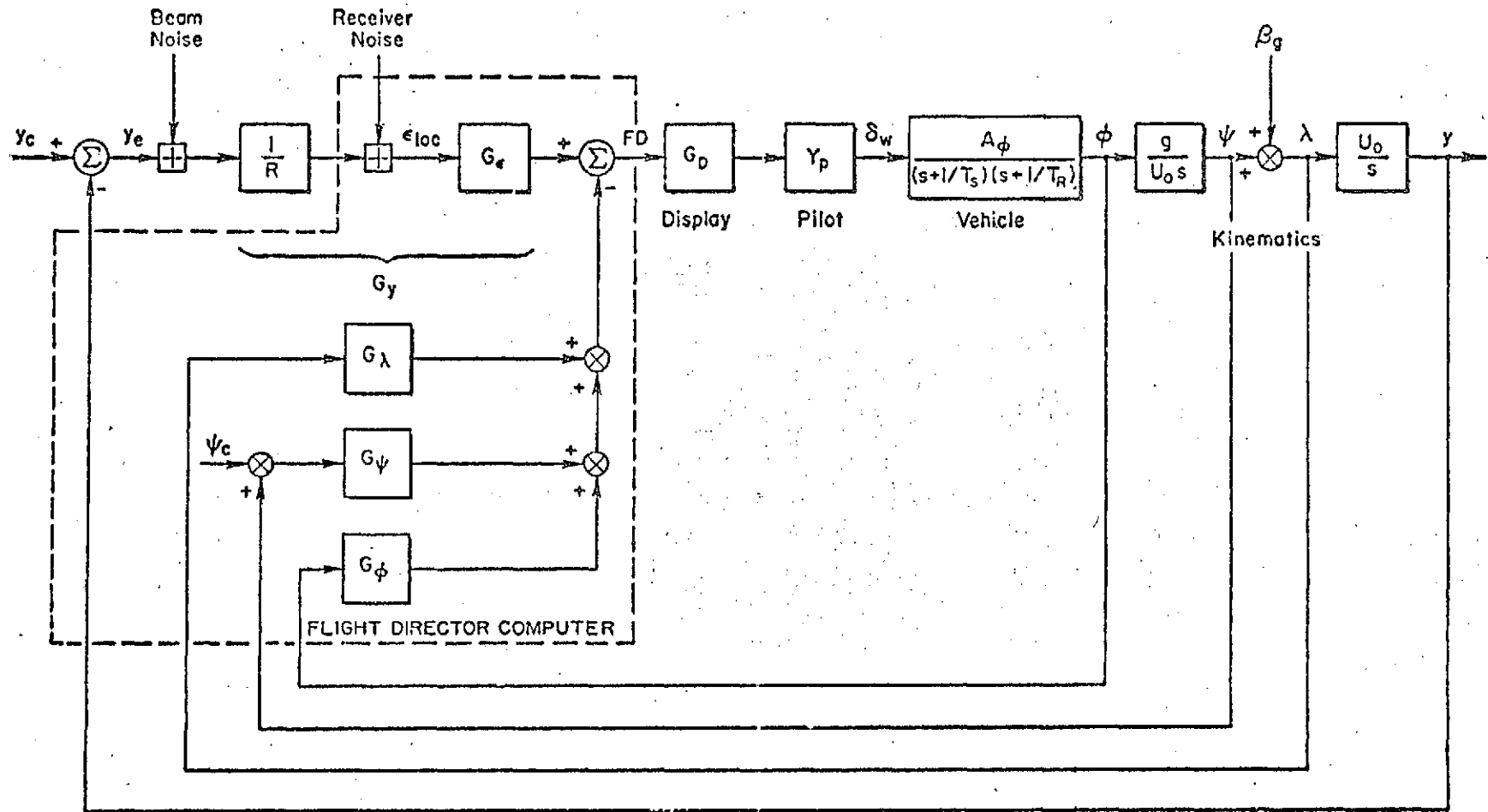
Figure 13. Simplified Lateral Axis Flight Director System
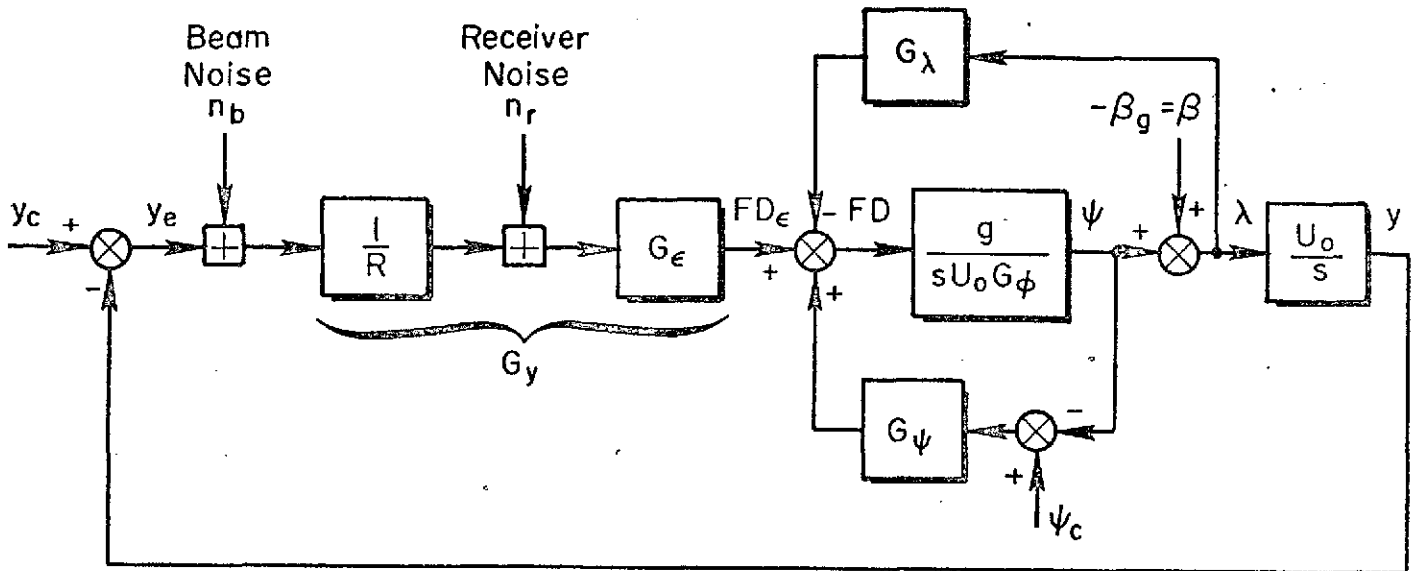
Figure 14. Simplified Lateral Block Diagram (Tight Roll
Loop Closed by Pilot and/or SAS)

If the range variation is removed (or ignored as when fixed-gain conditions are assumed), $G_y \equiv G_\epsilon/R$ and the equations for Fig. 14 are constant coefficient and can be Laplace transformed to give:

$$\left[\frac{G_\varphi}{g} s^2 + \frac{(G_\psi + G_\lambda)s}{U_o} + G_y\right]y = G_y(y_c + n_b + Rn_r) + G_\psi(\psi_c + \beta_g) + \frac{U_o}{g} G_\varphi s\beta_g \quad (8)$$

To determine the steady-state localizer error, y_e, to a lateral gust disturbance (v_g) or a beam command (y_c), Eq. 8 was solved for $(y-y_c)/v_g$ and $(y-y_c)/y_c$ as shown below:

$$\frac{y_e}{v_g} = \frac{s + \dfrac{G_\psi}{G_\varphi}\dfrac{g}{U_o}}{s^2 + \dfrac{(G_\psi + G_\lambda)}{G_\varphi}\dfrac{g}{U_o}s + \dfrac{G_y}{G_\varphi}g} \quad (9)$$

$$\frac{y_e}{y_c} = \frac{s\left(s + \dfrac{(G_\psi + G_\lambda)}{G_\varphi}\dfrac{g}{U_o}\right)}{s^2 + \dfrac{(G_\psi + G_\lambda)}{G_\varphi}\dfrac{g}{U_o}s + \dfrac{G_y}{G_\varphi}g} \quad (10)$$

Each of the feedback transfer function blocks (G's) may assume three possible forms. The first has a free s in the denominator, such as $G_y = K_y + (K_{\bar{y}})/s = (K_y s + K_{\bar{y}})/s$; the second has a free s in the numerator (e.g., $G_y = sK_{\dot{y}}$); and the last represents just a pure gain feedback. It can be assumed that G_φ and G_ψ would not contain a denominator free s (integral equalization) since this could force a localizer standoff. Therefore, the practical guidance and control possibilities for all three flight director feedbacks are constant or washed out roll angle, constant or washed out heading, and beam error or beam error plus integrated beam error. Thus,

$$G_\varphi = k_\varphi \quad \text{or} \quad sk_\varphi$$

$$G_\psi = k_\psi \quad \text{or} \quad sk_\psi$$

$$G_y = k_y \quad \text{or} \quad k_{\bar{y}}/s$$

However, the heading feedback function (path damping) may be replaced by lateral flight path angle or, with the introduction of microwave landing systems, by direct beam differentiation. In this case the possible feedbacks are:

$$G_\varphi = k_\varphi \quad \text{or} \quad sk_\varphi$$

$$G_\psi = 0$$

$$G_y = k_y + k_{\bar{y}}/s \quad \text{or} \quad k_y + k_{\dot{y}}s$$

Table 3 shows the magnitude of the steady-state beam error to three orders of beam command, i.e., step, ramp, and parabola, and two wind inputs, i.e., constant crosswind and crosswind shear, as a function of various combinations of feedback equalization. For example, Line 3 shows that straight gain feedbacks of bank angle, heading, and localizer deviation would produce no error to a step beam command (such as would appear for engagement), a constant error to a steady crosswind or ramp change in beam angle, and an ever-increasing error to a crosswind shear or curved path command. By washing out the heading feedback (Line 2) there is no steady-state error to a steady

TABLE 3

STEADY-STATE CONSIDERATIONS FOR
LATERAL FEEDBACK SELECTION
(Assumes $1/T_s \equiv 0$)

CONFIG. NO.	FEEDBACKS			STEADY-STATE ERROR		
	G_φ	G_ψ	G_y	TO STEP BEAM	TO STEP v_g OR DUAL ANGLE BEAM	TO v_g SHEAR OR CURVED PATH
				Path damping with heading		
1	k_φ *	sk_ψ	$k_y + k_{\overline{y}}/s$	O	O	O
2	k_φ	sk_ψ	k_y	O	O	OFFSET
3	k_φ	k_ψ	k_y	O	OFFSET	∞
4	k_φ	k_ψ	$k_y + k_{\overline{y}}/s$	O	O	OFFSET
	G_φ	G_λ	G_y	Path damping with beam rate or λ		
5	sk_φ	O	$k_y + k_{\dot{y}}s$	O	O	O
6	sk_φ	k_λ	k_y	O	OFFSET-y_c / O-v_g	∞-y_c / O-v_g
7	sk_φ	sk_λ	k_y	O	O	OFFSET-y_c / O-v_g
8	k_φ	O	$k_y + k_{\dot{y}}s$	O	O	OFFSET
9	k_φ	O	$k_y + k_{\dot{y}}s + (k_{\overline{y}})/s$	O	O	O

NOTE: sk_φ, sk_ψ, sk_λ represent washout equalization

$k_{\dot{y}}s$ represents beam rate

$k_{\overline{y}}/s$ represents beam integral

No s represents a finite, non-zero gain at DC

*With heading feedbacks (Lines 1-4) the form of k_φ does not change the steady state error results

crosswind or ramp change in beam angle. This equalization is typically found in CTOL approach control systems.

Since wind shear and curved path approaches are much more pertinent to STOL aircraft, the more important conclusions to be drawn from Table 4 are as follows:

1. A parallel integrator $(k_{\overline{y}}/s)$ on beam deviation is the only way to get curved path or wind shear compensation when heading feedback is used (e.g., Line 1).

2. Lateral flight path angle does not require a washout (free s) for counteracting wind inputs (e.g., compare Lines 6 vs. 2).

3. Without beam integral, beam rate $(k_{\dot{y}}s)$, along with washed out attitude (Line 5) is the only set that has zero path error to curved paths and wind shears.

4. With beam integral it is not necessary to wash out attitude in order to assure zero error to curved paths and wind shears.

Although beam integral or beam rate plus washed-out attitude appear most desirable, the pilot-centered requirements and practical aspects must also be considered. First, beam integral feedback does not meet the pilot-centered requirement for unattended operation. That is, if the pilot does not continually respond to the director commands, a small localizer deviation will be integrated up to appear as a large director command. If the pilot then centers the bar, the aircraft is driven off the localizer to a point where the integrator output is cancelled by the localizer error. The aircraft will then return to the beam with a time constant near that of the integral term. Second, pure beam rate feedback over a wide frequency region is not a realizable signal even for scanning beam landing systems. We can, however, realize a good beam rate feedback at low frequencies, and then, via complementary filtering, simulate the high-frequency portion with lateral flight path angle. This gives good gustproofing but leaves the steady-state localizer errors dictated by Lines 6 or 7 in Table 3. In this table, both forms of k_λ produce zero steady-state error for wind shear inputs but Line 7 (washed-out λ) results in smaller steady-state error to following a curved path input. The difference in performance may be more academic than real for an approach of finite time duration, so the final choice should be based on simulation. In

either case, the desired feedback quantities are bank angle, lateral flight path angle, and localizer deviation.

The weighting of the selected feedbacks is based on both the performance (guidance and control) and additional pilot-centered requirements. This is done by a tradeoff in path-following response with effective controlled element response. A simplified approach for preliminary investigation is accomplished by deriving approximate transfer functions for y/y_c and FD/δ_W using Fig. 14. This results in the following transfer functions which indicate the compromise which must be struck between high beam-following bandwidth and a wide range of potential crossover frequencies (and hence pilot gain) for the manual closure.

$$\frac{y}{y_c} \doteq \frac{gG_y}{G_\varphi s^2 + \dfrac{G_\lambda g}{U_o} s + gG_y} \tag{11}$$

$$\frac{FD}{\delta_W} = \frac{-A_\varphi [G_\varphi s^2 + \dfrac{G_\lambda g}{U_o} s + gG_y]}{s^2(s + 1/T_S)(s + 1/T_R)} \frac{\text{units FD}}{\text{rad } \delta_W} \tag{12}$$

As expected, the systems characteristic equation in Eq. 11 is the same as the numerator of the effective single loop being closed by the pilot. Therefore, increasing the bandwidth of the y/y_c response, i.e., increasing frequency of y/y_c roots, decreases the stability of the FD/δ_W response. The crux of the design problem is thus to achieve the maximum y/y_c bandwidth while, at the same time, providing the pilot with an acceptable controlled element (in the region of anticipated crossover frequency) as the flight·director signal.

All forms for the frequency response of the effective controlled element have a K/s^2 slope at low and at high frequency due to the fundamental feedbacks of lateral position and roll attitude, respectively. The feedback weighting determines the response in between these initial and final slopes. With the conventional feedbacks of localizer deviation, lateral flight path

angle (or heading), and roll attitude, the response may be made to have a
K/s-like region, as illustrated by Fig. 15. However, the path mode response,
and hence the beam acquisition inverse time constant, will be slow due to the
low-frequency roots of $s^2 + (gG_\lambda/U_oG_\varphi) + (gG_y/G_\varphi)$.

For rapid and well-damped localizer intercept, a path mode frequency
of 0.2 rad/sec and a damping ratio of 0.707 were selected. At a 60 kt
approach speed this selection resulted in the following gain ratios:

$$\omega_n^2 = gG_y/G_\varphi = 0.04$$

$$2\zeta\omega_n = gG_\lambda/U_oG_\varphi = 0.282$$

To select a specific gain for each feedback signal the consistency of the
flight director to attitude and localizer status displays must be considered.
This is discussed in the next subsection.
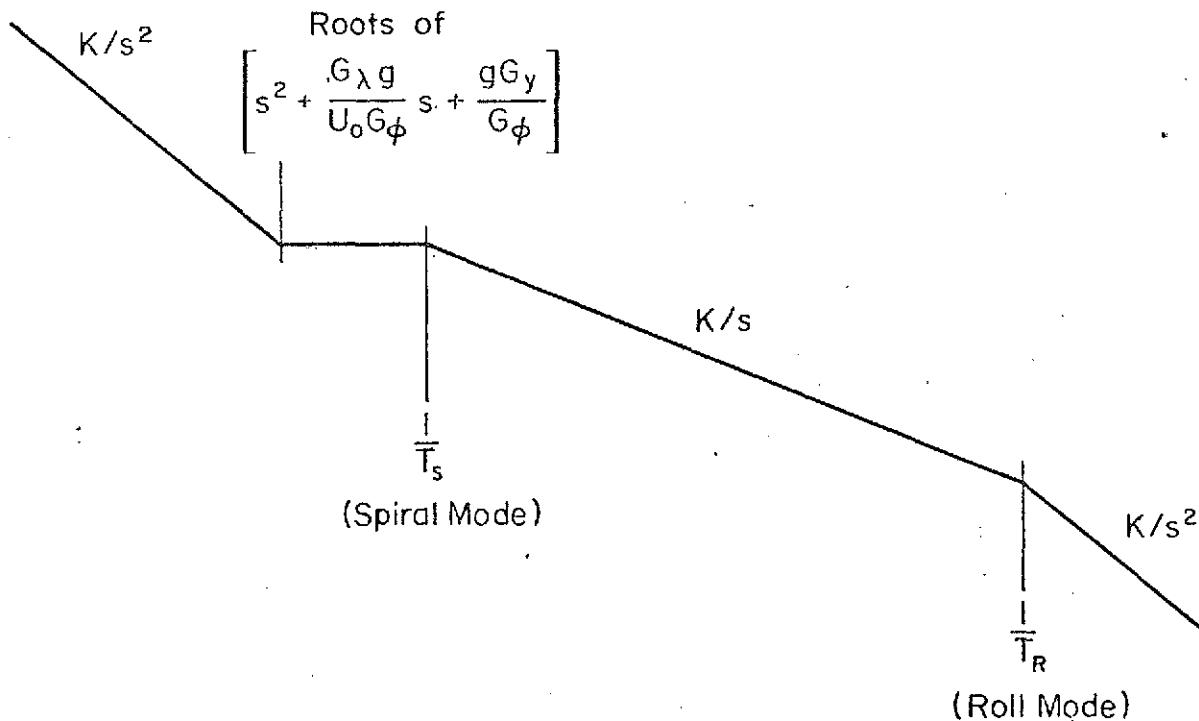
Figure 15. Sketch of Conventional Form for the Effective
Controlled Element Frequency Response

B. SELECTION OF NOMINAL FEEDBACK GAINS

The main problem in setting display or feedback gains is how to maintain command bar consistency at high and low frequency. For example, if the gain ratios previously selected do not provide enough separation between the lateral deviation and attitude gains, the director compatibility with localizer displacement at low frequencies will force too high an attitude gain. This will then not be compatible with the attitude status display at high frequencies.

For a 7-1/2 deg STOL approach, the glide slope is intercepted at 11,500 ft from the transmitter when the altitude is 1500 ft. If we assume that the full 2-1/2 deg localizer deviation occurs at this distance, then the HSI will display a ±500 ft lateral error. Full-scale deflection of the command bar on a typical flight director indicator is approximately ±1.0 in. To make the low-frequency director display compatible with the HSI display, the gain K_y must be about 0.002 in./ft. Since the pilot's foveal resolution is about 0.01 in. when viewed from a distance of 3 ft, the minimum resolvable lateral error will be about 5 ft if the feedback is not range compensated. This resolution should be more than ample when we consider the ±75 ft lateral window at decision altitude applicable to CTOL aircraft.

Assuming a lateral gain 0.002 in./ft and the desired gain ratio, $gG_y/G_\varphi = 0.04$, the attitude feedback gain should then be 1.6 in./rad. This means that just over 30 deg bank attitude will produce maximum director displacement. Also, the movement of the sky pointer on the attitude display moves about 1 in. for a bank angle of 30 deg. Thus, the director and attitude display should reflect compatible motions at high frequency.

For an approach speed of 60 kt and an attitude gain of 1.6 in./rad, the lateral flight path gain should be 1.4 in./rad. With the gain, $K_\lambda = 1.4$ in./rad, an intercept angle of 45 deg produces maximum director deviation.

C. EFFECTIVE CONTROLLED ELEMENT

The actual effective controlled element will differ somewhat from the simplified version since lateral deviation is not exactly $g\varphi/s^2$ and lateral flight path angle is not exactly $g\varphi/U_o s$. A system survey of the actual effective controlled element with feedback gains:

$$K_\varphi = 1.6 \quad \text{in. FD/rad}$$

$$K_\lambda = 1.4 \quad \text{in. FD/rad}$$

$$K_y = 0.002 \quad \text{in./ft}$$

is shown in Fig. 16. The response has a mid-frequency region of K/s-like slope and the pilot can easily put in lead equalization at the roll mode without any increase in workload. Lead equalization at $1/T_R$ would provide a continuous K/s-like response from about 0.3 rad/sec. Anticipated closure of this loop by the pilot would be about 1 rad/sec, which will require a pilot gain of 2 rad δ_w per inch of director displacement. The closed-loop path mode will have a damping ratio and frequency of about 0.67 and 0.23, respectively.

D. PRACTICAL ASPECTS

1. Feedback Signal Derivation

The first order of business in reducing the design concept to practice was to derive the most efficient way to obtain lateral flight path angle, λ. The most efficient way is to pseudo-integrate lateral acceleration (measured at the vehicle c.g.) independent of bank as shown in Fig. 17. This produces lateral flight path angle at frequencies greater than 1/T but has no low-frequency gain. Lateral flight path angle must be complemented with derived radio beam rate as shown in Fig. 18 in order to maintain the beam reference.

A more sophisticated mechanization using a second-order complementary filter is shown in Fig. 19. This mechanization may be necessary in order to adequately filter beam noise.

2. Command Limiting

The next item to be included in a practical system with washed-out feedbacks is command limiting. This sets maximum values for the beam inter-cept angle and roll attitude. The technique used is best described in Fig. 20. The addition for command limiting is shown in the dashed box. Operation is such that in the linear region the two additional x_n feedback paths cancel
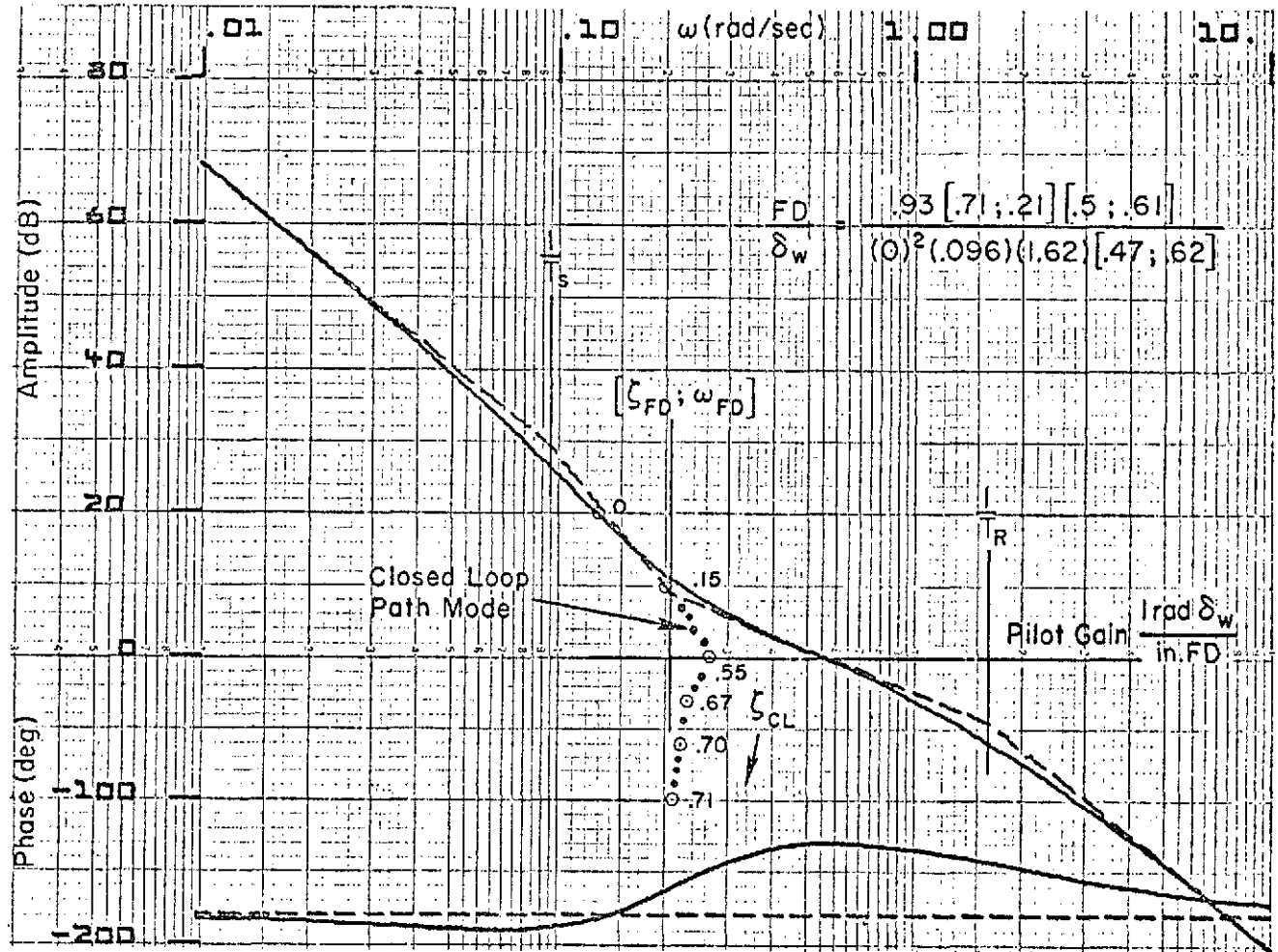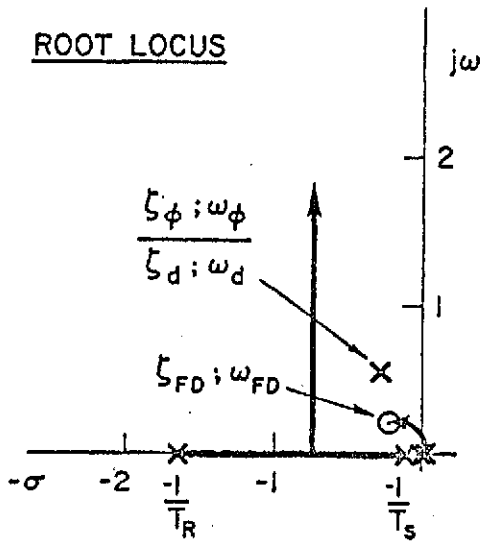
Figure 16. System Survey of Lateral Effective Controlled Element
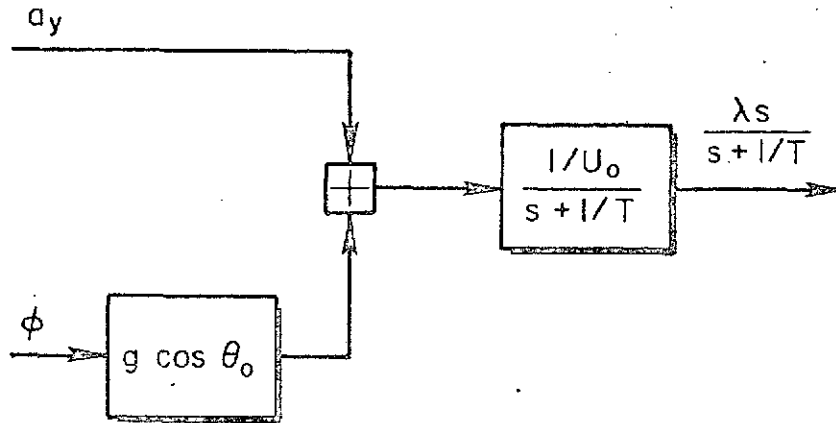
Figure 17. Obtaining Washed-Out Lateral Flight Path Angle
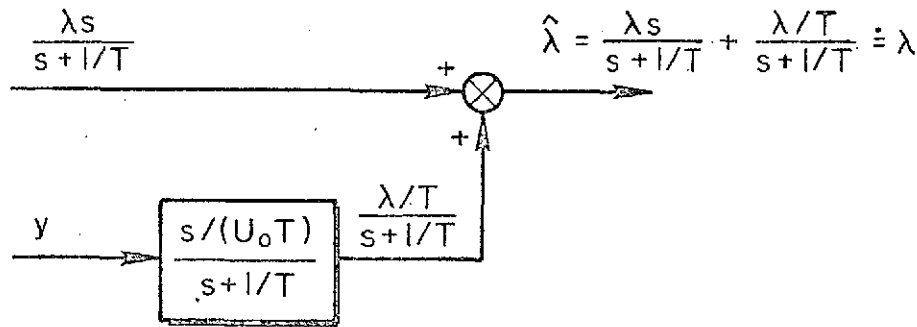
Figure 18. Approximation to Lateral Flight Path Angle
Throughout Complete Frequency Region

and only the washed-out feedback of x_n acts. In the nonlinear region, the incremental gain on x_{nc} is zero and the commanded value of x_n is either $+x_{nCL}$ or $-x_{nCL}$.

3. Range Compensation

Without any range compensation, the system gains will result in unstable response at about 3500 ft short of a CTOL runway. However, if pseudo-integrated lateral acceleration independent of bank angle is used for the path damping, as was shown in Fig. 19, the system will remain stable until about the glide path intersection point (i.e., 1000 ft onto the runway). We will assume, however, that range compensation will be included in an operational system.
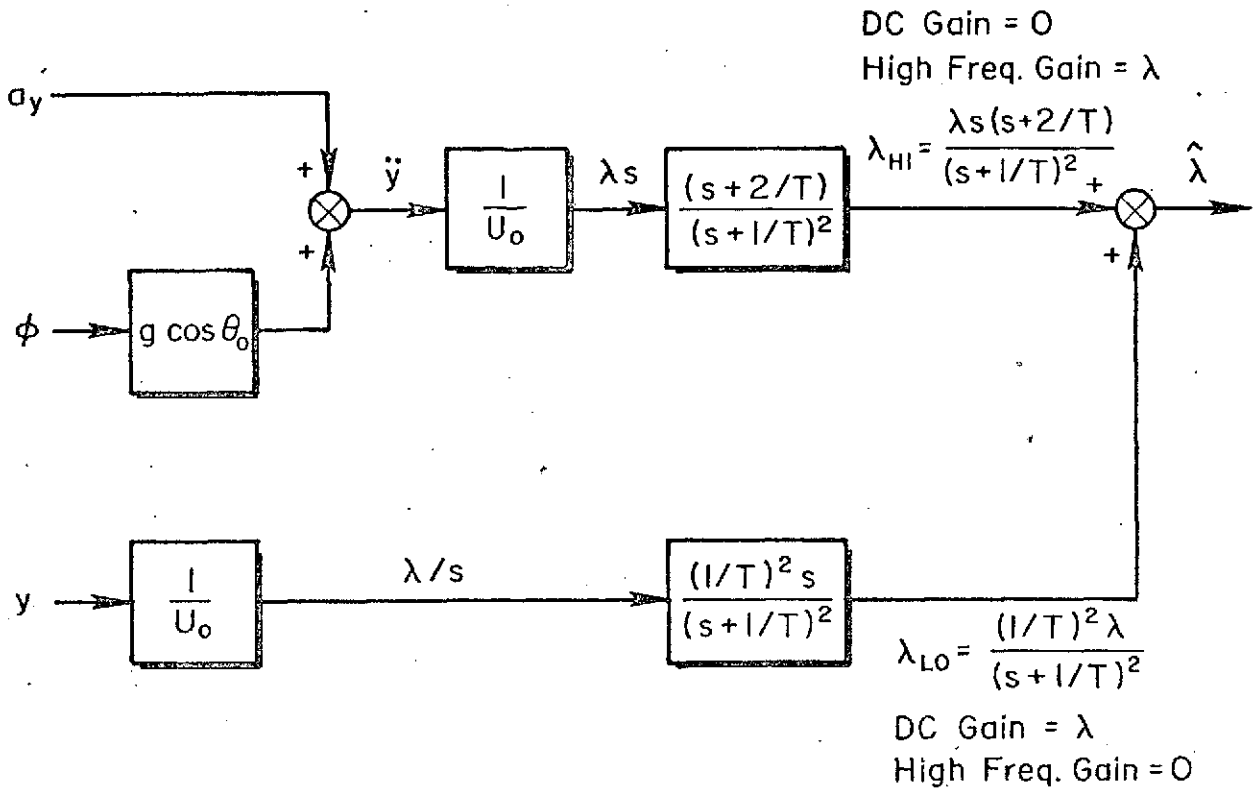
Figure 19.   Derivation of Lateral Flight Path Angle
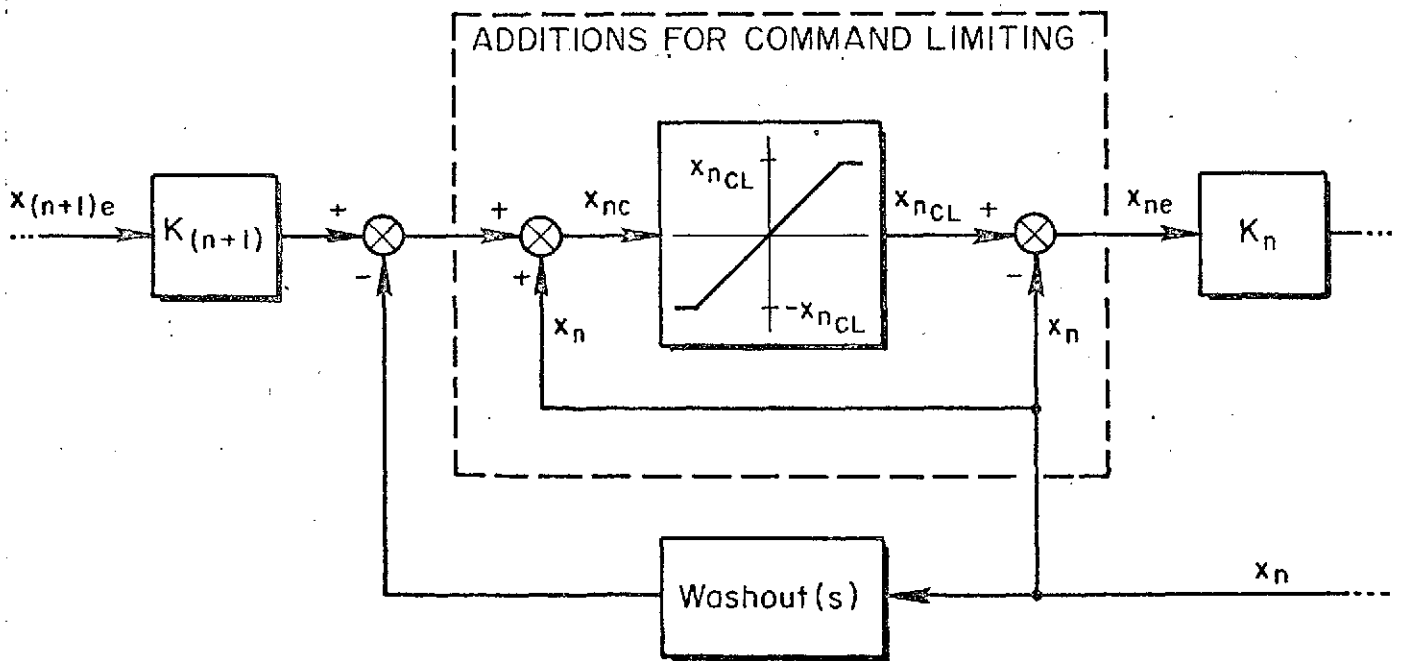
Figure 20.   Schematic for Effective Command Limiting
for Use with Washed-Out Feedback

SECTION V

LONGITUDINAL FLIGHT DIRECTOR SIMULATION

This section presents and discusses the longitudinal results obtained from the flight director simulation program conducted on the NASA Ames FSAA simulator.

The specific objectives for the longitudinal evaluation were as follows:

1. Determine nozzle and column director display gains. Check approximate pilot gain.

2. Check preliminary design. Vary gain ratios to determine pilot rating sensitivity.

3. Determine effective lead and lag for "busy display" when pitch rate and nozzle position feedback are used in column and nozzle guidance laws, respectively.

4. Determine range compensation limits in view of guidance scheme to be used (e.g., SPN-10).

5. Measure closed-loop performance in presence of deterministic wind inputs. Compare tracking performance in presence of random gust and beam noise inputs to predicted closed-loop performance.

6. Determine mode selection requirements and performance of director for glide slope engage.

A. DISPLAYS, TESTS, AND EVALUATION PROCEDURES

The experimental scenario including cockpit displays, flight conditions, tasks, disturbance forms, and performance metrics which were applied in the simulation evaluation are briefly outlined in the following paragraphs.

1. Attitude-Director Display

The attitude director indicator was the Sperry HZ-6B shown in Fig. 21. This display utilizes conventional cross pointers for the wheel and column, but has no unique thrust vector or nozzle command cue. Based on pilot preference, the nozzle command was mechanized on the FAST-SLOW donut

Go-Around
Light

Roll Pointer

Minimum Decision
Altitude Light

Attitude Sphere

Fixed Airplane
Symbol

Speed Command
Replaced by
Nozzle Command
Cue

Glide Slope Display

Longitudinal Flight Director
Command Bar

Lateral Flight Director
Command Bar

Radio Altitude Display

Self Test Switch

Trim Knob

Inclinometer

Rate-of-Turn Indicator

Expanded Localizer Display

Figure 21. Sperry HZ-6B Attitude Director Indicator

located on the left side of the indicator as shown in Fig. 21. The sense was such that a fast indication (high donut) commanded a forward push on the nozzle lever in order to bring it back toward the center.

2. Flight Condition

Only one type approach was evaluated. The initial conditions were 1500 ft altitude, 60 kts, trimmed on the 7.5 deg glide slope. No glide slope capture from level flight was simulated. Flaps and thrust were not changed from their initial settings of 65 deg and 93% respectively. For some tailwind conditions, however, thrust was reduced in discrete steps to increase the rate of descent capability. There was no longitudinal stability augmentation system, but a lateral SAS whose effects were previously described was operating.

3. Tasks

The task was basically an IFR approach from beam acquisition to breakout at an altitude of 200 ft. Other director modes such as altitude hold and heading hold were not evaluated. Flare logic was not mechanized since the pilot would transition to VFR upon breakout at 200 ft altitude. From breakout through touchdown the task was VFR. Compatibility of pilot technique and performance between this task and the IFR task was checked.

4. Disturbance Inputs

The flight director/pilot/vehicle system was subjected to disturbances from random turbulence, deterministic wind profiles, and random beam noise. These inputs reduce the accuracy to which the aircraft can be flown to follow path commands. A block diagram of the flight director/pilot/vehicle system with environment disturbances is shown in Fig. 22.

FAA Advisory Circular 120-20 specifies wind profiles relative to runway heading and the resulting minimum localizer and glide slope tracking performance. Table 4 presents the wind conditions from Ref. 6 (and Ref. 7) in tabular form so that all the combinations are covered.
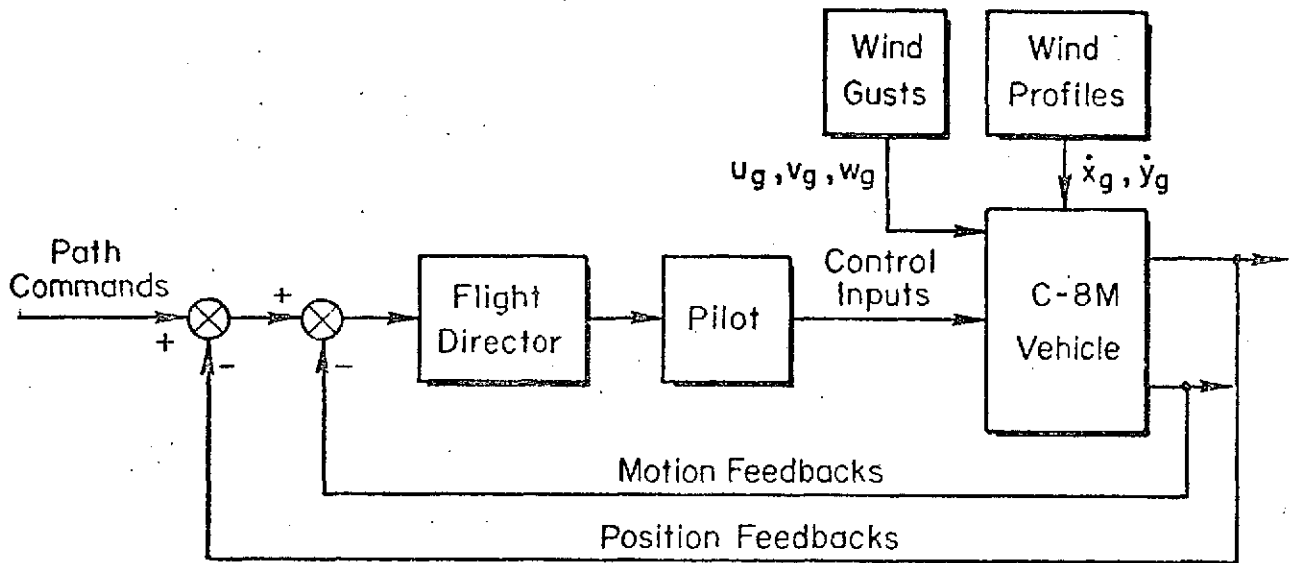
Figure 22. Flight Director/Pilot/Vehicle System
Showing Disturbance Inputs

TABLE 4

WIND PROFILES FOR FLIGHT DIRECTOR PERFORMANCE EVALUATIONS

WIND	INITIAL ALT.	INITIAL[*] WIND SPEED	FINAL[*] WIND SPEED	FINAL ALT.
Decreasing Tailwind Shear	500	+30 kt	+10 kt	0
Increasing Tailwind Shear	500	−10 kt	+10 kt	0
Decreasing Tailwind Shear; Calm on Ground[†]	600	+20 kt	0	100
Decreasing Crosswind Shear	500	+35	+15	0
Increasing Crosswind Shear	500	−5	+15	0

[*] + indicates tailwind or crosswind from left side. − indicates headwind or crosswind from right side.

[†]Critical condition described in Ref. 7 (not specified in Ref. 6).

The minimum <u>localizer</u> tracking performance for the above wind conditions is specified as follows:

1. The airplane should be stabilized on the localizer for the purpose of demonstration before the outer marker is intercepted on a normal inbound approach.

2. From the outer marker to an altitude of 300 ft above runway elevation on the approach path, the flight director should cause the airplane to track within ±35 microamperes, i.e., ±0.6 deg = ±1/2 dot (95 percent probability) of the indicated localizer course. The performance should be free of sustained oscillations.

3. From an altitude 300 ft above runway elevation on the approach path to the decision altitude (100 ft), the flight director should cause the airplane to track to within ±25 microamperes, i.e., ±0.40 deg = ±1/3 dot (95 percent probability) of the indicated course. The performance should be free of sustained oscillations.

The minimum <u>glide slope</u> tracking performance for the wind profiles is specified as follows:

1. For the purpose of the demonstration, the airplane should be stabilized on the glide slope before an altitude of 700 ft above the field level is reached.

2. From 700 ft altitude to the decision altitude (100 ft), the flight director should cause the airplane to track the center of the indicated glide slope to within ±3 microamperes, i.e., ±0.17 deg = ±1/2 dot, or ±12 ft, whichever is the larger, without sustained oscillations.

NASA turbulence models specified for space shuttle simulations (Ref. 8) were used for random gust inputs.

The gust levels were defined by the following equations:

$$\sigma_u = \sigma_v = 4 \text{ fps}$$

$$\sigma_w = \frac{\sqrt[3]{h}}{3} \quad \text{for } 100 \text{ ft} < h < 1750 \text{ ft}$$

Beam noise was not simulated.

5. Performance Evaluations

The desirability of the director systems was based on pilot opinion ratings, performance measures, and strip chart recordings. The performance measures included the following parameters measured from inside the outer marker (from 1300 to 300 ft altitude) and inside the middle marker (from 300 to 50 ft altitude).

rms and maximum deviations from localizer and glide slope	$\ddot{\epsilon}_{LOC}$, ϵ_{GD}
rms and maximum airspeed excursion and vertical acceleration at the pilot station	$\ddot{u}_a$, $a_{z_{PILOT}}$
rms and maximum attitudes	ϕ, θ, ψ, β
rms and maximum control deflections	δ_{column}, δ_{wheel}, δ_{nozzle} δ_{pedal}
rms flight director excursions	FD_C (column), FD_N(nozzle), FD_L (lateral)

B. FINAL SYSTEM

The primary objective of the experimental program was to evaluate the analytically derived system, determine display gains, and check the approximate crossover frequency. This objective was accomplished and the final system found best by two pilots was very similar to the nominal system derived in Section II. The only differences were that airspeed was complemented with longitudinal acceleration, the nozzle display scaling was increased, and a lead-lag (i.e., lagged pitch rate) quickener was used in the stick director.

This system produced pilot ratings of from 2-1/2 to 3. Furthermore one pilot stated that this would be the minimum numerical rating possible for this vehicle without longitudinal SAS. Glide slope tracking was significantly improved over the no flight director case with essentially no change in rms control activity or pitch attitudes.

A block diagram of the final system is presented in Fig. 23. The optimum gain settings for this mechanization are given in Table 5 below.
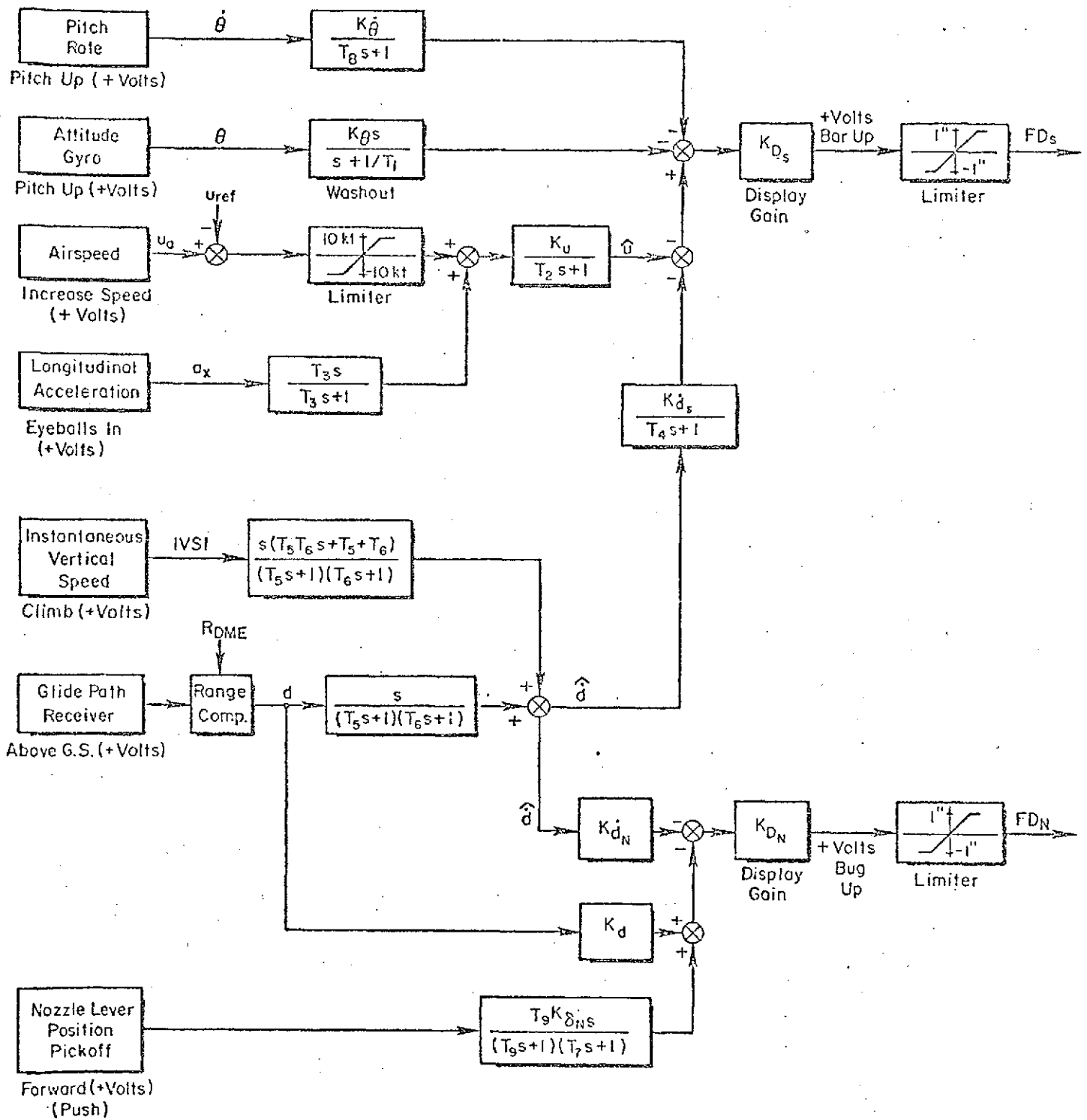
Figure 23. Longitudinal Flight Director Block Diagram

TABLE 5

GAINS FOR LONGITUDINAL FLIGHT DIRECTOR SYSTEM

$K_\theta = 1.0$ Units FD/rad $T_1 = 3.0$ sec $K_{D_s} = 5.73$ in./unit

$K_{\dot\theta} = 1.0$ Units FD/rps $T_2 = 1.0$ sec

$K_u = -.01$ Units FD/fps $T_3 = 20$ sec

$K_{\dot d_s} = 0.01$ Units FD/fps $T_4 = 0$ sec

$T_8 = 0.67$ sec

$K_d = 0.5$ Units FD/ft $T_5 = 2.0$ sec $K_{D_N} = 0.16$ Dots/Unit

$K_{\dot d_n} = 1.0$ Units FD/fps $T_6 = 1.0$ sec

$K_{\delta_n} = 80$ Units FD/rad Lever Angle $T_7 = 1.0$ sec

$T_9 = 10.0$ sec

With this mechanization the nozzle command cue maintains glide slope at and below path mode frequencies. Beam rate provides lead equalization. The nozzle position feedback provides a nearly immediate indication of response to pilot action. It is washed out (10 sec time constant) to avoid trim stand-off errors. The stick director maintains trim airspeed. Beam rate feedback is utilized in conjunction with washed out pitch attitude to provide path damping and improve windproofing performance. Lagged pitch rate was found to be desirable to extend the effective controlled element's K/s-like amplitude response.

The effective controlled element for the stick director is shown in Fig. 24. This is not the same transfer function as given in Section III since the trim conditions and ratio of hot/cold thrust were changed in the simulation to reflect more up to date information on the airplane's characteristics. Appendix B contains the revised aircraft data and transfer functions. Also the inclusion of lagged pitch rate feedback adds a lead/lag of approximately $(s + 0.8)/(s + 1.5)$ to the transfer function. The cross-over line shown in Fig. 24 was chosen as typical from examination of strip
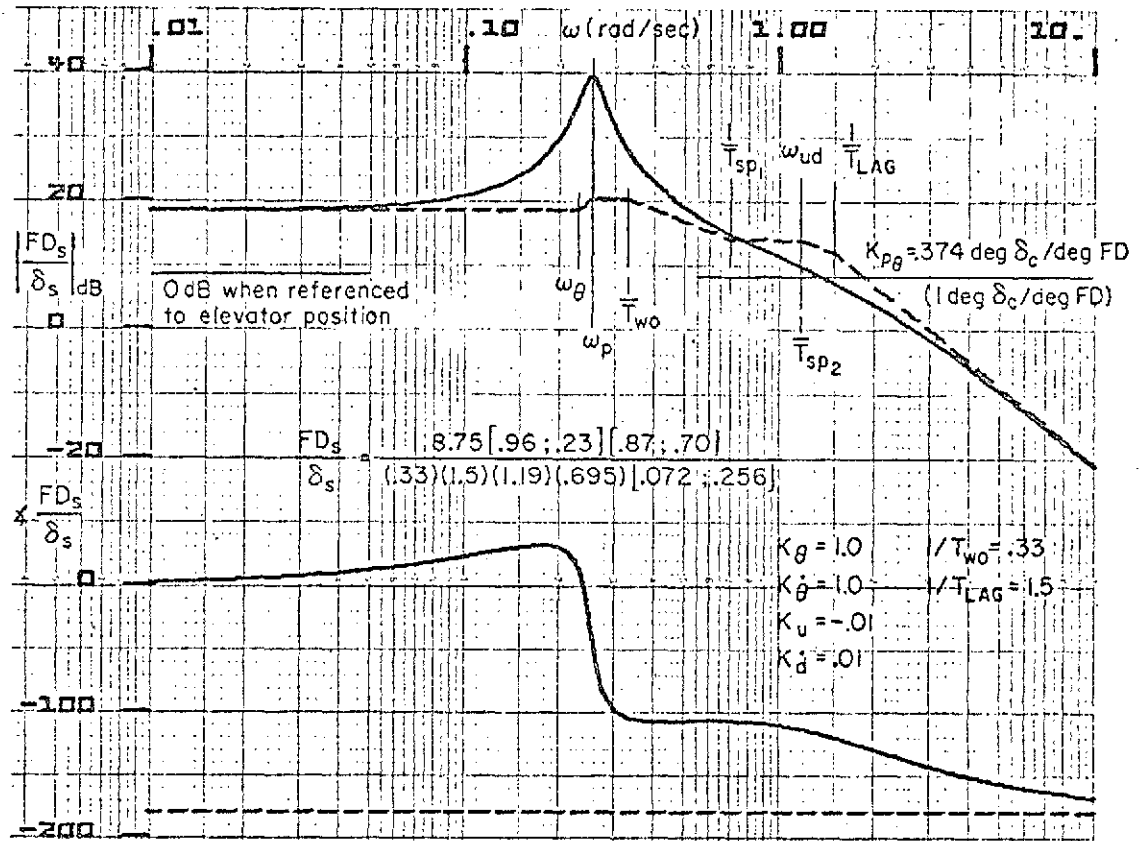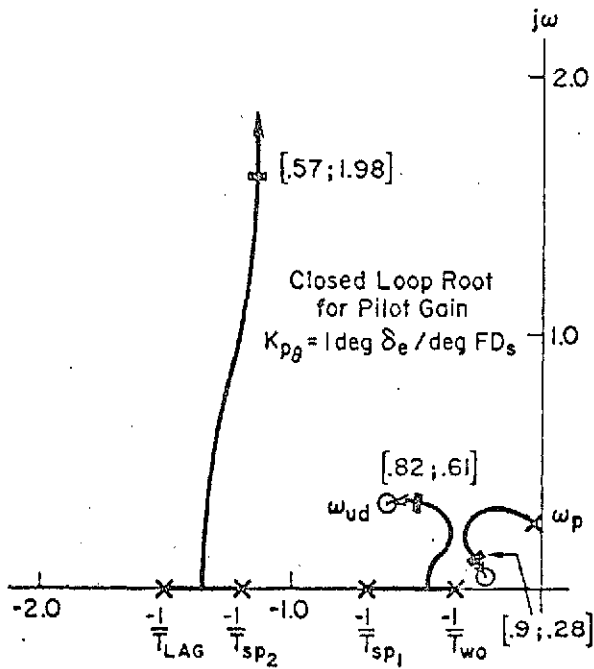
Figure 24.   Stick Director Effective Controlled Element

chart recordings. An example of these time histories is presented in
Fig. 25. By comparing the δ_e trace to the FD_S trace some estimate can
be made as to the pilot's gain. A rough scan shows that the FD_S trace
is, on the average, higher amplitude than the δ_e trace. This means the
pilot's gain is at least 1 deg/deg FD_S (e.g., if the traces were of equal
amplitude, the pilot gain would be 2.0 due to the scale factor difference).

For the nozzle director the pilot gain is approximately 40 deg δ_N/dot,
on the average, with no response for deviations less than 1/4 dot. Maximum
excursion is +10 deg, −30 deg from trim. The nozzle effective controlled
element with the stick loop closed at 1.3 rad/sec is shown in Fig. 26.
The zero dB line for a pilot gain of 40 deg δ_N/dot is also shown for pilot B.
For pilot A the display gain was 0.08 dots/unit and his average gain was on
the order of 40-50 deg/dot as can be found by examining the strip chart
recording of Fig. 27.

Table 6 summarizes the pilot ratings for the final longitudinal director
system as a function of lateral SAS and directors on or off. A primary
result is that the longitudinal director changes the longitudinal rating
from 5-7 with no director to 2-1/2 to 3. With lateral SAS off the dif-
ference is not so apparent since the main problem is lateral control.

TABLE 6

PILOT RATING SUMMARY
LONGITUDINAL FLIGHT DIRECTOR EVALUATION

FLIGHT DIRECTOR	LATERAL SAS	PILOTS	
		A	B
ON	Lateral SAS On	2-1/2	3
	Lateral SAS Off	5 to 5-1/2	Not Tested
OFF (Lateral Flight Director On)	Lateral SAS On	5	5 7 With Shears and Lat. Task
	Lateral SAS Off	5-1/2 to 6	Not Tested
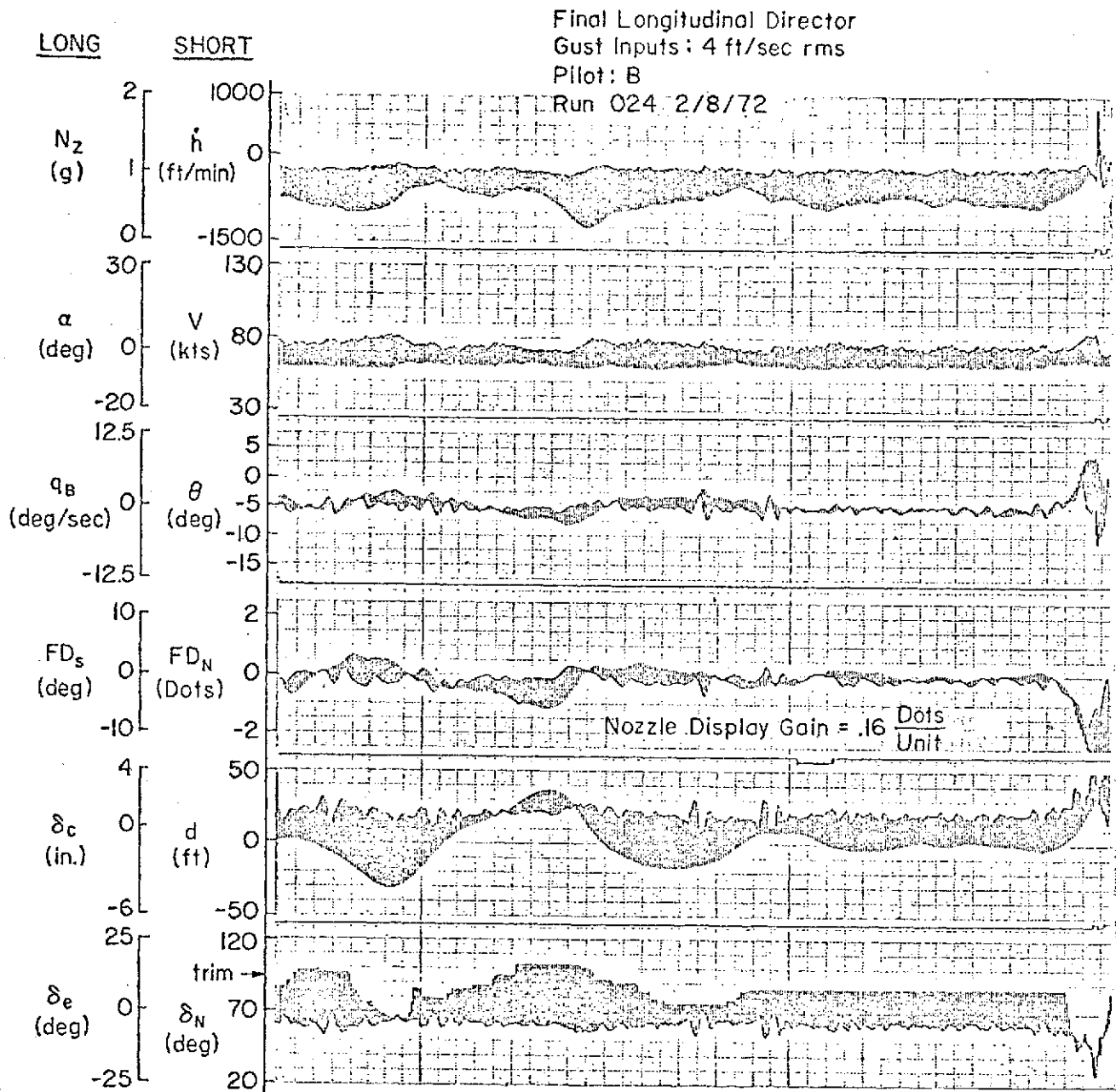
Figure 25. Example Time History of Flight Director Approach
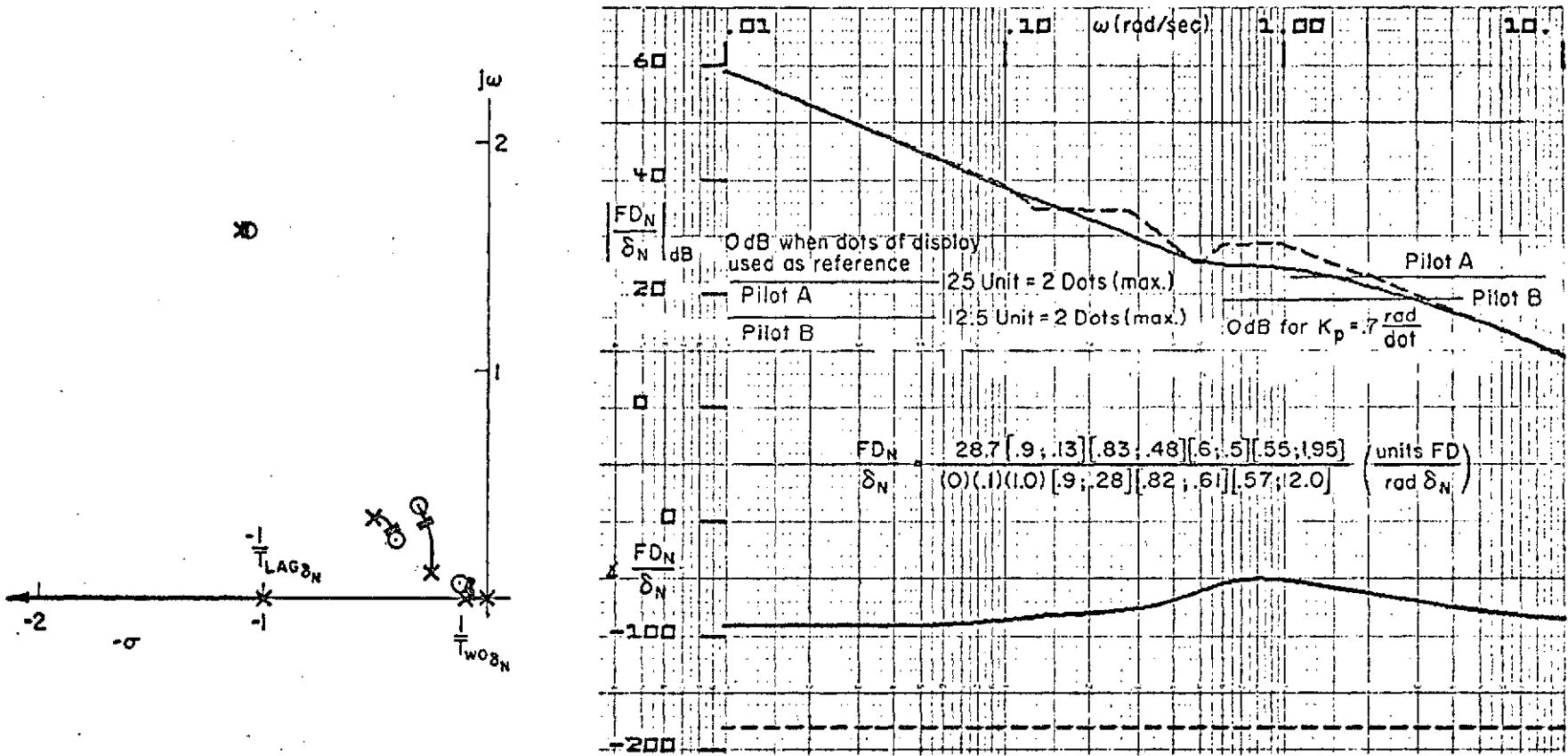
Figure 26.   Nozzle Effective Controlled Element with Stick Director Loop
Closed at 1.3 rad/sec
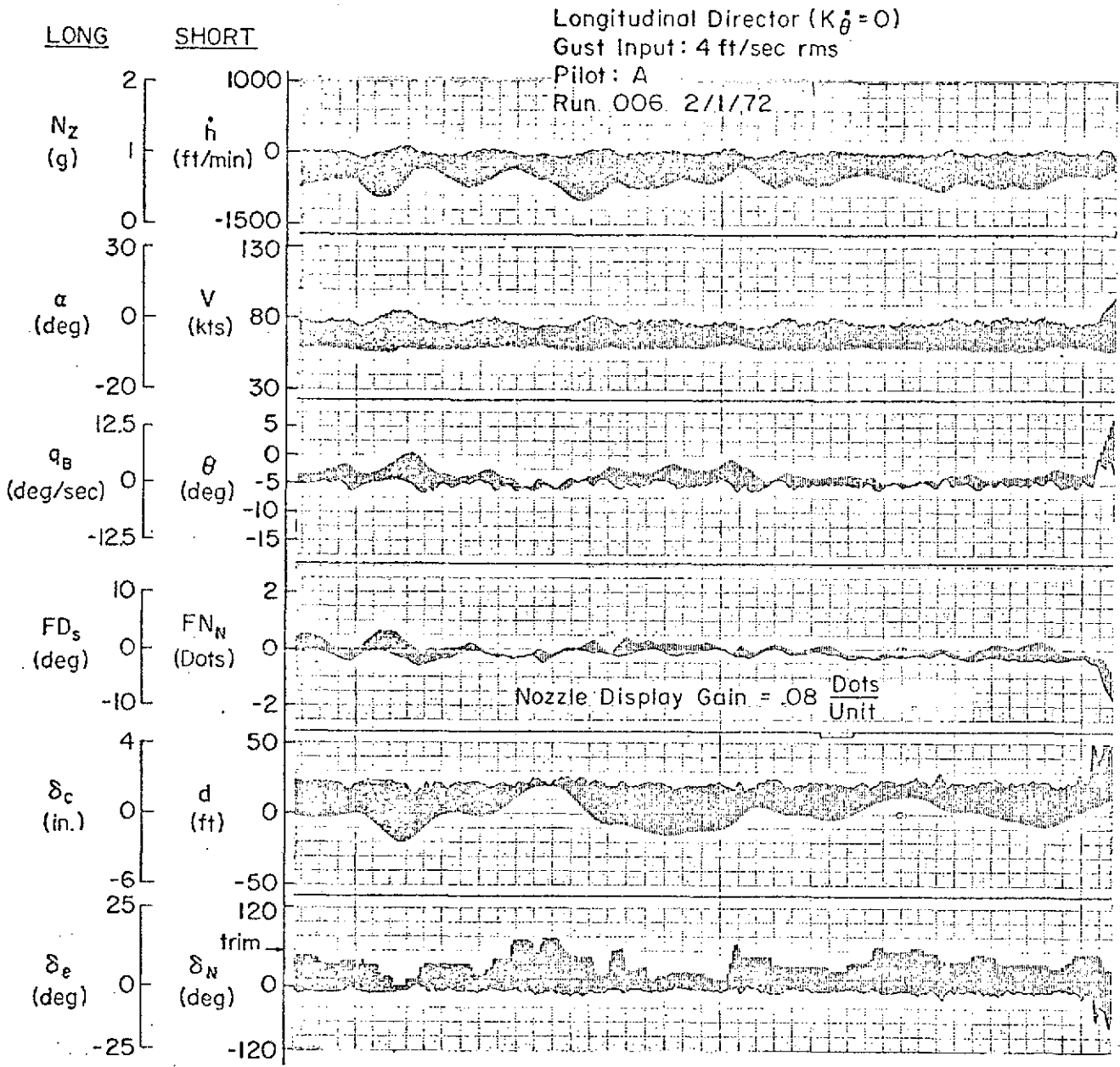
Figure 27. Example Time History of Flight Director Approach

Several problems were uncovered during the simulation. Primarily these had to do with the nozzle controller and included the following:

- Low control power so glide slope tracking performance is limited.

- Rate of descent capability from trim is only 250 fpm which is insufficient to compensate for a 10 kt tailwind.

- Excess control cross-coupling.

Additional problems were with the throttle sensitivity and related angle of attack limits. It was found that when α neared 10 deg the pilot would not follow the stick director. This occurs when thrust is reduced just slightly. A limit should be included in the director mechanization to reflect some angle of attack margin.

Two problems that were not addressed were course softening and the glide slope capture mode. Since the glide slope transmitter is located 250 ft from the runway threshold it was necessary to range compensate the beam.

C. RESEARCH ASPECTS

The remaining objectives of the experimental design are:

1. Vary gain ratios to determine pilot rating sensitivity to final design.

2. Determine effective lead and lag for "busy display" when pitch rate and nozzle position feedback are used in column and nozzle guidance laws respectively.

3. Measure closed-loop performance in presence of deterministic wind inputs. Compare tracking performance in presence of random gust and beam noise inputs to predicted closed-loop performance.

The sensitivity of the stick director to gain changes in K_u of $\pm 50\%$ were not noticed by the pilots. In the nozzle director, a gain change in K_d of -50% was not significant but an increase of 50% made the low frequency motions too predominant. Table 7 presents the pharaphrased pilot commentary for each of the feedback gain changes.

TABLE 7

PILOT COMMENTS SUMMARY

PILOT: A

DATE: 2/1/72

DIRECTOR	FEEDBACK	COMMENT
$N_{O_{Z_{Z_{L_E}}}}$ Gain: 25 units = 2 dots	$K_{\delta_\nu} = .5$ units/deg $K_d = 0.5$ $K_{\dot{d}} = 1.0$ $K_{\delta_\nu} = 1.0$ $K_{\delta_\nu} = 0.25$	Workload for 3 axis high. Display gain OK. Tailwind of 10 kts exceeds aft nozzle lever capability, must reduce power, not desirable. Nozzle now more demanding of attention. Tend to overcontrol it. Don't see any response in nozzle director, don't like.
	$K_d = 0.25$ $K_d = 0.75$ $K_d = 0.5$	Just as easy to fly as nominal. Busier on nozzle — seems like more turbulence. Would rate poorer. Best system. POR = 2 1/2.
$S_{T_{I_{C_K}}}$ Gain: 5.7 in./ unit	$K_{\dot{\theta}} = 0$ $K_{\dot{d}} = 0.01$ $K_u = -.01$ $K_\theta = 1.0$	SHEAR A: Will not respond to director if $\alpha > 10$ deg when reduce power.
	$\left. \begin{array}{c} K_{\dot{\theta}} = 1.0 \\ T_{LAG} = 0.5 \end{array} \right\}$ $T_{LAG} = 0.33$	Much better. Reduces workload. Minimizes attitude excursions. POR = 2 1/2. Chasing bar too much.
	$K_u = -.015$	Not different.

TABLE 7 (CONTINUED)

PILOT: B

DATE: 2/8/72

DIRECTOR	FEEDBACK	COMMENT
N O Z Z L E	$K_D = .08$ dots/unit $K_{\delta_\nu} = 0.5$ $K_d = 0.5$ $K_{\dot{d}} = 1.0$	Not enough response to nozzle changes in director.
	$K_{\delta_\nu} = 1.0$	Much nicer response to nozzle changes.
	$K_D = .16$ dots/unit $K_{\delta_\nu} = 0.5$	Same as previous. Can easily recover large glide slope offsets with director alone.
S T I C K Gain: 5.7 in./ unit	$K_\theta = 1.0$ $K_{\dot{\theta}} = 0$ $K_{\dot{d}} = 0.01$ $K_u = -.01$	No anticipation in attitude. Should tell me when attitude is changed. Don't like.
	$K_{\dot{\theta}} = 1.0$ $T_{LAG} = 0.667$ $T_{LAG} = 0.5$	Very good. POR = 3. Best can get with this aircraft. Not too busy. Now tighter pitch loop. Requires more attention.
	$K_u = -.005$	Not much different.

With regard to the "busy" display criterion (Item 2) some interesting results were obtained. First the stick director; recall from Section III that since $1/T_{sp_2}$ was greater than 1 rad/sec it was not apparent whether the pilot would generate a lead at $1/T_{sp_2}$ without inducing a pilot rating degradation or whether the K/s region could be extended with lagged pitch rate feedback without producing a "busy" display. Both pilots preferred the built-in lead with the lag set at 1.5 rad/sec. Pilot B felt the 2 rad/sec lag made the display too busy, whereas pilot A felt the 2 rad/sec lag was acceptable but 3 rad/sec was too busy.

For the nozzle director it was found that in order to produce an acceptable director command, the effective controlled element must be capable of being closed at greater than 1 rad/sec. This criterion validated the use of nozzle position feedback. For example Fig. 28 shows that without nozzle position feedback the high frequency (i.e., > 1 rad/sec) is highly attenuated, and an unreasonably high pilot gain would be required to close the loop at an acceptable crossover. On the other hand, the pilot does not desire to close the loop at 0.5 rad/sec. This appears to be "not responding" for a flight director. Both pilots felt the increased high frequency gain obtained with nozzle position feedback produced a desirable response. It should be noted that increasing display gain has the same effect (see pilot B's comments). To make the choice we turned to the performance aspects presented in Section III which showed that increased nozzle position feedback produced undesirable midfrequency droop in the closed loop beam tracking response. Therefore the display gain should be adjusted to the practical maximum first and then nozzle position added only as needed to give 1-2 rad/sec crossover with a reasonable pilot gain.

D. PERFORMANCE COMPARISONS

Since the longitudinal director system was not designed for beam capture, quantitative results were limited to comparisons of the no flight director approach versus the nominal director approach.

$$\frac{FD_N}{\delta_N}\bigg]_{FD_s \to \delta_s} = \frac{6.95\,(.5)(.182)(.738)(2.31)}{(0)[.9;.28][.82;.61][.57;1.98]} \quad \frac{Units}{rad}$$

Stick Director
Closed at 1.3 rad/sec

O dB When Display
Dots Used As
Reference

$$K_p = \frac{.7\,rad\,\delta_N}{Dot} \quad Nominal$$

$$\frac{10\,rad\,\delta_N}{Dot}$$
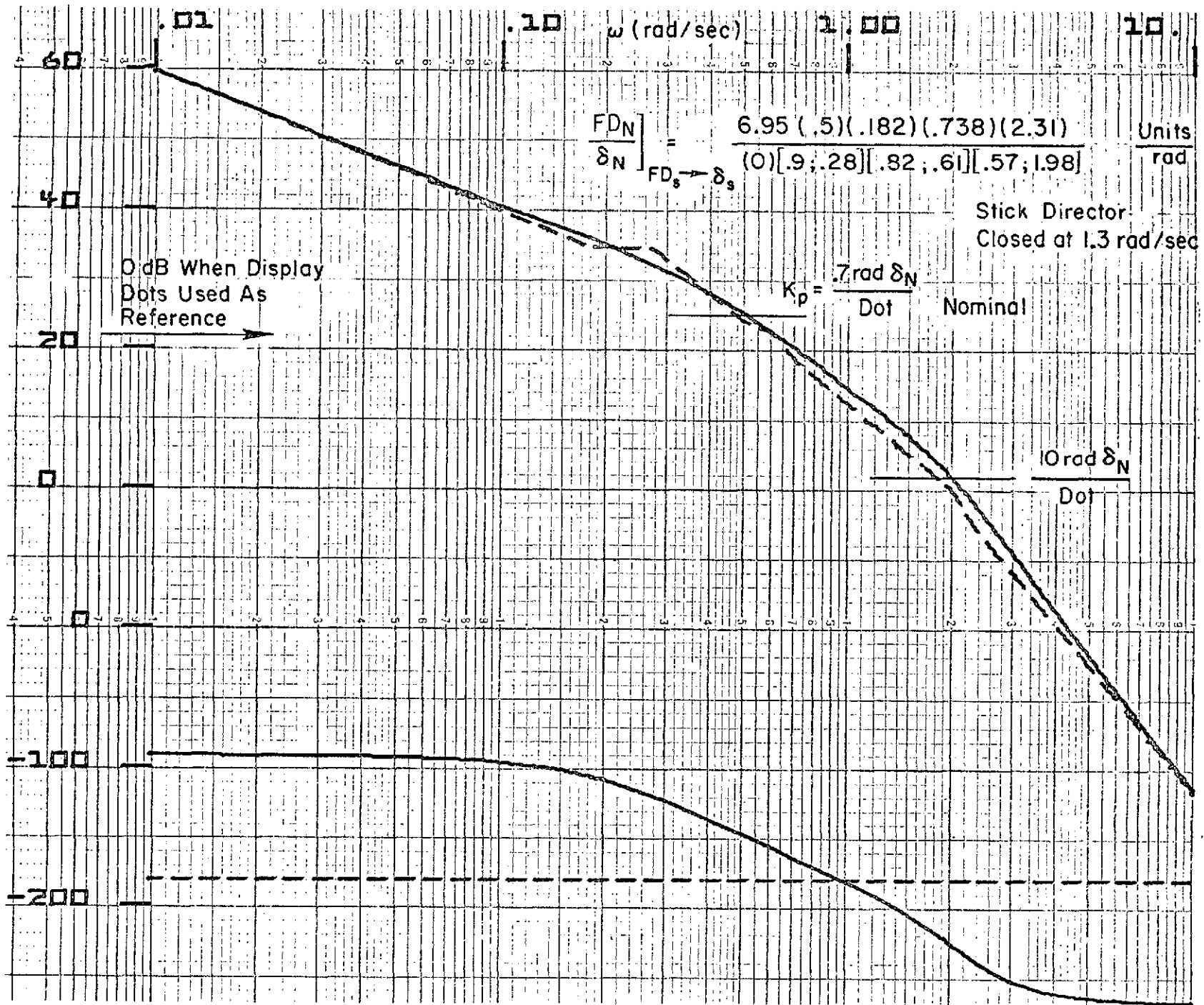
Figure 28. Nozzle Effective Controlled   ent Without Nozzle Position Feedback

Performance comparisons with and without the longitudinal director are presented in Table 8. The main difference is in glide slope tracking performance throughout the approach. Attitude and control deflections are about the same with and without director, which means the pilot is flying as he would conventional IFR but yet getting better performance for his workload.

TABLE 8

LONGITUDINAL FLIGHT DIRECTOR
RMS PERFORMANCE COMPARISON

VARIABLE	ϵ_{GS} (deg)		θ (deg)		δ_{COL} (deg)		δ_{NOZZLE} (deg)	
ALTITUDE RANGE	1300-300	300-50	1300-300	300-50	1300-300	300-50	1300-300	300-50
With FD*	0.118	0.177	1.43	0.45	0.28	0.21	9.5	1.5
No FD	0.246	0.855	1.36	0.82	0.30	0.37	9.3	10.1

*Avg. of 2 pilots; gust input; 4 ft/sec rms.

The glide slope tracking errors are difficult to compare to the predicted values in Section III, since the measurement was made as an angle and the w_g rms level varied with altitude. Also u_g and w_g components were used together. However a rough comparison does show the predicted beam errors to be similar to an average of the measured errors. For example, the rms glide slope error varies from 20.6 ft at 10,000 ft range (1300 ft altitude) down to 4.7 ft at 2300 ft range (300 ft altitude). For this altitude change σ_{w_g} varies from 3.64 ft/sec down to 2.64 ft/sec. The average beam deviation divided by the average σ_{w_g} produces an rms beam deviation of 4.3 ft/ft/sec. This is slightly higher than the 3.9 ft/ft/sec value predicted in Section III (Table 2) for a $w_g/(s + 0.5)$ spectrum.

SECTION VI

LATERAL FLIGHT DIRECTOR SIMULATION

A. FINAL SYSTEM

A lateral director system was derived that met both the pilot-centered and guidance and control requirements. It produced excellent crosswind shear performance and received pilot ratings of 1-2 for all tasks.

The block diagram for this system is given in Fig. 29. As discussed in Section IV, it utilizes heading, bank attitude, lateral acceleration, and range compensated localizer deviation feedbacks. The gains for the optimum system are specified in Table 9. These differ slightly from those derived in Section IV due to the addition of complementary filters.

TABLE 9. LATERAL DIRECTOR GAINS (CASE 2F)

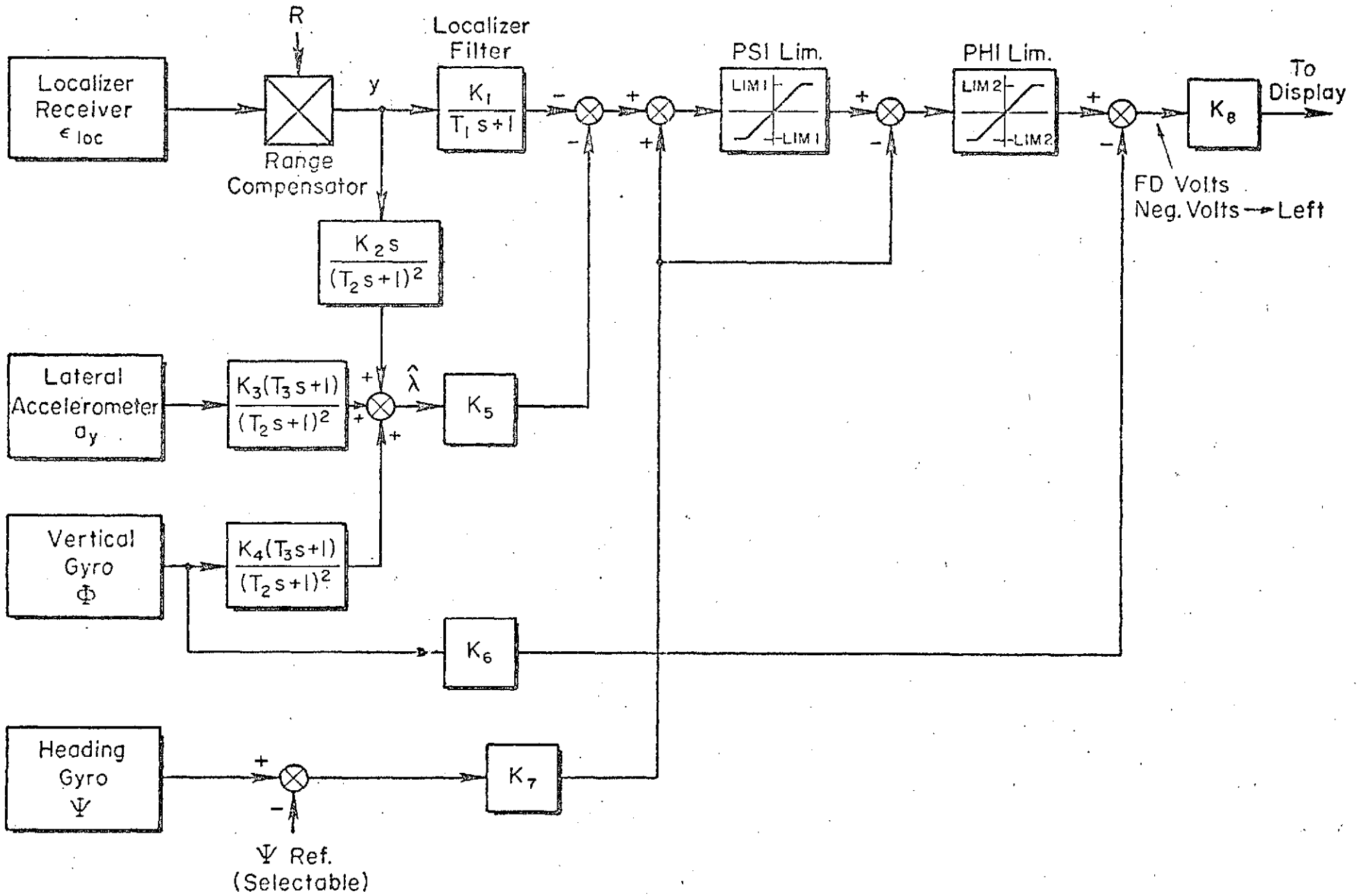|		
K_1	0.00194	volts display/ft lateral deviation
K_2	0.01	rad $\hat{\lambda}/(\text{ft/sec } \dot{y}_e)$
K_3	0.10	rad $\hat{\lambda}/(\text{ft/sec}^2 a_y)$
K_4	3.22	rad $\hat{\lambda}/\text{rad } \phi$.
K_5	1.55	volts display/rad $\hat{\lambda}$
K_6	1.61	volts display/rad ϕ
K_7	1.0	volts display/rad ψ
K_8	1.0	in display/volt (MAX 2.0)
T_1	1.0	sec
T_2	5.0	sec
T_3	2.5	sec
PSI LIM	0.78	volts (45 deg)
PHI LIM	0.45	volts (16 deg)

Figure 29. Lateral Flight Director System for Beam Acquisition and Approach

Basically, the system operates as follows: when the aircraft is more than 400 ft from the localizer, on a parallel course, the flight director commands a maximum bank angle of 16 deg. This was reduced from the original 30 deg limit since pilots felt there was too much longitudinal coupling when bank angle exceeded 15-16 deg. If the localizer deviation had been greater than 930 ft, a resulting turn rate of 5 deg/sec would be held until a maximum intercept angle of 45 deg was obtained. At 600 ft from the localizer the system starts reducing the lateral flight path angle in order to blend into the localizer. From this point on, the heading signals on either side of PSI limiter cancel out and the path damping is obtained via $\hat{\lambda}$.

A frequency response and root locus plot of the effective controlled element, FS/δ_W, defined by the gains ratios of Table 9 is shown in Fig. 30. The low-frequency region of conditionally stable response is apparently not influential to the pilot, who closes the loop in the mid-frequency region.

A time history of the intercept and tracking performance of this system is shown in Fig. 31. Note that an approximate gain is 100 deg δ_W/in. FD displacement. This represents a 1 rad/sec crossover of the effective controlled element in Fig. 30. Pilots felt this frequency of path mode control, i.e., 0.2 rad/sec, was good, and yet the directors did not demand a high degree of pilot workload.

The final system improved pilot ratings of from 7-10 with no lateral director and no lateral SAS to 4 to 4-1/2 when the director was turned on. A similar improvement was made when the lateral SAS was on. Then the ratings for one pilot improved from 4 to 4-1/2 without the director to 1-1/2 with the director. The improvement in rating for the second pilot was from 3-4 down to 1-2. These ratings are summarized in Table 10.

B. RESEARCH ASPECTS

As discussed in Section IV, the frequency response of the effective controlled element determines system performance and pilot acceptance. It was thought initially that a K/s + shelf type effective controlled element would be most desirable in meeting both these sets of requirements; therefore, several perturbations on this philosophy were tested.

Closed Loop
Roots for

$K_p = 1.75 \frac{rad}{in.}$

ω_{FD}

$\frac{-1}{T_R}$

$\frac{-1}{T_S}$

σ

$j\omega$

$\frac{FD}{\delta_w} = \frac{1.0\,[.73\,;\,.189]}{(0)^2\underbrace{(.096)}_{1/T_s}\underbrace{(1.62)}_{1/T_R}}\ \frac{in.}{rad}$

Numerator Roots
Approximated By:

$\left[s^2 + \frac{gK_\lambda}{U_0 K_\phi}s + \frac{gK_y}{K_\phi}\right]$

$K_\phi = 1.61$
$K_\lambda = 1.55$
$K_y = .00104$

$\left|\frac{FD}{\delta_w}\right|_{dB}$

$|G(-\sigma)|$

$\frac{1}{T_R}$

$\frac{1}{T_s}$

$K_p = 1.75 \frac{rad}{inch}$

$= 100\ deg/in.$

Locus of
Closed Loop Roots

Path
Mode

Attitude
Mode

$\angle \frac{FD}{\delta_w}$

$\omega\,(rad/sec)$
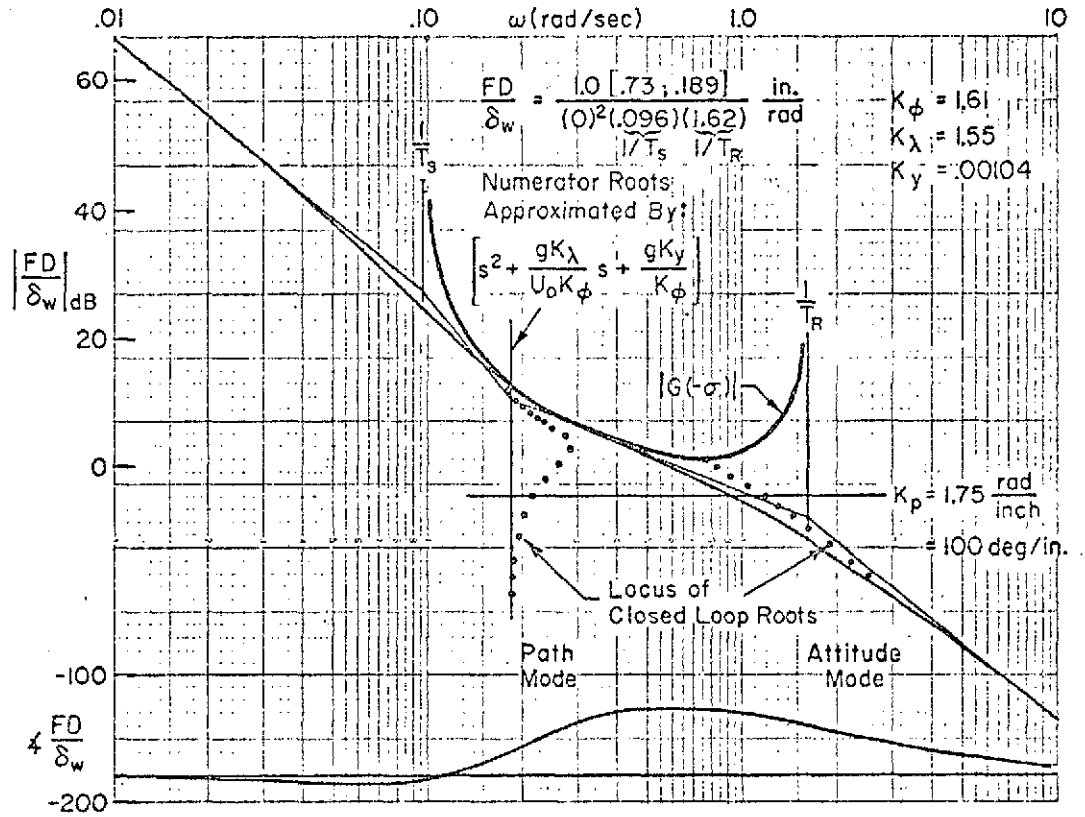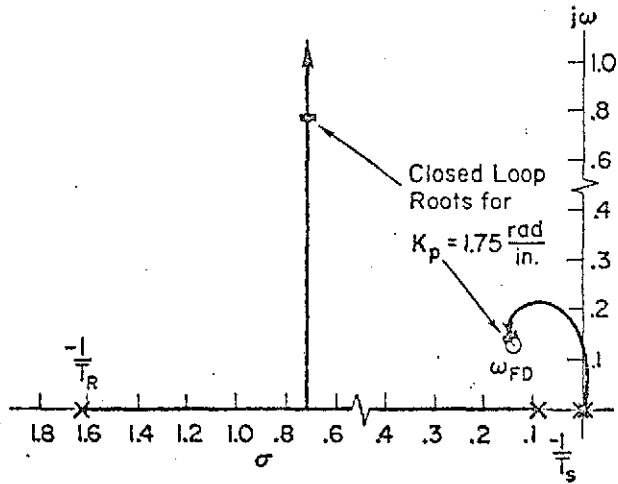
Figure 30. Effective Controlled Element Dynamics for
Lateral Director (Case 2F)
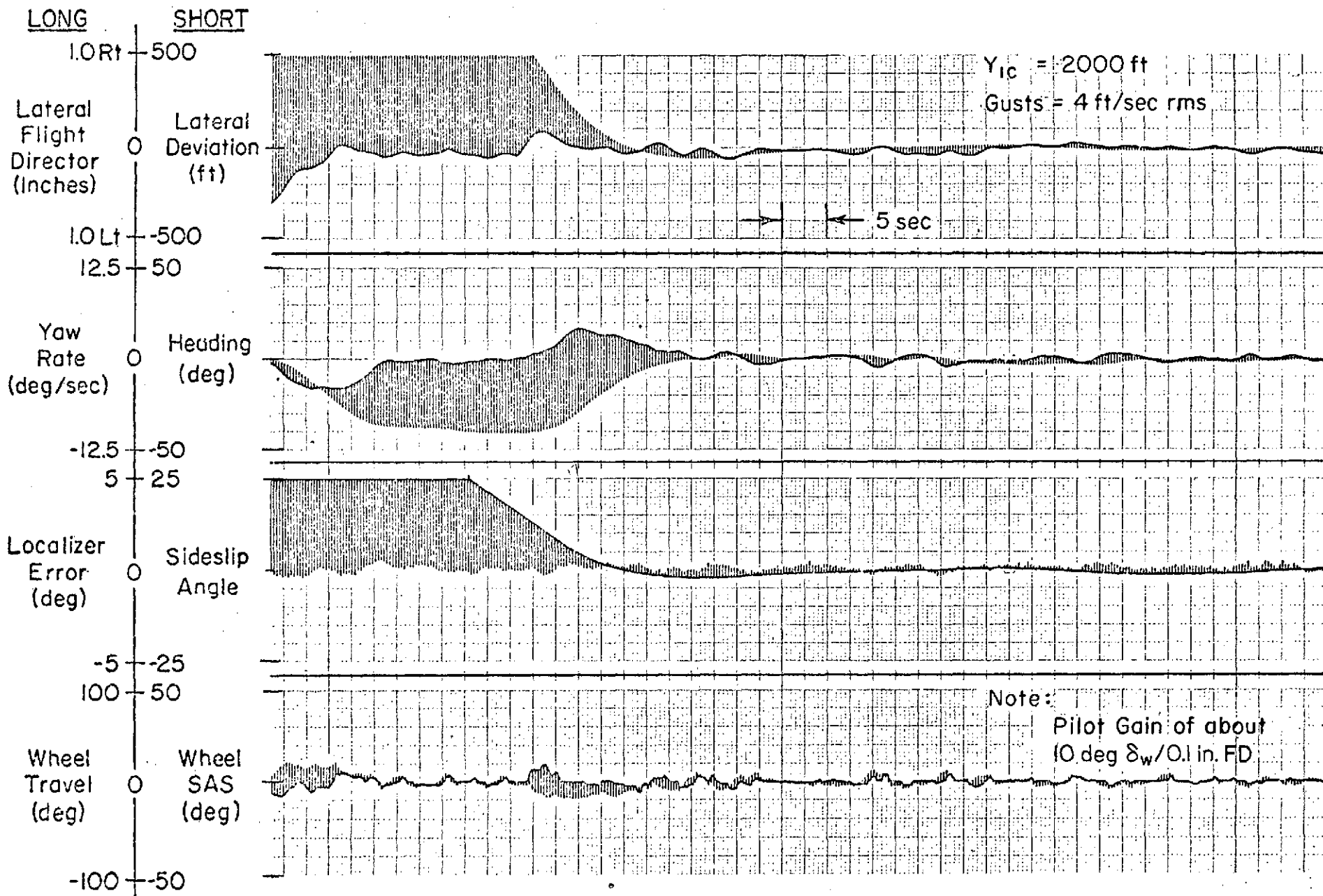
Figure 31. Time History of Intercept and Tracking Task with Lateral Director (Case 2F)

TABLE 10

PILOT RATINGS FOR FINAL LATERAL FLIGHT DIRECTOR SYSTEM
WITH AND WITHOUT LATERAL SAS

LATERAL FLIGHT DIRECTOR	LATERAL SAS	PILOTS	
		A	B
On	On	1-1/2	1-2
	Off	4 to 4-1/2	Not tested
Off	On	4 to 4-1/2	3-4
	Off	7 (Some Visual) — 10 (Total IFR)	Not tested

Table 11 presents the feedback gains used for these cases. However, during the simulation it became obvious that a forward loop lead on localizer error designed to cancel out the closed-loop spiral mode was not effective in the presence of the forward loop limiters. Therefore, the intercept

TABLE 11. EFFECTIVE CONTROLLED ELEMENT

CASE NO.	GAINS				·IDEAL NUMERATOR TRANSFER FUNCTION $N_{\delta_W}^{FD}$	ESTIMATED CROSSOVER FREQUENCY (RAD/SEC)	REMARKS
	K_p	K_φ	K_λ	K_y			
3	2.66	1.434	1.05	.0006	$2.62(.1)(.27)^2$		Used forward loop lead on y_e
3A	2.66	2.10	1.95	.001295	$2.62(.1)(.4)^2$	0.8	Same as 3
3C	2.66	3.19	3.99	.00299	$2.62(.1)(.62)^2$	1.0	No forward loop lead used. All path damping from $\hat{\lambda}$
3D	2.66	1.89	1.81	.001625	$2.62(.27)^3$	0.66	Same
3E	2.66	3.11	4.30	.00557	$2.62(.27)(.5)^2$	0.90	Same
2F	0	1.61	1.55	.00194	$1.0[.73; .19]$	1.0	No shelf. Conditionally stable

time constant as well as localizer tracking, after being blown off by wind inputs, was dominated by the time constant of the spiral mode. This can be seen in an intercept time history shown by Fig. 32. To eliminate this problem the spiral mode had to be driven to a higher frequency. This was done by increasing the frequency of the first-order numerator zero as shown by Cases 3D and 3E and, of course, the final system, 2F.

The ideal numerator transfer functions were used to derive the gains presented in Table 11. This was done by equating like powers of s in the following equation:

$$N_{\delta_w}^{FD} = A_\varphi \frac{\omega_c}{f} \left[K_p s^3 + \left(K_\varphi + \frac{K_p}{T_s} \right) s^2 + \left(\frac{gK_\lambda}{U_o} \right) s + gK_y \right]$$

where:

A_φ	=	high frequency gain of φ/δ_w numerator
ω_c	=	crossover frequency
f	=	frequency separation factor
K	=	feedback gains identified by subscript
T_s	=	spiral mode time constant
U_o	=	forward speed
g	=	gravity

However, since roll attitude is not simply the integral of roll rate and ω_φ does not exactly cancel ω_d, the actual effective controlled element dynamics were somewhat different. Frequency responses for actual effective controlled elements tested are presented in Figs. 33a-33e.

Pilot ratings showed Case 2F to be the most desirable. The best of the cases previously shown in Fig. 33 was Case 3D. This case seemed to the pilot as though it was giving about the same performance but was demanding "tighter" control. Figure 34 can be compared with Fig. 31 tc show the intercept performance of Case 3D and Case 2F, respectively. The more rapid convergence of Case 2F is due to the closed-loop path mode being at higher frequency than that of Case 3D. The director activity (continuous line on the first channel) does exhibit more high-frequency activity than that of Case 2F.

Time histories of intercept and localizer tracking for the no-flight-director case and the remaining two flight director cases (Cases 3C and 3E) are presented in Figs. 35, 36, and 37, respectively.

A tabulation of the pilot ratings and comments for each case tested is presented in Table 12.
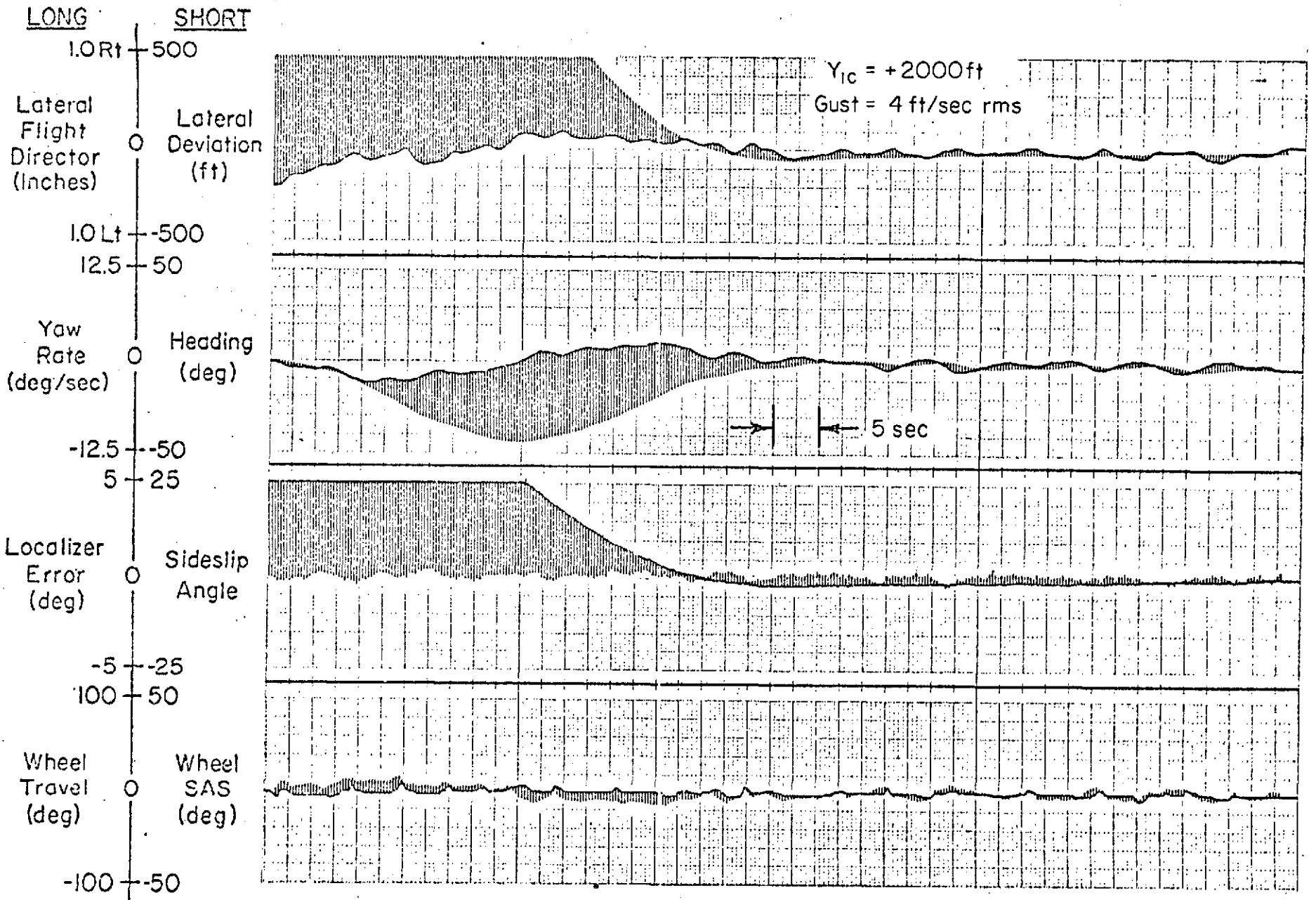
Figure 32. Time History of Intercept for Lateral Director (Case 3A)

$$\frac{FD}{\delta_w} = \frac{2.62\,(.083)[.74\,;.30][.53\,;.63]}{(0)^2(.096)(1.62)^2[.48\,;.62]}$$
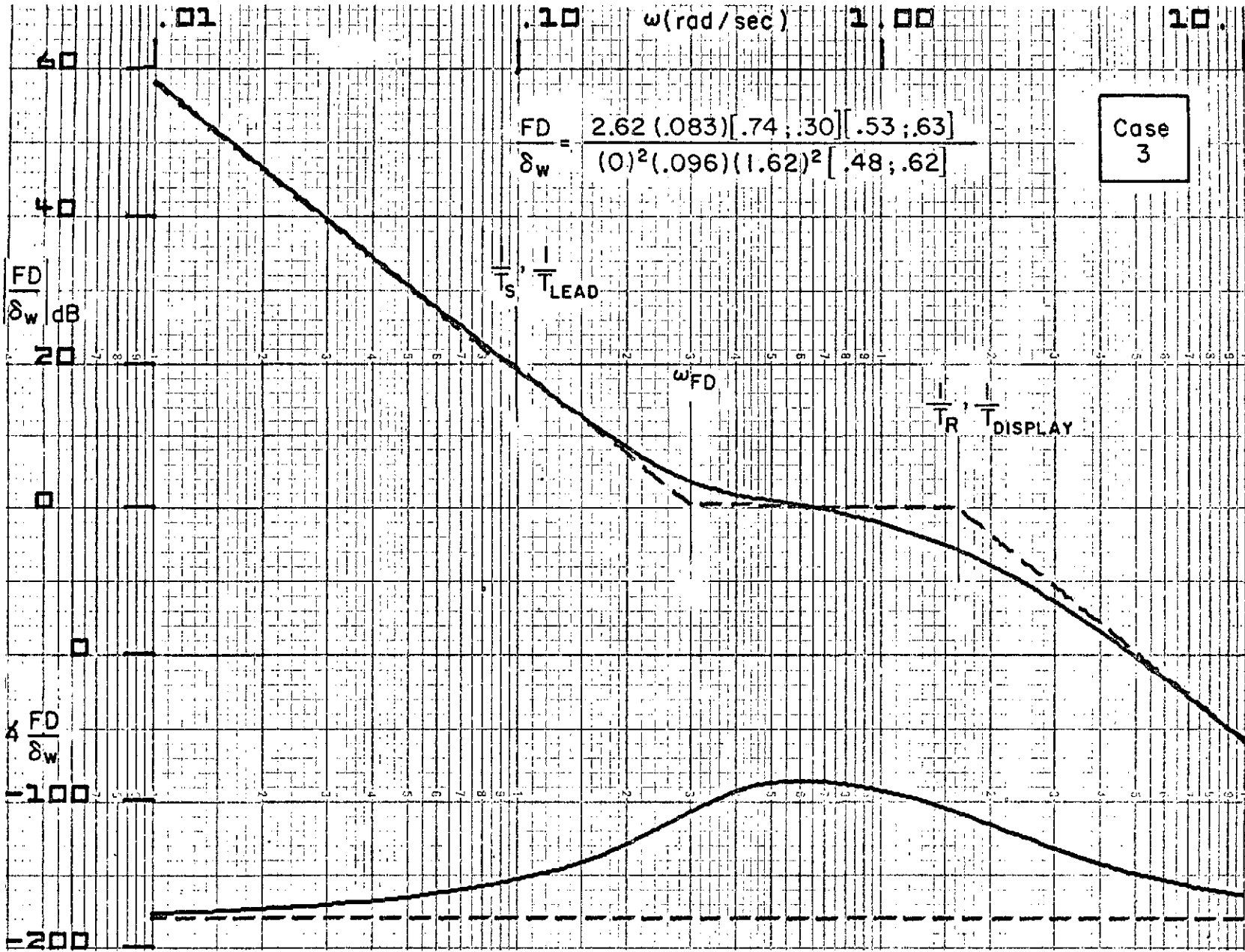
Case 3

Figure 33.   Effective Controlled Element for Lateral Director.   a)   Case 3

$$\frac{FD}{\delta_w} = \frac{2.52\,(.093)[.81\,;.42][.53\,;.63]}{(0)^2\,(.096)(1.62)^2[.48\,;.62]}$$

Case 3A

$\dfrac{1}{T_S}$, $\dfrac{1}{T_{LEAD}}$

$\left|\dfrac{FD}{\delta_w}\right|$ dB

ω_{FD}

$\dfrac{1}{T_R}$, $\dfrac{1}{T_{DISPLAY}}$

$\sphericalangle\,\dfrac{FD}{\delta_w}$
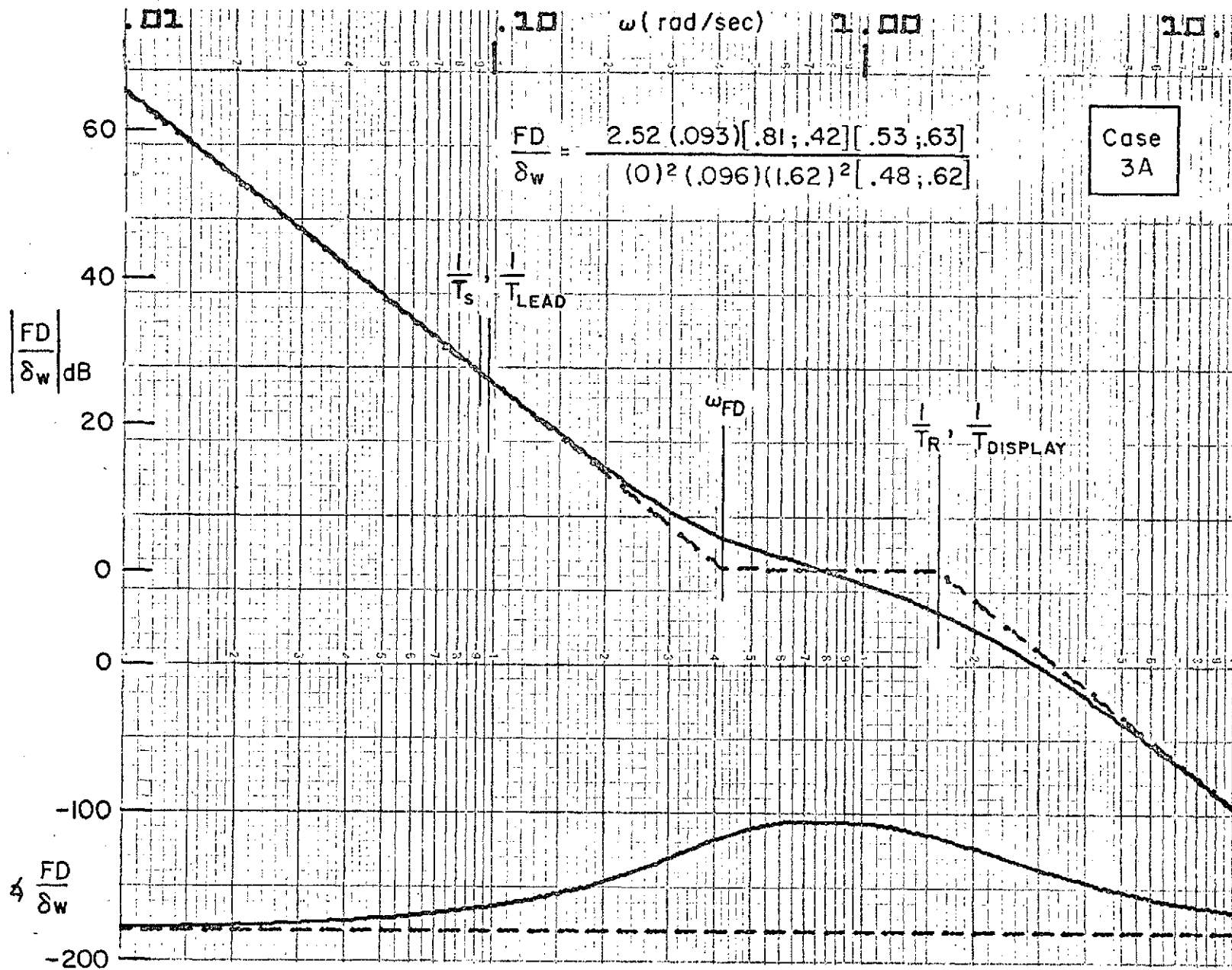
Figure 33. (Continued). b) Case 3A

$$\frac{FD}{\delta_w} = \frac{240\,(.097)[.51;.59][.86;.68]}{(0)^2(.096)(1.62)^2[.48;.62]}$$
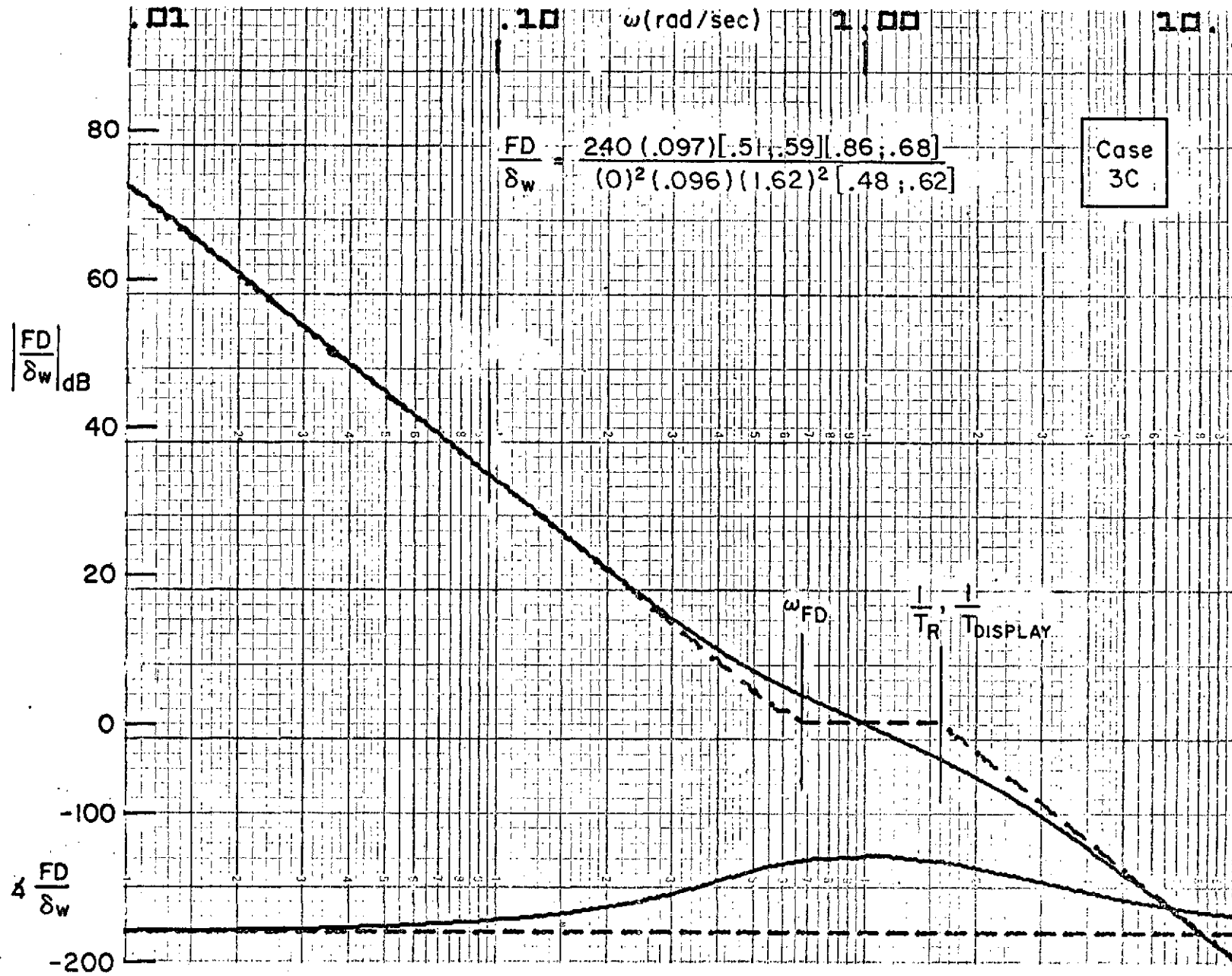
Case 3C

Figure 33 (Continued) c) Case 3C

$$\frac{FD}{\delta_w} = \frac{2.52\,(.151)[.74;.36]\,[.53;.63]}{(0)^2(.096)(1.62)^2[.48;.62]}$$
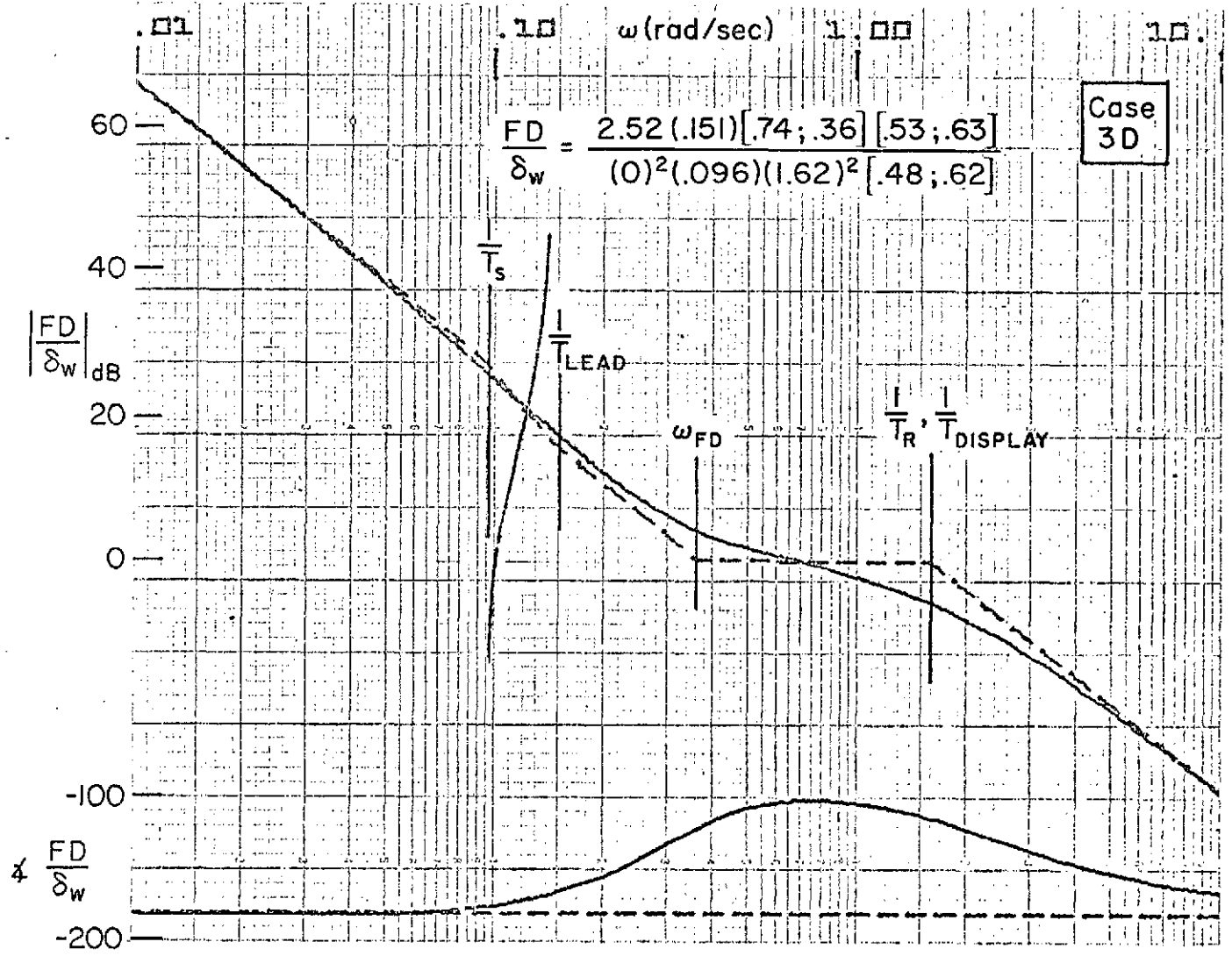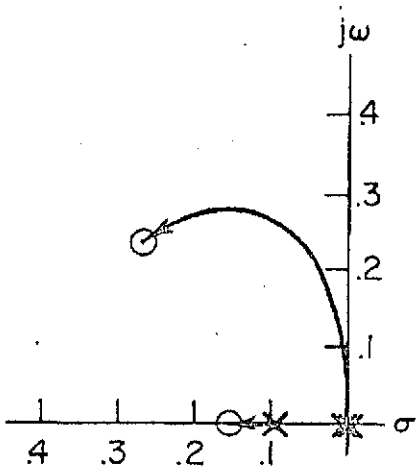
Case 3D

Figure 33 (Continued). d) Case 3D
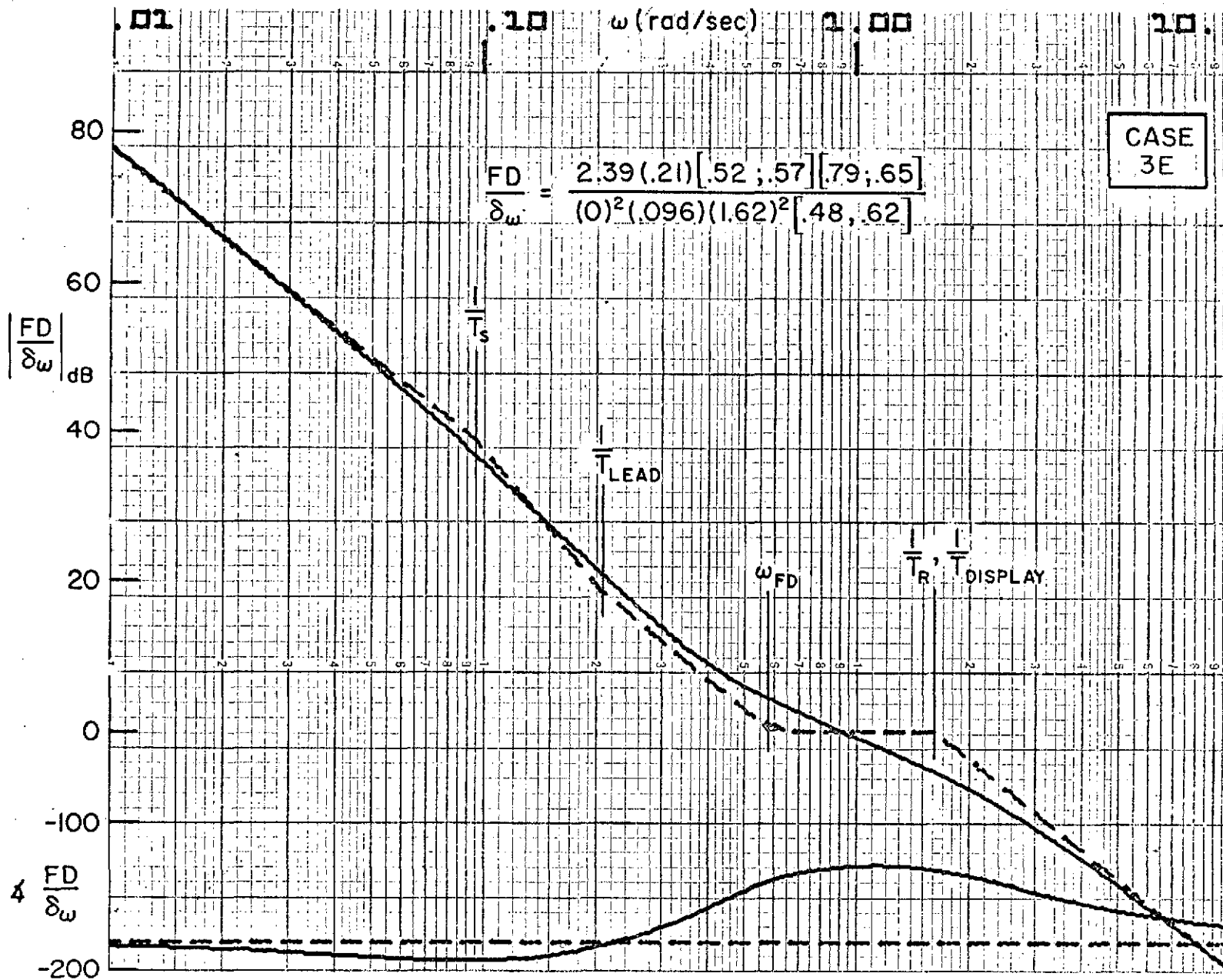
Figure 33 (Concluded). e) Case 3E
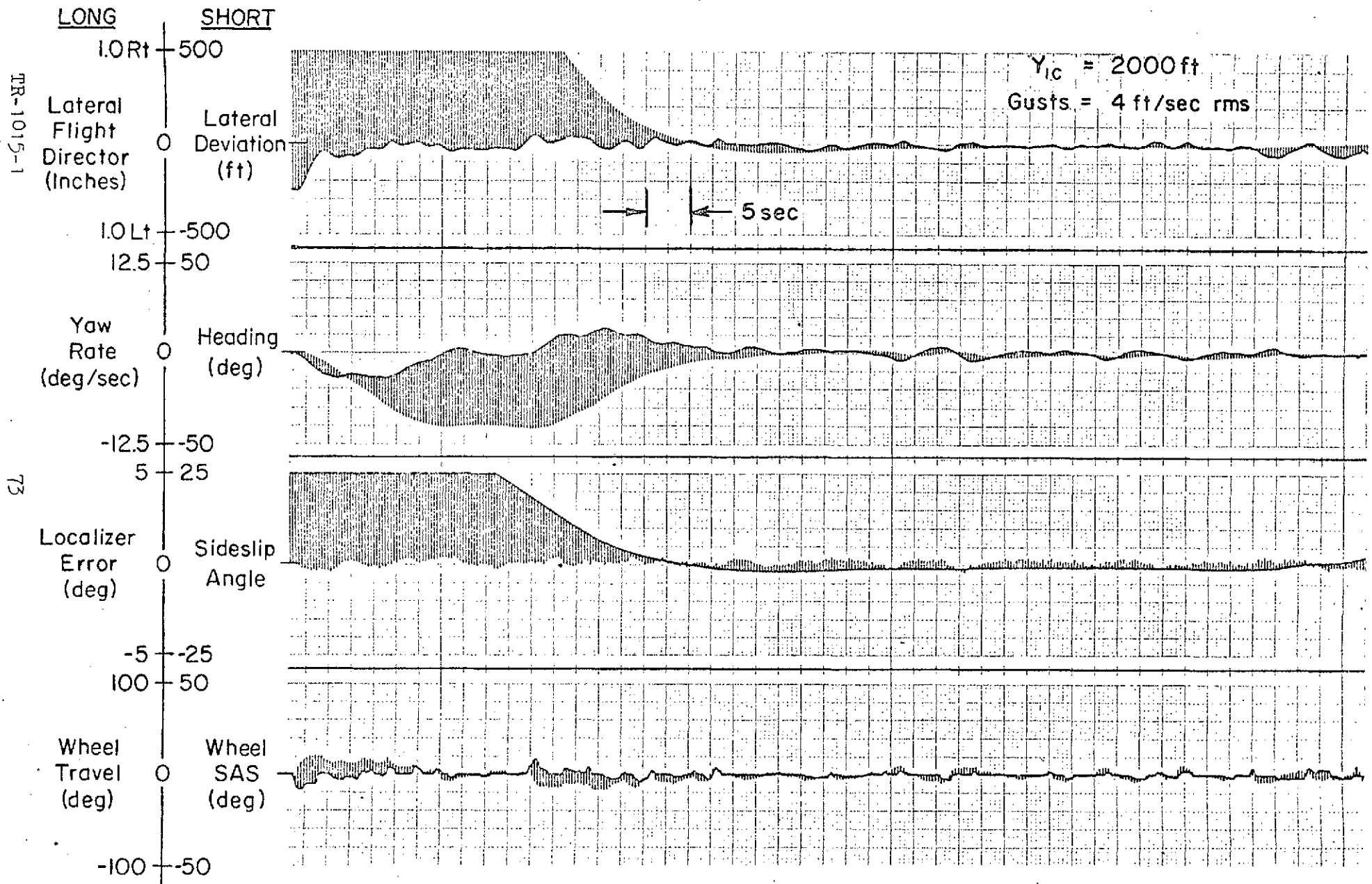
Figure 34. Time History of Intercept and Tracking Task with Lateral Director (Case 3D)
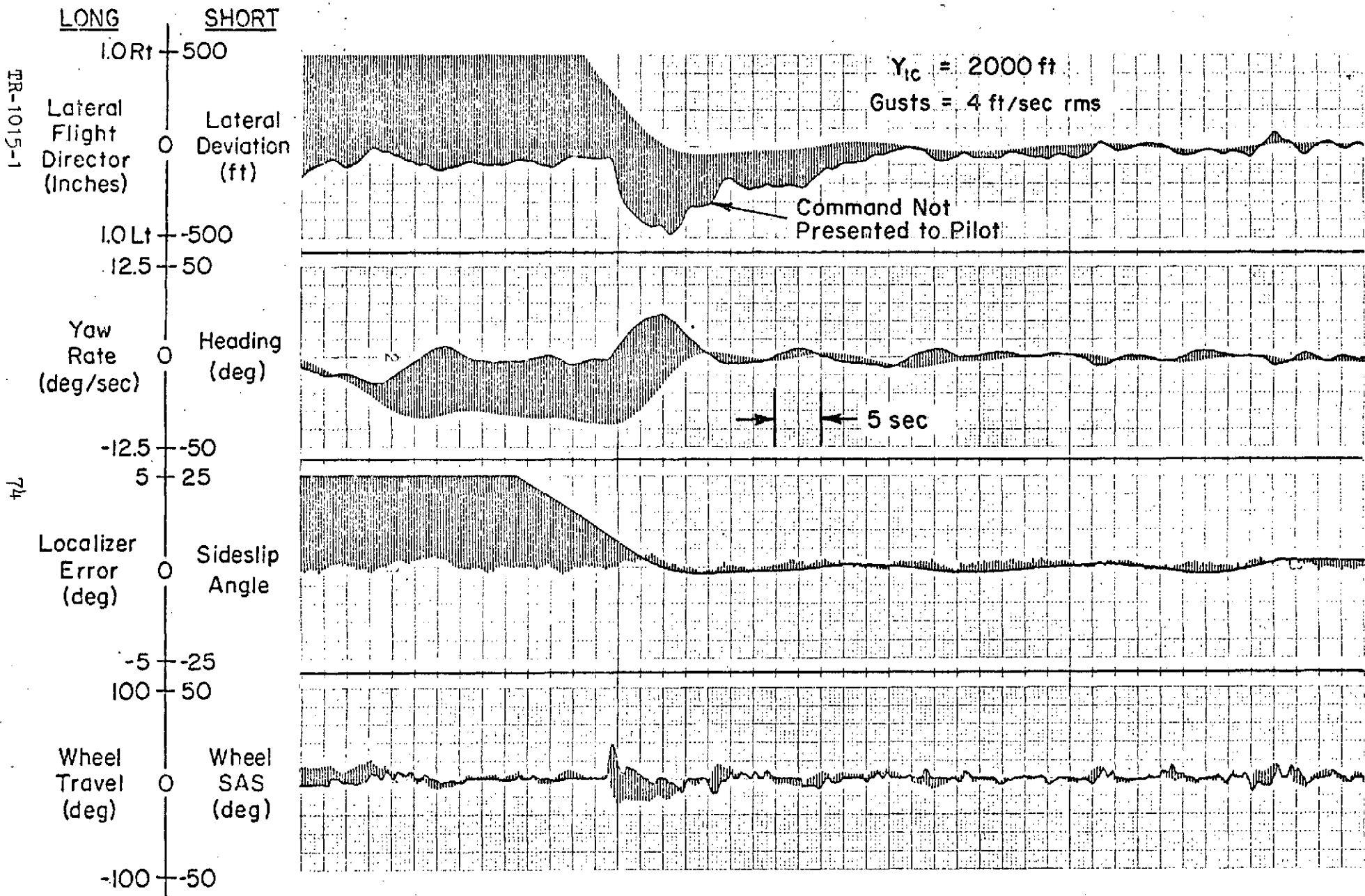
Figure 35. Time History of a Non-Flight Director Intercept and Localizer Tracking

74

LONG   SHORT

1.0 Rt — 500

Lateral   Lateral
Flight   Deviation
Director   0   (ft)
(inches)

Y_{IC} = 2000 ft

Gusts = .4 ft/sec rms

1.0 Lt — -500

12.5 — 50

Yaw
Rate   0   Heading
(deg/sec)   (deg)

5 sec

-12.5 — -50

5 — 25

Localizer
Error   0   Sideslip
(deg)   Angle

-5 — -25

100 — 50

Wheel   Wheel
Travel   0   SAS
(deg)   (deg)

-100 — -50
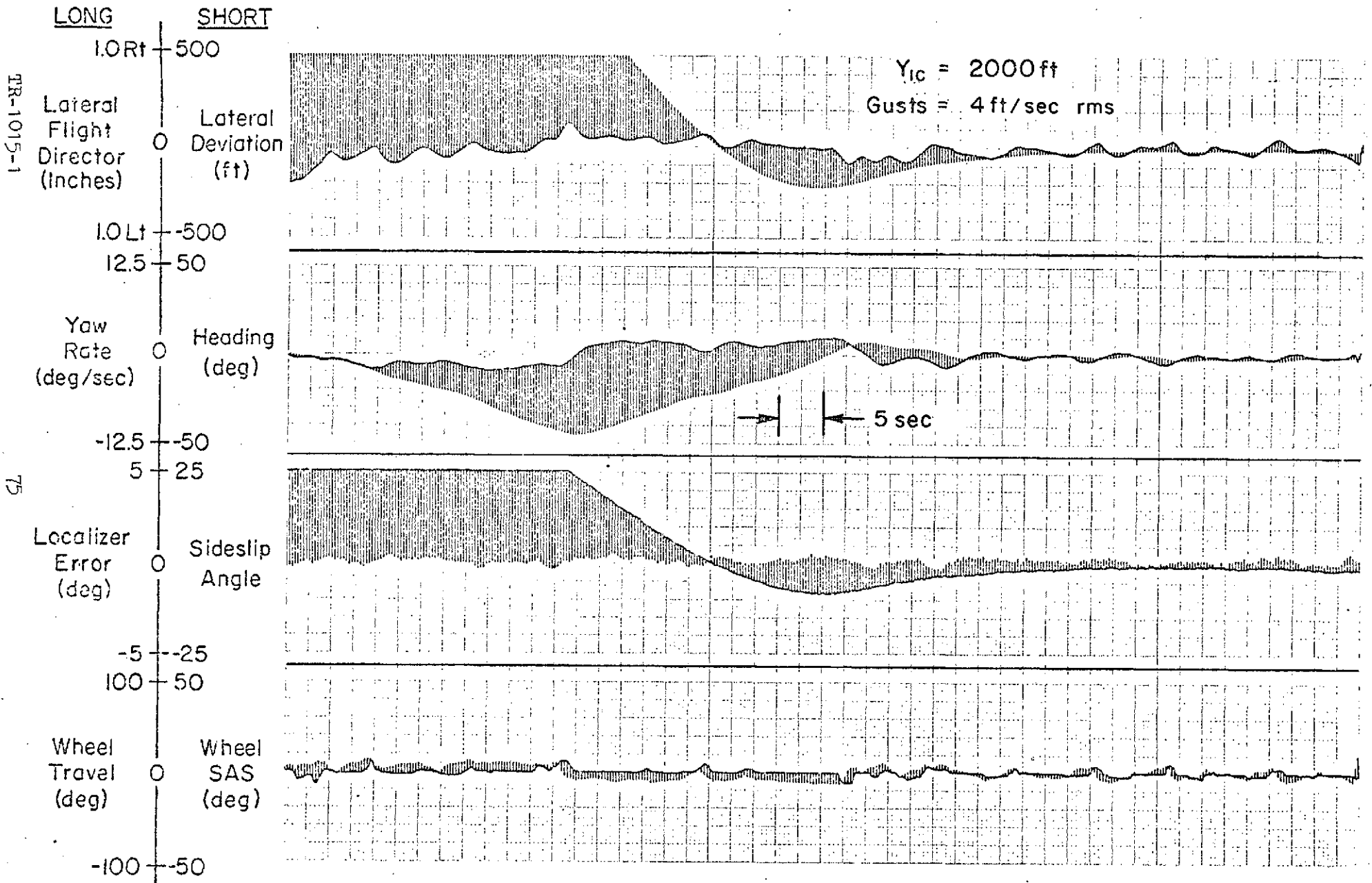
Figure 36.   Time History of Intercept and Localizer Tracking for Case 3C
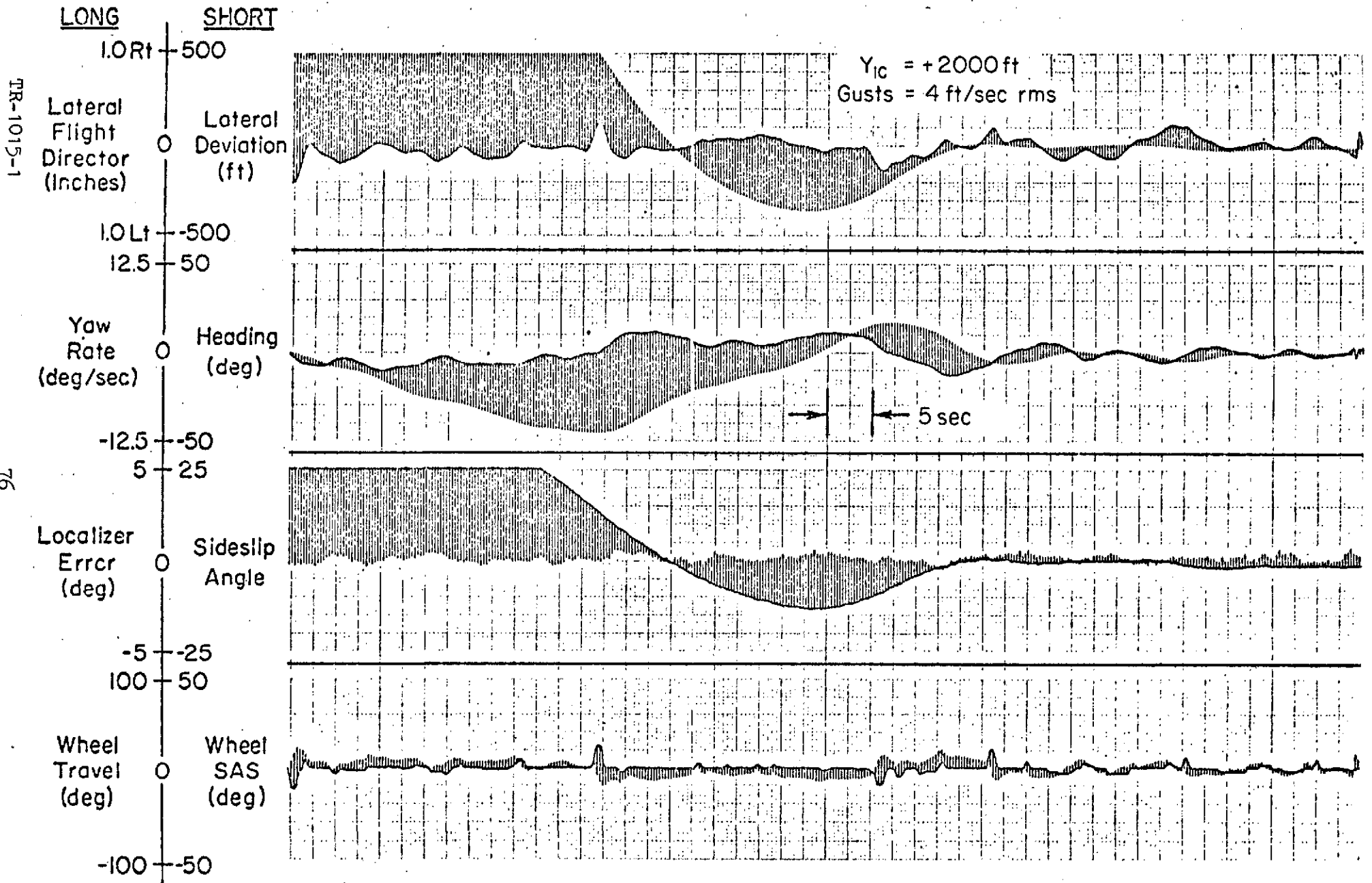
Figure 37. Time History of Intercept and Localizer Tracking for Case 3E

TABLE 12

PILOT RATINGS AND COMMENTS

PILOT	CASE	POR	COMMENTS
A	3	2-1/2	Long tail — produces slight standoff at end if you have to correct late for it. Gusts have no effect.
	3A	2-1/2	Less standoff error. Just as easy as Case 3. Couldn't see any difference in FD motion.
	3C	3-1/2 — 4	Poorer performance — working harder to get more overshoots.
	3D	2	Much better performance. Liked FD bar response. Not tight control. With loose control get big overshoot on intercept. No offset for wind shear input. May tend to overbank.
	3E	3-1/2 — 4	Director makes large changes abruptly (coming off limiters). Causes initial overshoots. Not hard to track although wanders back and forth too much.
	No FD	4 — 4-1/2	Longitudinal performance degraded because of attention required for lateral. Wind shear is most severe part to cope with.
	4	4	Wind shear: just keeps drifting further away. Poor performance. This primary cause of degraded rating.
	2F	1-1/2	Don't have to spend as much time on FD. 3D requires higher frequency inputs and I'm working harder.
	SAS Off No FD	7	Was only possible because could get some visual cues through clouds. Totally IFR is usually impossible.
	SAS Off 3D	4-1/2	Not a problem. All have to do is follow the needle although this requires constant attention and high effort.

(continued)

TABLE 12 (concluded)

PILOT	CASE	POR	COMMENTS
B	3D	2 – 3	Not as good as 2F for localizer holding, gives slight offset. Very self-compelling, needs monitoring. No problem, nice and tight.
	2F	1 – 2	More time to monitor status. Not as tight as 3D and performance seems same. Picks up drift angle up to 20 deg with no overshoot. Wish current equipment had this sense.
	3E	3 – 4	Too sluggish — more demanding and get reduced performance. Like another set of raw data. Seems like command responses are delayed. Not smart.
	4	3 – 4	Most precise. Could do better without a FD. Produced standoff to the wind shear. Raw data say all screwed up but director says OK.

C. WINDPROOFING WITH LATERAL FLIGHT PATH ANGLE FEEDBACK

Included as a separate test case (Case 4) was a more conventional mechanization of Case 3D that used washed-out heading feedback for path damping instead of lateral flight path angle. Figure 38 shows that the effective controlled element response is nearly the same as that of Fig. 33d (Case 3D). However, since lateral flight path angle will not produce a localizer standoff error for any type of wind input (see Table 3), Case 3D (or any other effective controlled element that uses $\hat{\lambda}$) should exhibit better windproofing than a corresponding system using washed-out heading.

The difference in windproofing performance can be appreciated by comparing strip chart recordings of an approach in wind shear for the two systems. Figures 39 and 40 show the difference in windproofing between Cases 4 and 3D when subjected to a crosswind shear of −5 kt at 500 ft increasing linearly to +15 kt at the ground. The washed-out heading system operating in Fig. 39 produced a large localizer error since heading was not changing rapidly enough. At 200 ft altitude the pilot was forced to go visual to salvage the approach. With a lateral flight path angle system, virtually no lateral error was produced, and the pilot remained on the instruments down to an altitude of less than 75 ft.

D. PERFORMANCE COMPARISONS

To lend support to the foregoing results, a comparison of rms performance measures was made between the no flight director vs. best director case, between the best K/s + shelf type effective controlled element and the no roll rate case, and between the windproofing performance of lateral flight path angle vs. washed-out heading systems. Table 13 compares the rms localizer error, ϵ_{loc}, bank angle, φ, and wheel activity, δ_w, in the presence of wind shears and initial offsets for these director systems. In summary, the no flight director case required more wheel activity and attitude excursions to produce 5 times poorer tracking performance. Cases 3D vs. 2F did not have significant control and attitude differences, although the tracking performance of Case 2F was somewhat better. The lateral flight angle method of windproofing reduced rms localizer error and attitude excursions by a factor of 6, with significantly less wheel activity than the washed-out heading case.

$$\frac{FD}{\delta_w} = \frac{2.61(.69)[.47;.083][.89;.5][.33;.54]}{(0)^2(.067)(.096)(1.62)^2(.5)[.48;.62]}$$
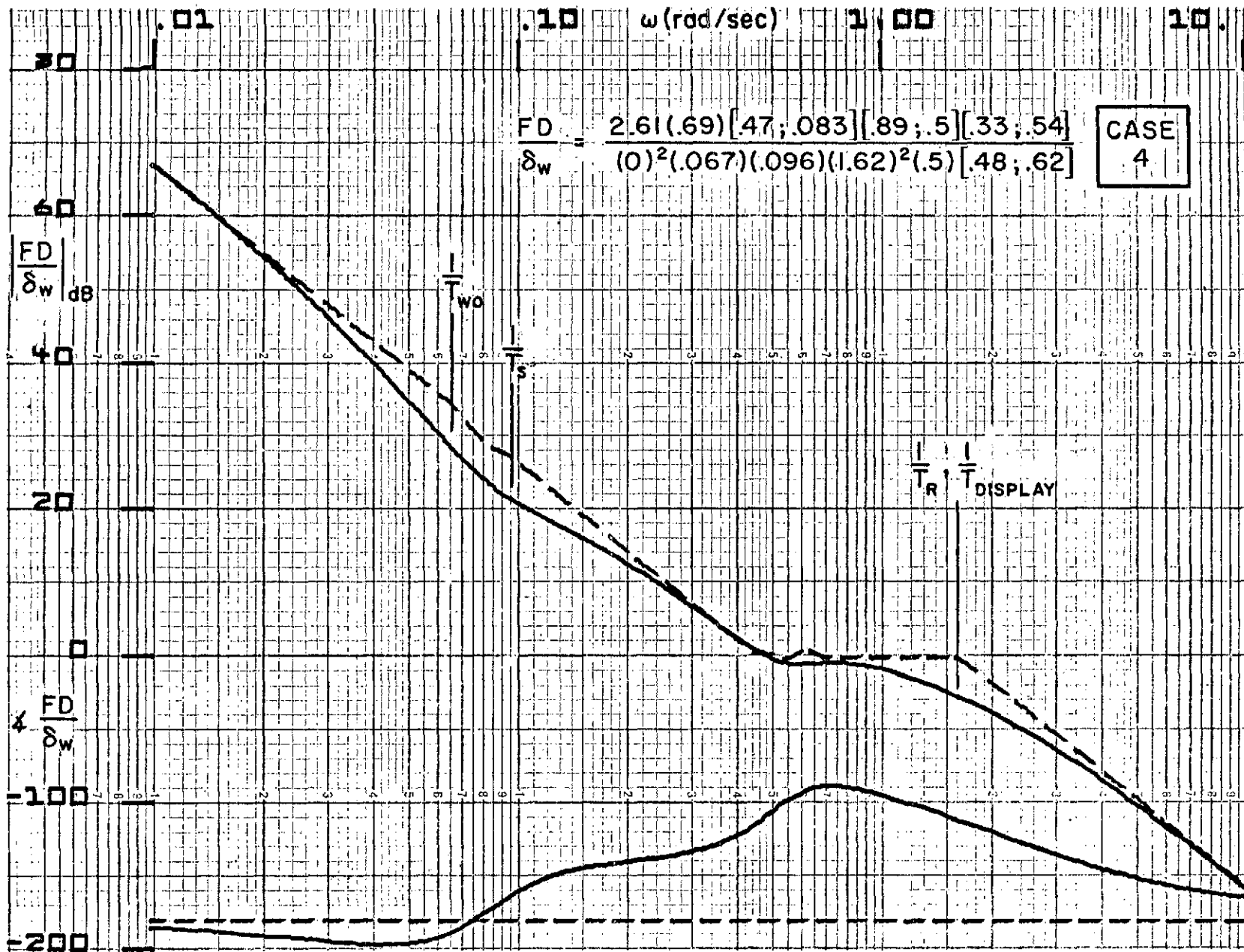
CASE 4

Figure 38. Effective Controlled Element Response for Washed Out Heading Director (Case 4)
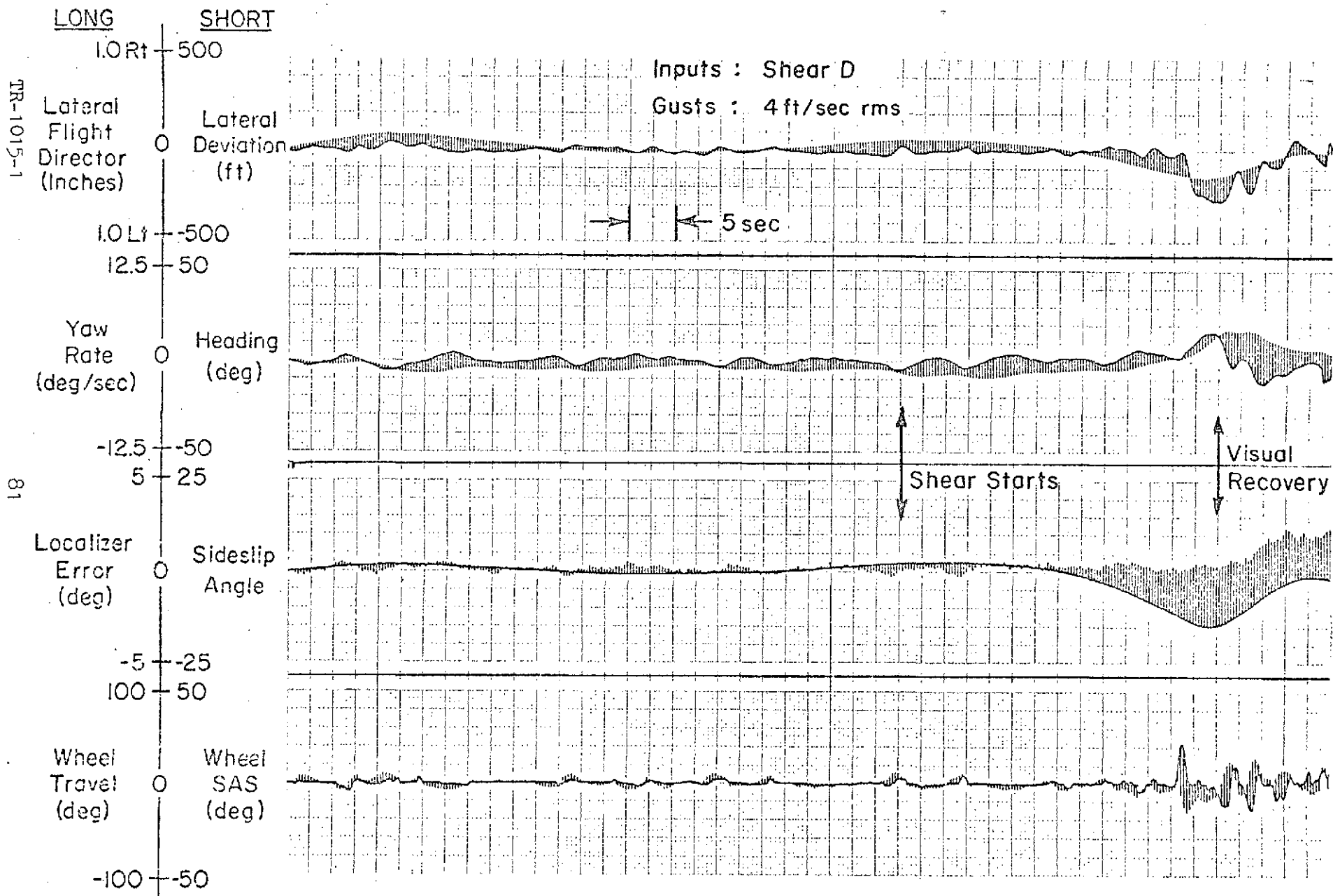
Figure 39. Effect of Wind Shear D on Washed Out Heading Flight Director (Case 4)
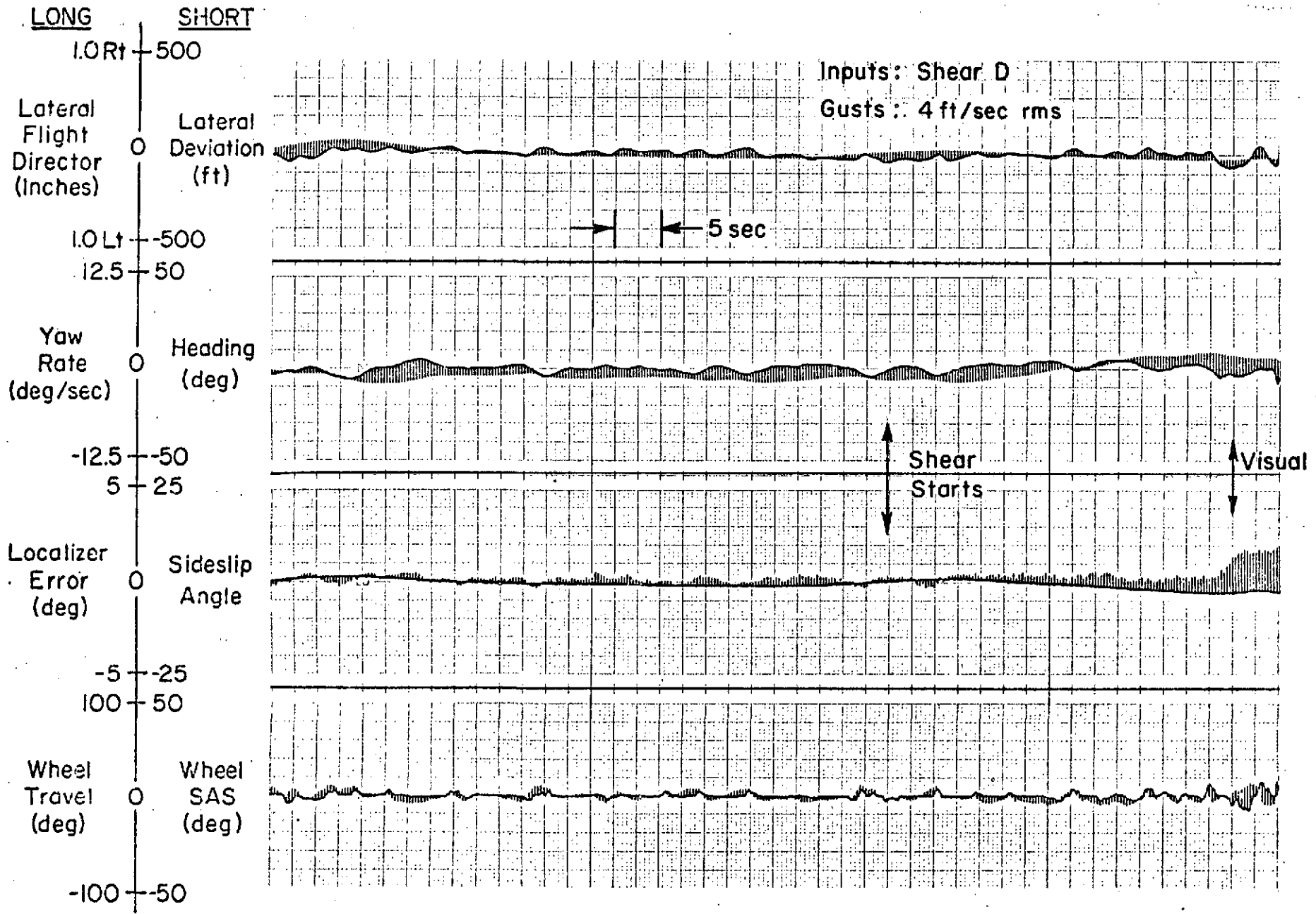
Figure 40. Effect of Wind Shear D on Windproofed Director (Case 3D)

TABLE 13

RMS PERFORMANCE COMPARISONS

VARIABLES & SYSTEMS / INPUTS	ϵ_{loc} (deg)		φ (deg)		δ_w (deg)		COMPARISON OF
	NO FD	2F	NO FD	2F	NO FD	2F	
Shears[1]	0.216	0.0420	3.48	1.05	8.48	4.16	No Flight Director vs Best Flight Director
Offset[2]	2.61	2.29	4.78	3.85	5.67	1.43	
	3D	2F	3D	2F	3D	2F	
Shears[3]	0.251	0.178	0.990	1.22	2.08	3.30	Effective Controlled Elements
Offset[4]	2.57	2.23	3.91	4.15	3.11	4.08	
	ψ_{wo}	$\hat{\lambda}$	ψ_{wo}	$\hat{\lambda}$	ψ_{wo}	$\hat{\lambda}$	
Shears[5]	0.640	0.103	4.14	0.710	9.81	2.50	Path Damping Mechanizations

[1] Average of shear E and shear D (including gusts); data for 300 → 50 ft during approach (2 runs)

[2] 2000 ft initial lateral offset (including gusts); data for 1300 → 300 ft (1 run)

[3] Same as (1) but data for 1300 → 300 ft (2 runs)

[4] Same as (2) but has 2 runs

[5] Same as (1) but 2 runs at each shear condition (2 pilots)

The major problem in the lateral axis was the incompatibility of the forward loop limiters. Since the maximum bank angle was limited to 16 deg by pilot preference, the PHI limiter is set at 45% of the maximum display range. Hence, a large lateral offset can never drive the flight director more than about 1/2 scale. To get around this problem the display gain was increased by a factor of 2. This resulted in an unacceptably busy display. Changing the ratio of K_φ/K_y would also solve the problem but would force a reduction in K_λ which would then increase the path mode time constant, again an undesirable result. It was concluded that a nonlinear display gain would be the best solution. However, this required a program change which was not able to be done in the time available.

E. SUMMARY OF RESULTS

A summary of the results for the lateral flight director evaluation is as follows:

1. K/s + shelf type effective controlled elements do not allow enough path and attitude mode amplitude separation. A display gain set for high frequency command bar consistency does not give enough localizer resolution at low frequency.

2. A closed-loop path mode of from 0.1 to 0.2 rad/sec produces good subjective performance.

3. Pilot closure of the flight director loop is at about 0.8-1.0 rad/sec. Wheel travel never exceeds 30 deg, regardless of command.

4. Lateral flight path angle improves "face validity" and performance over a conventional washed-out heading-type director when compensating for wind shears.

5. The flight director system makes a significant improvement in performance and pilot workload over the raw data situation. It can also save the approach in case of a SAS failure during a 60 kt IFR approach.

6. Gusts on or off did not make any difference in pilot rating or the ability to perform the task.

REFERENCES

1. McRuer, Duane T., and Henry R. Jex, "A Review of Quasi-Linear Pilot Models," IEEE Trans., Vol. HFE-8, No. 3, Sept. 1967, pp. 231-249.

2. McRuer, Duane, Dunstan Graham, Ezra Krendel, and William Reisener, Jr., Human Pilot Dynamics in Compensatory Systems — Theory, Models, and Experiments with Controlled Element and Forcing Function Variations, AFFDL-TR-65-15, July 1965.

3. McRuer, D., and D. H. Weir, "Theory of Manual Vehicular Control," Ergonomics, Vol. 12, No. 4, 1969, pp. 599-633.

4. Weir, D. H., R. H. Klein, and D. T. McRuer, Principles for the Design of Advanced Flight Director Systems Based on the Theory of Manual Control Displays, NASA CR-1748, Mar. 1971.

5. Allen, R. W., W. F. Clement and H. R. Jex, Research on Display Scanning, Sampling, and Reconstruction Using Separate Main and Secondary Tracking Tasks, NASA CR-1569, July 1970.

6. Criteria for Approval of Category II Landing Weather Minima, FAA Advisory Circular 120-20, 6 June 1966.

7. Melvin, William W., Effects of Wind Shear on Approach with Associate Faults of Approach Couplers and Flight Directors, AIAA Paper No. 69-796, July 1969.

8. Wind Model for Space Shuttle Simulations, NASA, Ames Research Center, 1 July 1971. Transmitted to STI from Everett Palmer, 28 July 1971.

9. Graham, Dunstan, Warren F. Clement, and Lee Gregor Hofmann, Investigation of Measuring System Requirements for Instrument Low-Approach, AFFDL-TR-70-102, Feb. 1971.

10. Klein, Richard H., and Warren F. Clement, Application of Manual Control Display Theory To The Development Of Flight Director Systems For STOL Aircraft, Systems Technology, Inc., Technical Report 1011-1, January 1973 (Forthcoming AFFDL-TR-72-152).

APPENDIX A

AWJSRA VEHICLE DYNAMICS AT 60 KT
ON 7-1/2 DEG GLIDE SLOPE

NOMINAL TRIM

SIMULATOR COMPUTER SYSTEMS BRANCH
NASA-AMES RESEARCH CENTER

AUGMENTOR WING JET STOL RESEARCH AIRCRAFT

TIME = .00   DATE 16:52 JAN 13, '72

VEQ =	.60000E 02	KTS	ALFA =	.13000E 01	DEG	BETA =	-.10381E-09	DEG
GAIN =	-.74973E 01	DEG	IT =	.10000E 01	DEG	ALFT =	-.65779E-01	DEG
WAIT =	.40000E 05	LB	BSCG =	.34120E 03	IN	QBAR =	.12216E 02	P/F2
DC =	.20712E 01	IN	DJ =	.00000E 00	DEG	DP =	.00000E 00	DEG
DE =	-.43729E 01	DEG	DF =	.55000E 02	DEG	DNUP =	.94097E 02	DEG
DAR =	.32593E 02	DEG	DCHR =	.30000E 00	DEG	DGPR =	-.19531E-02	DEG
DAL =	.32098E 02	DEG	DCHL =	.30000E 00	DEG	DGPL =	-.19531E-02	DEG
DR =	.00000E 00	DEG	THP =	.35799E 04	LB	THS =	.35799E 04	LB
PHI =	.00000E 00	DEG	THET =	-.51992E 01	DEG	PSI =	.90000E 02	DEG
PB =	.00000E 00	R/S	QB =	.00000E 00	R/S	RB =	.00000E 00	R/S
PBD =	.33450E-05	R/S2	QBD =	-.50573E-03	R/S2	RBD =	-.11136E-04	R/S2
ALT =	.20008E 04	FT	XCG =	-.91368E 04	FT	YCG =	.69049E-09	FT
UB =	.10439E 03	F/S	VB =	-.18917E-09	F/S	WB =	.23703E 01	F/S
VH =	-.30518E-02	F/S	VEE =	.10051E 03	F/S	ALTD =	-.01722E 03	F/M
VHW =	.00000E 00	F/S	VEW =	-.91563E-02	F/S	VDW =	-.76294E-02	F/S
TAL =	.12037E 01	FP	TAM =	-.75465E 04	FP	TAN =	-.47975E 01	FP
TTL =	.12037E 01	FP	TTM =	-.11126E 03	FP	TTN =	-.47975E 01	FP
FAX =	-.27026E 04	LB	FAY =	.11333E 00	LB	FAZ =	-.32450E 05	LB
FTX =	-.43190E 04	LB	FTY =	.11333E 00	LB	FTZ =	-.39697E 05	LB
AXP =	-.10030E 00	G	AYP =	-.35376E-05	G	AZP =	-.90906E 00	G

LONGITUDINAL DIMENSIONAL DERIVATIVES
AND TRANSFER FUNCTIONS

FC#5 C-8

GEOMETRY:

VT	ALPHA	GAMMA	LX A	LX P
101.3	1.300	-6.300	.0	.0

DIMENSIONAL DERIVATIVES

XU STAR	ZU STAR	MU STAR	Z WD	M WD
-.05200	-.2800	.001470	-.01510	-.004340
XW	ZW	MW	MQ	
.1230	-.5350	-.003350	-.9140	
XDE	ZDE	MDE		
.1520	-.4570	-1.300		
XDNU	ZDNU	MDNU		
-5.400	.4280	-.09450		

CONDITION: FC#5 C-8

DENOMINATOR:
    .10151E 1
    (.11940E 1) (.69500E 0)
    ((.72288E- 1, .25622E 0, .18521E- 1, .25555E 0))
    < .55297E- 1>

CONDITION: FC#5 C-8

DE NUMERATORS:

U   - DE
    .15430E 0
    (.87190E 0)
    ((.79569E 0, .12734E 2, .10132E 2, .77128E 1))
    < .21813E 2>
W   - DE
    -.45700E 0
    (.28906E 3)
    ((.14295E 0, .29997E 0, .42882E- 1, .29689E 0))
    <-.11887E 2>
THE - DE
    -.13176E 1
    (.43883E 0) (.13953E 0)
    <-.80679E- 1>

HD   - DE h/δ_e
     .44181E 0
    (-.13960E   2) (.11002E   2) (-.26777E- 1)
    < .18170E   1>
AZ   - DE a_z/δ_e
     -.45700E 0
    (-.13830E   2) (.11002E   2)
    ((-.19931E 0, .57062E- 1,-.11373E- 1, .55917E- 1))
    < .22642E   0>

DNU NUMERATORS: (Not Lever Angle)

U   - DNU
     -.54815E 1
    (-.26057E   0) (.13286E   1) (.77540E   0)
    < .15644E   1>
W   - DNU
     .42800E 0
    (-.17898E   2)
    ((.52872E- 1, .33597E   0, .17764E- 1, .33550E   0))
    <-.86466E   0>
THE - DNU
     -.97784E- 1
    ((.93006E   0, .39417E   0, .36660E   0, .14482E   0))
    <-.15193E- 1>
HD   - DNU
     .51375E- 1
    (.12183E   0) (-.30759E   2) (.41890E   1)
    <-.80645E   0>
AZ   - DNU
     .42800E   0
    ((.63539E   0, .40554E   1, .25767E   1, .31315E   1))
    ((.78658E   0, .77829E- 1, .61219E- 1, .48059E- 1))
    < .42637E- 1>

CONDITION: FC#5 C-8

DE / DNU COUPLING NUMERATORS:

```
U   -DE /W  -DNU
    -.24027E  1
    ( .29683E   3) ( .71234E- 3)
    <-.50805E   0>
U   -DE /THE-DNU
    -.71302E  1
    ( .51634E   0)
    <-.36816E   1>
U   -DE /HD -DNU
     .23936E  1
    (-.14083E   2) ( .10982E   2)
    <-.37019E   3>
U   -DE /AZ -DNU
    -.24027E  1
    (-.14771E   2) ( .11048E   2) ( .26349E- 1)
    < .10332E   2>
W   -DE /THE-DNU
     .59959E  0
    ( .33429E   1)
    < .20043E   1>
W   -DE /HD -DNU
    -.20941E  0
    ( .35605E   2) (-.27061E   2)
    < .20177E   3>
W   -DE /AZ -DNU
    -.60722E  2
    ( .33429E   1) ( .27711E-.1)
    <-.56250E   1>
THE-DE /HD -DNU
    -.24127E- 1
    (-.69460E   2)
    < .16758E   1>
THE-DE /AZ -DNU
    -.59959E  0
    ( .33429E   1) ( .00000E   0)
    <-.20043E   1>
HD -DE /AZ -DNU
     .20941E  0
    (-.13980E   2) ( .11002E   2) (-.14602E   0)
    < .47031E   1>
```

LATERAL DIMENSIONAL DERIVATIVES
AND SAS-ON WHEEL TRANSFER FUNCTIONS

GEOMETRY:

VT	ALPHA	GAMA	LX	LZ
101.3	.0	-7.500	18.5	-2.370
IX	IZ	IXZ	AG	
287200.	41670.	27910.0	3.510	
S	B	RHO	W	A
865.0	78.7	.002377	400.0	1116.9

NON-DIMENSIONAL DERIVATIVES

CYB	CLB	CNB	
-1.285	.0	.2370	
CLP	CNP	CLR	CNR
-.5090	-.2680	.7300	-.3980
CYDW	CLDW	CNDW	
-.3200	.2110	-.01440	
CYDR	CLDR	CNDR	
.6540	.08220	-.3610	

UNPRIMED DIMENSIONAL DERIVATIVES

YV	LB	NB	
-.1076	.0	.4725	
LP	NP	LR	NR
-.5723	-.2077	.8208	-.3084
YDW	LDW	NDW	
-2.715	.6104	-.02871	
YDR	LDR	NDR	
5.50	.2378	-.7197	

PRIMED DIMENSIONAL DERIVATIVES

YB	LBP	NBP	
-10.9	.04622	.4756	
LPP	NPP	LRP	NRP
-.5964	-.2476	.7960	-.2551
YDW S	LDW P	NDW P	
-.02681	.6115	.01225	
YDR S	LDR P	NDR P	
.05478	.1689	-.7084	

DENOMINATOR:

.73000E 0
(.95717E- 1) (.50464E 0) (.16213E 1) (.33425E 1)
((.47531E 0, .62085E 0 , .29510E 0, .54624E 0))
< .73654E- 1>

NUMERATOR: B /DWC

-.19571E- 1
(.12639E 0) (.37299E 0) (-.87207E 0)
((.97493E 0, .33961E 1 , .33109E 1, .75568E 0))
< .92793E- 2>

NUMERATOR: P /DWC

44639E 0
.42118E- 1) (.50030E 0) (.33250E 1)
((.47894E 0, .63039E 0 , .30192E 0, .55338E 0))
< .12429E- 1>

NUMERATOR: R /DWC

.89425E- 2
(.57360E 0) (.15495E 1) (.92182E 1)
((.55109E 0, .11358E 1 , .62592E 0, .94775E 0))
< .94513E- 1>

NUMERATOR: PHI/DWC   (Body Axes)

.44522E 0 φ_β
(.50369E 0) (.33179E 1)
((.49510E 0, .63441E 0 , .31410E 0, .55119E 0))
< .29946E 0>

NUMERATOR: LMP/DWC λ/δ_w

-.19571E- 1
(.50087E 0) (-.20927E 1) (.29216E 1) (.38738E 1)
((.46187E 0, .63794E 0 , .29486E 0, .56602E 0))
< .94465E- 1>